UiT The Arctic University of Norway

Faculty of Biosciences, Fisheries and Economics, Department of Arctic and Marine Biology

Circadian disruption by light and its effect on the immune function of the Atlantic Salmon (*Salmo salar*)

Therese Solberg

Master's thesis in Biology, BIO-3950, May 2022

UiT The Arctic University of Norway

Faculty of Biosciences, Fisheries and Economics, Department of Arctic and Marine Biology

Circadian disruption by light and its effect on the immune function of the Atlantic Salmon (*Salmo salar*)

Therese Solberg

Master of Science in Biology - Arctic Animal Physiology

May 2022

Supervisor:

Alexander West, UiT – The Arctic University of Norway

Co-supervisors:

David Hazlerigg, UiT – The Arctic University of Norway

Eva-Stina Edholm, UiT – The Arctic University of Norway

Acknowledgements

I would like to give a huge thank you to my supervisors Alexander West, David Hazlerigg and Eva-Stina Edholm for giving me this opportunity to work on this project.

Thank you, Alex, for giving me the support and security I needed throughout this project. Thank you for opening my world to molecular biology, for all your help at the lab, with analyses and all your helpful feedback. Thank you for all your enthusiasm, encouragement, and patience. I am very grateful for all that you have taught me.
Thank you, Eva-Stina, for giving me a better understanding of immunology, for all your help with the SAV3 experiment, and for making time for my questions throughout my master.
Thank you, David, for all your help regarding statistics.

I would also like to thank Anja Striberny. Thank you for all your help with the ECG bio-logger implantation.
A special thank you goes to Chandra Sekhar Ravuri for all for your guidance and help at the lab.
Thank you to the personnel at Havbruksstasjonen in Kårvik, without you this project would not have been possible.
Thank you to my fellow master students, for all the laughs throughout this master journey.

Finally, I would like to thank my family and friends for supporting me and keeping my spirit up when I needed it.

Therese Solberg

Therese Solberg
Tromsø – May 2022

Abstract

The Atlantic salmon (*Salmo salar)* is an anadromous salmonid that begins its life cycle in freshwater streams then, develops, in a process known as smoltification, into a marine-adapted fish prior to its migration to the sea. Smoltification is a photoperiod regulated process which involves extensive change in the salmons' physiology. In recent years smoltification procedures in aquaculture has been linked to a downregulation of the immune system, but the underlying cause remains unknown.

In mammals, the circadian clock drives 24h cycles in immune system capacity and recent work links circadian clock disruption, including through exposure to constant light, to an impaired immune response. These data are particularly relevant in an aquaculture context where constant light is used routinely in smoltification protocols. Here, we hypothesise that the downregulation of the immune system in aquaculture smoltification protocols is a consequence of circadian clock disruption caused by exposure to constant light. To investigate our hypothesis, we performed two different smoltification protocols, one under long photoperiod 18 h L: 6 h D (LD), providing both photoperiodic stimulation and circadian entrainment, and a second under constant light (LL), which receives photoperiodic stimulation but in a potentially disruptive circadian environment. We next characterised the smolt phenotypes of each of these groups then compared their immune competence by SAV3 immune challenge.

Both LD and LL protocols induced classical smolt characteristics. In contrast to earlier work, we did not observe a decrease in the expression of a panel of immune genes, and there were not a difference between the LD and LL groups, suggesting that the immune marker genes *Cd3e*, *Csf1r* and *IL10rb* are not robustly associated with smoltification. Following SAV3 challenge, qPCR analysis of immune response markers in head kidney and heart, revealed no difference in viral response between LD and LL groups. These findings were supported by an *in vitro* leukocyte experiment, which showed that LL and LD were similarly stimulated by the viral mimic poly I:C and that there was no distinct time-of-day difference in immune response. Taken together, our results do not support the notion that the immunosuppression observed during smoltification is a consequence of circadian disruption. Instead, we propose that it may be an adaptive response, which may be important for successful migration.

We also present here a complementary pilot study to investigate how salmon circadian physiology is affected by light, using heart rate as circadian output. Here, we implanted ten Atlantic salmon with ECG bio-loggers (Star Oddi, DST-micro-HRT), then entrained them to a light/dark cycle for 14 days before transferring them to a constant light environment. Several of the sutures broke during the experiment which affected bio-logger placement and likely the quality of the data. From the retrieved data, our analysis showed big inter-individual variability in keeping with other studies of salmonids. We suggest technical improvements to the implantation protocol for future studies.

Keywords: Atlantic salmon (*Salmo salar*), smoltification, SAV3, immune response, circadian, ECG, heart rate

Table of Contents

List of Tables

List of Figures

List of abbreviations

AC: Accessory cell

dH_2O: distillated water

GH: Growth hormone

IFN: Interferon

LD: Light dark cycle

LL: Constant light

MHC: Major histocompatibility complex

MRC: Mitochondrion rich cell

NKA: Na^+, K^+ ATPase

PVC: Pavement cell

RPM: Revolutions per minute

SD: Standard deviation

1 Introduction

1.1 Smoltification

The Atlantic salmon (*Salmo salar*) is a anadromous fish species, meaning it spends the first part of its life cycle in fresh water streams, where it is hatches and develops, then migrates to the sea once it reaches a threshold size (Wedemeyer et al., 1980). Before migration the freshwater salmon parr preadapts and transforms into a marine ready smolt, in a process known as smoltification.

Smoltification involves many different coordinated processes, which changes the salmons' physiology and behaviour in preparation for its new marine life (Stefansson et al., 2008). Vertical bands on their body, known as parr marks, gradually disappear (See Figure 1), and they become silvery due to disposition of purines, which are products from protein catabolism (Johnston & Eales, 1967; Wedemeyer et al., 1980). The salmon also changes its behaviour, going from a bottom dwelling territorial fish to a pelagic schooling fish, which reduces risk of predation, as the salmon moves from a freshwater to a marine environment (Handeland et al., 1996; Stefansson et al., 2008). In addition, during smoltification the condition factor decreases. The condition factor reflects the weight length relationship of the salmon, so a decreased condition factor means that the salmon becomes longer and narrower as the fish transform from a freshwater parr to a marine ready smolt (Hoar, 1939).

Figure 1: *Salmon parr prior to smoltification and salmon smolt after 6 weeks of winter photoperiod and 6 weeks of summer photoperiod. The parr marks disappear and the salmon becomes silvery. Figure: Therese Solberg, fish photos taken at Havbruksstasjonen in Tromsø, Kårvik.*

1.2 Development of osmoregulatory capacity during smoltification

One of the best studied transitions that occurs during smoltification is the change in osmoregulatory capabilities. As a group, teleosts maintain stable osmolarity in their extracellular fluid, regardless of the osmolarity of their environment (Evans et al., 2005; Stefansson et al., 2008). When the salmon are in freshwater streams, they have a higher osmolality in their body compared to the outside environment, meaning they are prone to lose

ions to their environment and gain water by osmosis. To avoid this and keep their osmotic pressure stable, the salmon must absorb ions from their environment, with uptake of ions through food and by active uptake through the gill surface (Evans et al., 2005; Stefansson et al., 2008). In seawater the salmon have the opposite problem, where it will gain ions by diffusion and lose water by osmosis. The salmon therefore actively must secrete excess ions and the gill must reverse its osmoregulatory functions (Evans et al., 2005; Stefansson et al., 2008). During smoltification the salmon therefore goes from a hyper-osmoregulator to a hypo-osmoregulator (See Figure 2).

The gill epithelium of teleosts consists primarily of two cell types, pavement cells (PVCs) which makes up the majority, and mitochondrion rich cells (MRCs)(Evans et al., 2005). PVCs are believed to play an important role in gas exchange due to their thin appearance (Evans et al., 2005). MRCs on the other hand, play a big role in salt uptake and secretion (Evans et al., 2005). MRC have a high concentration of mitochondria and Na^+, K^+ ATPases (NKAs) compared to other cell types. Interestingly, the number and properties of MRCs are distinctly different between juvenile freshwater parr and smolts (See Figure 2) with smoltification stimulating an increase in MRCs, and an increase in NKA activity (McCormick et al., 1995; Zaugg & Wagner, 1973). The increase in NKA activity is believed to be linked to the regulation of the NKA subunits. The NKA enzyme are made up by 3 sub-units (Alpha, Beta and Gamma) each with their own isoforms. During smoltification expression of the isoform NKA alpha 1b sub-unit increases, suggesting that this isoform is, at least in part, responsible for delivery of sea-water gill phenotype (McCormick et al., 2013; Nilsen et al., 2007).

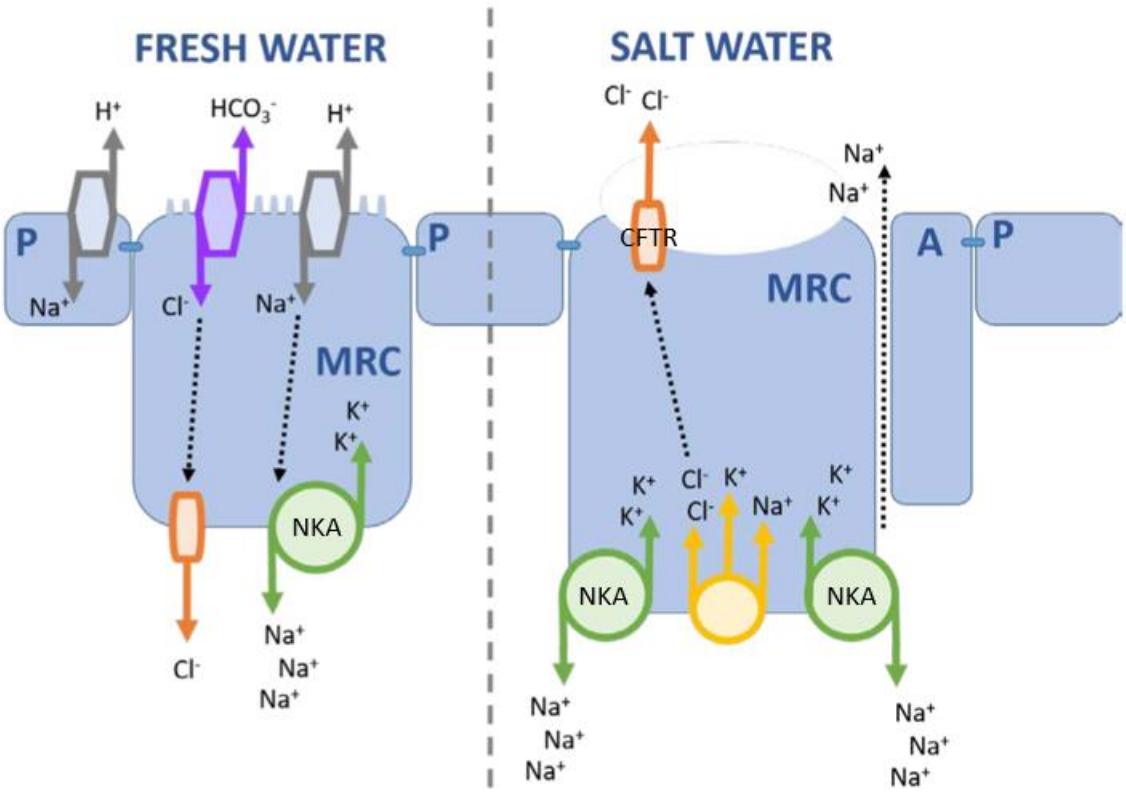

***Figure 2**: Simple illustration of a salmon mitochondrion rich cell (MRC) in freshwater and in saltwater, respectively. A: accessory cells. P: Pavement cell. **In freshwater**: the MRC actively take up sodium and chloride ions by exchanging them for HCO_3^- and H^+, both products from the reaction between CO_2 and water. The junction between Pavement cells and MRCs are tight to prevent ion leakage. **In Saltwater**: Chloride ions are secreted into the outside environment by the transporter protein CFTR. The MRCs are seen in complexes with other MRCs, and another cell type called accessory cells. The junctions between the cells are loosely linked to promote sodium leakage. The Figure are from Iversen (2020) PhD. Thesis Figure 4.*

1.3 Coordination of smoltification

Smoltification is coordinated by change in day-length (photoperiod), which indicates the change in season (Stefansson et al., 2008). The silvering of the salmon during smoltification, decrease in condition factor, NKA activity increase and MRC development, all seem to be under hormonal control, where environmental cues (light) are transduced through neuroendocrine output (Björnsson et al., 2011; Stefansson et al., 2008). Both growth hormone (GH) and cortisol increase during smoltification (Young et al., 1989). Plasma GH and cortisol respond to increased daylength, with concomitant NKA activity (McCormick et al., 1995) and implantation of slow-release cortisol and GH pellets stimulate hypo-osmoregulatory activity in Atlantic salmon (Bisbal & Specker, 1991; Boeuf et al., 1994).

Increased cortisol levels and GH levels are therefore believed to play a fundamental role in the salmons' hypo-osmoregulatory capability (Bisbal & Specker, 1991; Boeuf et al., 1994).

Thyroid hormone is another important hormone which is believed to been implicated in the seasonal smoltification physiology (Dickhoff et al., 1978). In mammals and birds, seasonal changes in reproductive physiology are mediated by localized regulation of active levels of thyroid hormone (T3) by the enzyme deiodinase (coded by the *dio2* gene) hypothalamus. (Dardente et al., 2014). Recent work suggests that thyroid hormone metabolism also plays an important role in seasonal smoltification in salmon (Lorgen et al., 2015). There are 2 paralogs of the *dio2* gene in the Atlantic salmon genome, *dio2a* and *dio2b*. Interestingly, each *dio2* paralogue plays a specific role during smoltification. *Dio2b* expression is induced in the brain by photoperiod during the smoltification process, while *dio2a* is activated in the gill when the salmon is exposed to seawater (Lorgen et al., 2015). This indicates that the salmon have both a preparative and an activation stage of smoltification which are both locally dependent on T3.

Recent transcriptomic studies of the gill have identified many novel genes whose expression changes during smoltification (Houde et al., 2019; Iversen et al., 2020). We can distinguish between genes whose expression are directly responsive to a long photoperiod, such as *NKA* and *CFTR 1*, and genes whose expression are dependent on a short winter photoperiod, such as the *S100A* calcium binding gene and Calpain 2 (*CAPN2*) gene (Iversen et al., 2020). The regulation of *CAPN2* and *S100A* genes coordinates with the induction of *Dio2b* in the gill suggesting that their regulation may be coordinated by thyroid hormone metabolism

1.4 New directions in smoltification research

Smoltification is an extensive research area within salmon biology, however, little attention has been given the interrelationships between the extensive change of salmon physiology during smoltification and its relationship to the immune system. In aquaculture, smoltification is associated with increased disease incidence, especially in the seawater transfer phase (Garseth et al., 2021), where gene expression studies of several salmon tissues, including the gill, head kidney and intestine, have shown that there is a downregulation of several immune genes during smoltification (Johansson et al., 2016). In addition, the salmon immune response seems to be reduced just after seawater transfer (Moore et al., 2018; Nuñez-Ortiz et al., 2018).

Complementing these studies a single-nuclei RNA-seq study of the gill revealed that immune gene suppression during smoltification may be a consequence of immune cell depletion (West et al., 2021). These data suggests that the gill develops into a weakened immune state during smoltification.

1.5 The salmon immune system

Like other vertebrates, the salmon immune system is composed of an innate immune system, which provides immediate protection against infection, and an adaptive system (or acquired) which has a delayed response, but can provide a more specialized defence (Abbas et al., 2016; Jørgensen, 2014; Mutoloki et al., 2014).

The innate immune system of vertebrates depends on different phagocytes that engulf and destroy the pathogen such as macrophages and dendrites (Jørgensen, 2014). The innate immune response can directly recognise pathogens through common structures through pathogen recognition receptors. One of these receptors is the Toll like receptor 3 (TLR3) which can recognise nucleic acids, both double stranded and single stranded RNAs (Jørgensen, 2014). The adaptive immune response on the other hand depends on T and B lymphocytes, and antigen presenting Major histocompatibility molecules (MHC), where T-cells, together with MHC, are responsible for the cellular response, and the B cells are responsible for the humoral response, secreting antibodies (Abbas et al., 2016). Unlike the innate immune system who can act immediately upon antigen recognition, adaptive immunity require expansion and differentiation of T and B lymphocytes in response to antigens (Abbas et al., 2016).

There are two major classes of MHC molecules: MHC class I (MHCI) and MHC class II (MHCII). MHCI present antigens to CD8 positive T-cells, who upon recognition induce cell apoptosis of the infected cell. MHCII on the other hand, present antigens to CD4 positive cells, also known as T-helper cells, who upon antigen recognition become effector cells, who coordinate the activity of other immune cells through cytokine release (Abbas et al., 2016). All nucleated cells express MHCI on the surface of their cell membrane. Hence, when a cell is infected it will display the antigen in form of a peptide, which act as a marker for Cd8 positive T cells to kill them (Abbas et al., 2016). MHCII on the other hand, are only presented by professional antigen presenting cells, such as dendrites. The dendrite engulfs the pathogen

and presents them to T-cells, upon recognition the T-cell will be activated and the adaptive immune response sets in (Abbas et al., 2016).

When a virus infects a host cell, the cell secretes an immune signalling molecule, called a cytokine, which warns other uninfected cells (Abbas et al., 2016). The main anti-viral cytokine is called Interferon alpha (IFN alpha) and are an important part of the innate immune response. IFN alpha causes other non-infected cells to produce, among other things, antiviral peptides which inhibit viral replication. IFN alpha are also secreted by dendritic cells upon recognition of general markers for viruses, such as double stranded RNA, through binding of TLRs (Abbas et al., 2016). Atlantic salmon possess several IFNs including IFN alpha (Robertsen, 2018).

1.5.1 Salmon immune organs

Although, teleosts share many of the same primary and secondary immune organs as mammals, the groups lacks both bone marrow and lymph nodes (Jørgensen, 2014). In mammals, leukocytes are produced in the bone marrow (Abbas et al., 2016), but in teleost (such as the salmon) the head kidney is believed to be the main site of leukocyte production, thus serving as a primary lymphoid organ (Zapata, 1979). In mammals T cells develop in the thymus, and it is assumed that it has the same function in teleosts (Mutoloki et al., 2014). Lymph nodes in mammals function as a key secondary lymphoid organ, that together with the spleen are the main sites for B- and T-cell activation (Abbas et al., 2016). Even though the salmon don't have lymph nodes, it has a spleen, where antigens are presented to T lymphocytes to generate an adaptive immune response (Flajnik, 2018).

The gill mucosal membrane forms a barrier between the fish and the external milieu. The thin epithelium which is only a few cells thick, may aid in respiratory needs but there is also an entry pathway for pathogens (Koppang et al., 2015). Since the salmon is always in direct contact with its water environment it is constantly surrounded by different pathogens. Therefore, it is not surprising that the salmon (and other fish) have evolved a counter measure to protect themselves from possible infections. There have been reported organized lymphoid tissue within the gill, known as Gill Associated lymphoid tissue (GIALT), where transcriptome analysis has both characterized CD8 positive T-cells and CD4 positive T-cells, which play a big role in the adaptive immunity (Haugarvoll et al., 2008; Koppang et al., 2015;

Rességuier et al., 2020). Because of this it is believed that the gill plays a large role in the salmons' first line of defence against antigens and are an important site for immune system reactions (Haugarvoll et al., 2008; Koppang et al., 2015; Rességuier et al., 2020).

1.5.2 Immunosuppressed phenotype and the aquaculture environment

As the salmon migrates into its new marine environment it is subjected to a number of different pathogens which may be harmful for the salmon. Therefore, the observed down regulation of the immune system makes little sense. This raises the question why the salmon would supress their immune system? It is, however, worth emphasising that immune reduction results have only been observed in an aquaculture setting and it is not known if this immunosuppressed phenotype during smoltification occurs in the wild. It is therefore difficult to say if the immune downregulation observed point toward an adaptive response to avoid overstimulation of the immune system as the salmon migrates to the sea, or if it is a consequence of the artificial smolt production in the aquaculture environment.

As described in section 1.3 Coordination of smoltification, the different smoltification processes are coordinated by change in photoperiod (Sigholt et al., 1995; Strand et al., 2018). In nature the change in photoperiod occurs gradually, giving the salmon a daily input of different light conditions. In contrast, aquaculture commonly transfer the salmon from winter photoperiod directly into constant light. Although constant light stimulates the highest growth rates of salmon development (Kråkenes et al., 1991), unknown is whether there are any other side effects of salmon physiology. Constant light provides with summer photoperiod signals, however, it does not provide the salmon with time-of-day information. In mammals, light dark schedules are essential for the entrainment of the circadian system (see details below) and disruption of this system is linked to a wide variety of pathologies and disease progression (Logan & McClung, 2019; Xie et al., 2019). At present, little is known about what consequences circadian disruption through constant light exposure has on salmon physiology.

1.6 Circadian rhythms

The earth's rotation around its own axis and orbital movement around the sun underpins the stable daily and annual light environment. This rhythmic change in the environment have caused many organisms on earth to develop an inner time-keeping system, making them able

to anticipate the daily changes in their environment and coordinate different activities at certain times of the 24 -hour daily cycle (Koronowski & Sassone-Corsi, 2021). This 24-hour rhythm in physiological and behavioural outputs are called circadian rhythms. The circadian rhythm is based on a cell autonomous molecular oscillator called the circadian clock, which causes a rhythm of ~24 hours. The core of this clock is based on a transcriptional translational feedback loop of what we call clock genes, which again regulate the temporal expression of thousands of other genes (Koronowski & Sassone-Corsi, 2021).

The most instructive way to view the circadian system is by the aid of the "Eskinogram" model, developed by Arnold Eskin (See Figure 3). This system consists of an input pathway, where an external factor, such as light, gives input to the clock, an oscillator which consists of the temporal expression of the clock genes, and the output consisting of clock regulated events, such as a 24-hour rhythm in activity.

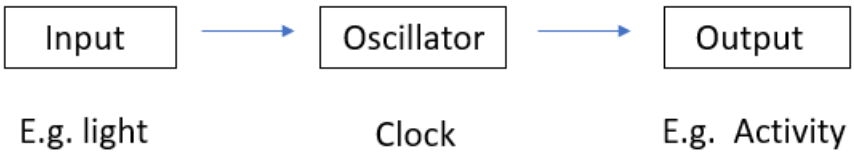

***Figure 3**: Eskinogram showing the circadian clock system.*

Since this endogenous rhythm is only approximately 24-hours, the circadian clock responsible for this rhythm needs to be synchronized to the external environment, in a process called entrainment. The most common environmental cue used for entrainment, called a zeitgeber, is the light/dark cycle caused by the earth's rotation. If the subject is put in constant conditions, e.g., in constant darkness (DD), the circadian rhythm will start to "free-run", and the rhythm will follow the endogenous rhythm of the molecular circadian clock (Koronowski & Sassone-Corsi, 2021).

How an organism entrains to light, depend on the species. In mammals, light is detected through photoreceptors in the eyes (Nelson & Zucker, 1981). Because not all cells have photoreceptors and are able to entrain directly to light, timing between peripheral tissue clocks must be coordinated internally. This is conducted by a master pacemaker located in the hypothalamus, called the suprachiasmatic nucleus (SCN) (Yoo et al., 2004). Little is known about the input pathway of Atlantic salmon, but in other fish species such as zebrafish, photoreceptors are expressed in every tissue type studied, and even peripheral tissues are able

to entrain directly to light *in vitro* (Whitmore et al., 2000). Zebrafish clock genes are shown to be directly responsive to light exposure, where light sensitivity is time of day dependent (Tamai et al., 2007).

Salmonid genetics are less well characterized compared to model mammals like mice, and complicated by four whole genome duplication events (Allendorf & Thorgaard, 1984). This means that the salmon have multiple copies of ancestral genes. For example, the 18 clock genes reported in mice, have ended up with 61 counterparts in the Atlantic salmon (West et al., 2020). Examination of the Atlantic salmon molecular clock shows that brain tissue has strong circadian oscillations (Bolton et al., 2021; West et al., 2020). For other tissues such as the gill, however, it has been reported to have both big variation between tissues, and inter-individual variation (West et al., 2020). This suggests that clock genes in different tissues are regulated differently from each other. Indeed, evidence suggests that many of the clock genes have diversified and taken on non-circadian functions (West et al., 2020).

At present, little is known about how the circadian output of salmonids are coordinated. One study conducted on pink salmon (*Oncorhynchus gorbuscha)* reported big inter-individual variation in activity patterns under constant conditions (LL), where half of the salmon showed a free-running rhythm and the other half were arrhythmic (Godin, 1981). One study conducted on Atlantic Salmon parr demonstrated a diel periodicity of locomotor activity under an artificial LD cycle (Varanelli & Mccleave, 1974).

The Atlantic salmon has also shown to have a diurnal change in heart rate under and LD cycle (Hvas et al., 2020; Svendsen et al., 2021; Zrini & Gamperl, 2021), which can clearly be seen in Figure 4. In the Svendsen et al. (2021) study it was shown that locomotor activity and heart rate are often closely linked, but sometimes this this is not always the case. Even though the salmon has a diurnal change in heart rate, little is known about how it is affected by constant light.

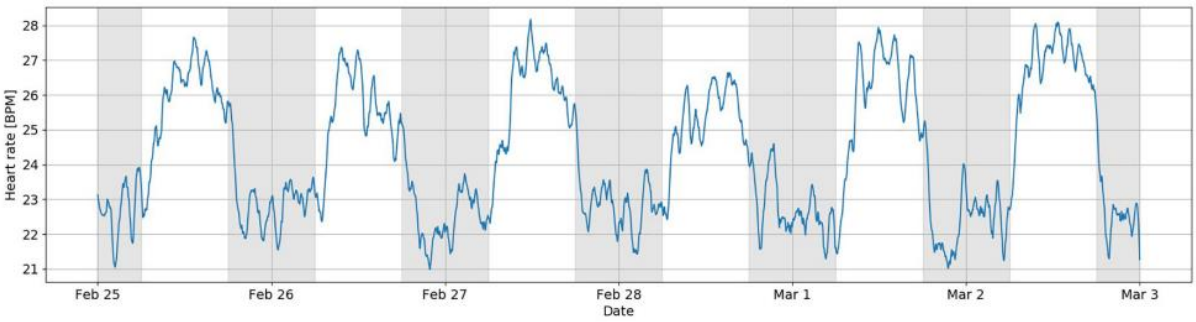

***Figure 4**: Figure from Svendsen et al. (2021) results section, where the X axis are given days and the Y axis is the average heart rate in beats per minute (BPM). The grey boxes are the average heart rate during nighttime and the white area are the average heart rate during the day.*

1.6.1 The circadian immune response

The immune system of mammals follows a circadian rhythm, with a change in both immune cell concertation and type of immune cells circulating in the blood at certain times of the day (Scheiermann et al., 2018). It has also been shown that disruption of the circadian clock by exposure to constant light has a negative effect on the immune response (Mizutani et al., 2017; Valdés-Tovar et al., 2015). Complementary studies on fish have linked the immune response to photoperiod and clock genes (Whiting et al., 2020) and there appears to be a link between light conditions and the innate immune response in zebrafish larvae, were larvae with bacterial infections had a higher bacterial clearance and chance of survival when infected during the light phase of the light/dark cycle and under constant light, compared to the dark phase (Du et al., 2017). There has also been suggested that constant light has a negative effect in parasitic lice clearance in rainbow trout (*Oncorhynchus mykiss*), and that constant light alter the expression of clock genes (Ellison et al., 2021). There are also data that suggest that the rainbow trout have a time-of-day immune cell response (Montero et al., 2019). However, to date, there has not been any studies linking the Atlantic salmon's immune system to the circadian clock, and there is little to no knowledge on how different light conditions affect the immune response. This is a significant knowledge gap.

1.7 Significance and purpose

Every year the aquaculture industry experience huge losses of Atlantic salmon. According to the Norwegian fish health report from 2021, over 50 million salmon is lost in the seawater phase in Norway alone, many due to disease. Aquaculture research shows that smoltification supresses immune gene expression in multiple tissues. However, the causative factors that generate this phenotype are not understood.

Aquaculture routinely exposes fish to constant light to stimulate smolt production. Drawing from comparative data in mammals, we hypothesise that constant light compromises the immune capacity by disturbing circadian organization.

Objective: To test the impact of circadian entrainment/disruption on the immune system during smoltification of Atlantic salmon, by comparing constant light (LL) and a light/dark cycle long photoperiod (LD). To address this aim we ask three specific questions:

- Does the use of LL and LD deliver different immune phenotypes in a smoltification protocol?
- Do salmon kept under LL have a weaker immune response compared to LD housed salmon?
- Do head kidney leukocytes have different immune responses when collected from LL and LD salmon from different times of day?

As an ancillary question we will also seek to better understand the outputs of the circadian clock by measuring heart rate, both under LD and under LL.

By fulfilling these aims we hope to give a better understanding of the link between the Atlantic salmons' circadian physiology and immune function. These data will improve our understanding of the impact of the aquaculture environment, in particular its effect on salmon welfare.

2 Material and methods

Atlantic salmon (*Salmo salar*) was used as the experimental animal in all *in vivo* experiments. All fish were hatched and kept at Havbruksstasjonen in Tromsø, Kårvik. The salmon were fed continually with normal pellet salmon feed (Skretting, Stavanger, Norway) through all experiments. The fish were always fasted 24 hours before being handled. Before any tissue and blood collections, the salmon was overdosed with benzocaine 120 ppm per 10 L. We waited until ventilation and operculum movement had stopped, and the fish gave no response to stimuli. This was done for all experiments.

2.1 SAV3 Experiment

The experiment was approved by the Norwegian food safety authority (Mattilsynet FOTS 27998) in the fall of 2021. The salmon parr hatched at havbruksstasjonen was put through photoperiod mediated smoltification after reaching an average size of 26,37 g, SD= 4,12.

The salmon were kept in 100 L freshwater circular tanks with circumferential waterflow and a natural temperature. The salmon started out under a LL photoperiod and was then exposed to a winter photoperiod (6h L: 18h D, lights on at 08:00 and off at 14:00) for six weeks (See Figure 5). The salmon cohort was then divided into two groups. Group 1 went through 6 weeks of constant light, and Group 2 went through 6 weeks of long photoperiod (18h L:6h D, lights on 20:30 and off 14:30). The water temperature was maintained at 10°C.

Gill, spleen, and head kidney tissue samples were collected at different timepoints (T1-T3, See Figure 5). 16 salmon were seawater challenged for each timepoint, 24 hours prior to collection.

2.1.1 SAV3 Immune Challenge

After 6 weeks of winter photoperiod, and 6 weeks of long photoperiod (LD) or LL, 192 salmon from the cohort were transferred to 8 circular seawater tanks with 24 fish in each tank. Four of the tanks contained Group 1 (LL smoltified fish) and the other 4 contained Group 2 (LD smoltified fish). Group 1 and Group 2 were kept at different rooms, still under their designated photoperiods (See Figure 6).

On experimental day 60, the salmon groups were then put through an immune challenge. 2 of 4 tanks in both groups were infected with $1x10^5$/100 µl Salmonid alphavirus subtype 3

(SAV3). The other 2 tanks were injected with 100 µl PBS for control (See Figure 6). The injection was administered on the midline, ~1 pelvic fin length in front of the pelvic fin. 12 of the fish in each tank were infected at ~17:30, during the mid-dark phase of Group 2 (LD smoltified group). The fish infected at 17.30 were marked with a tattoo. The other 12 untattooed fish in each tank were infected at 05:30, at the mid-light phase (See Figure 6).

SAV3 (PDV-H10-PA3) was provided by Professor Øystein Evensen, Norwegian University of life Sciences. The virus was incubated in CHH-1 cells in L15 + 5% FBS at 15°C and titrated as described in (Strandskog et al., 2011) according to the $TCID_{50}$ method (Reed & Muench, 1938).

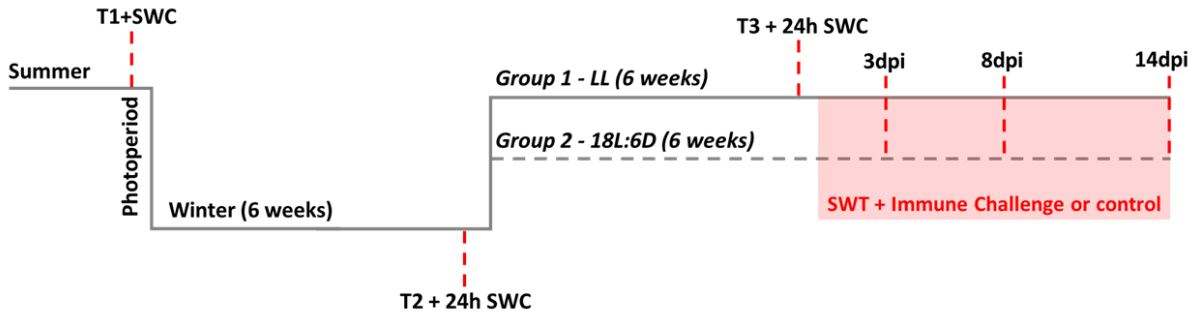

***Figure 5**: SAV3 experimental setup. T1-T3= timepoints of collection. SWC= seawater challenge. 3dpi = 3 days past infection, 8dpi=8days past infection, 14 dpi= 14 days past infection*

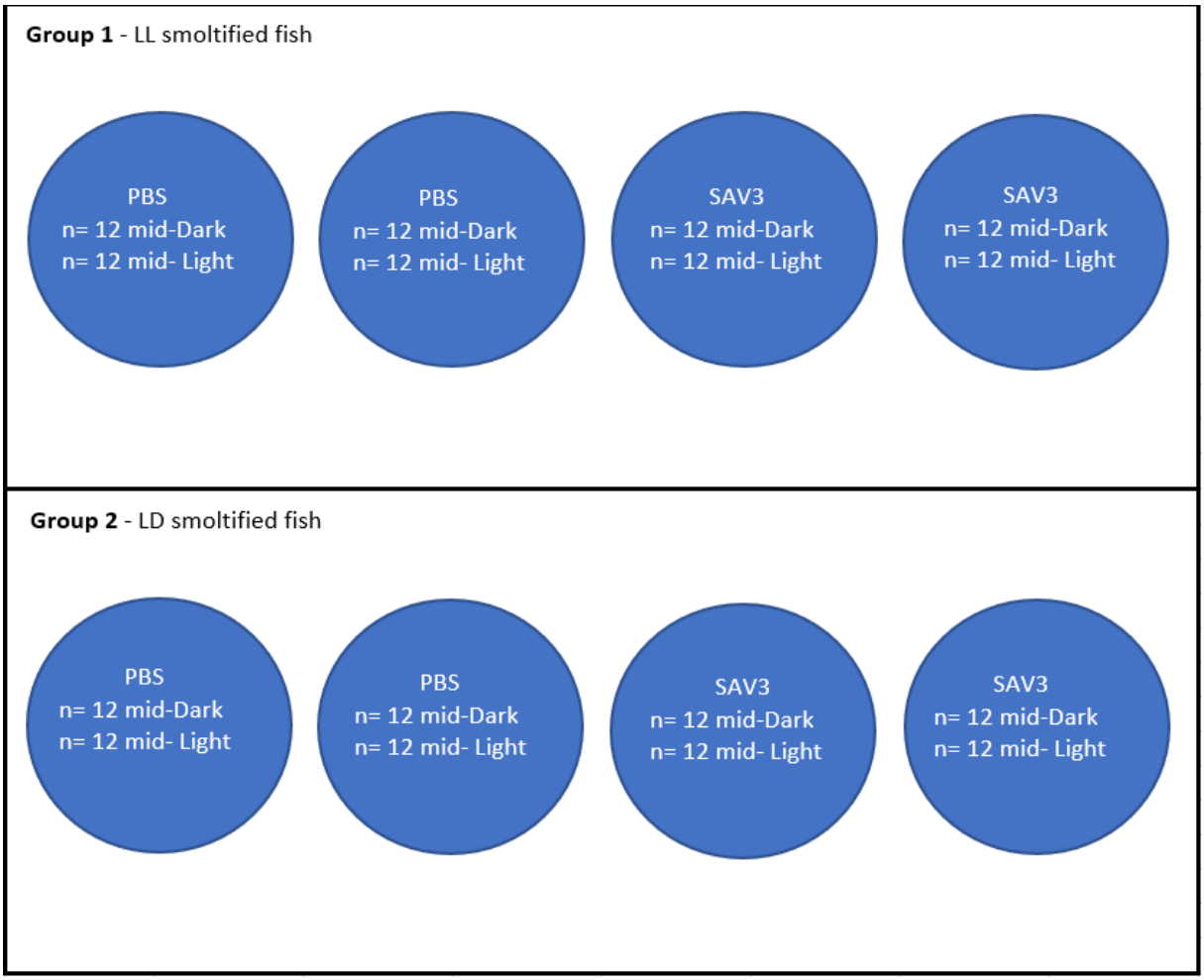

***Figure 6**: overview of infected fish.*

2.1.2 Tissue Collections

The sampling timepoints T1-T3 was conducted on experimental day 1, 42 and 63 respectively. Samples were collected from 16 salmon per group, including 24-hour seawater challenged salmon.

Blood samples were taken from the caudal vein using BD heparin vacutainers (Ref: 368494) and complement needles (27 gauge). The blood samples were stored on ice until centrifuged at 400xg for 10 min. Then 50-200 µl of plasma was transferred to a 1,5 ml Eppendorf microtube and stored at -80°C until further analyzed. Using a tweezer, a gill filament sample was taken and put in a 1,5 ml Eppendorf microtube containing 100 µl of SEI buffer (See table 1). Two gill arches were cut off from each fish. The gill tissue was cut from the arch and put into a 1,5 ml Eppendorf microtube. The fish were then cut open and spleen and head kidney

tissue samples were taken. All tubes containing a tissue sample were immediately snap-frozen on dry ice. All the samples were then stored at -80°C.

For the freshwater fish, gill, spleen, and head kidney histology samples were also taken. The histology samples were fixated in vials containing 10% Natural Buffered Formaldehyde (NBF). After ~24 h the NBF was removed, and the samples were washed with phosphate buffer. The samples were then stored in phosphate buffer at 5°C.

The SAV3 immune challenge collections was conducted 3 days past infection, 8 days past infection and 14 days past infection. Samples were collected from 8 fish from each tank, 4 tattooed and 4 untattooed. Gill, spleen, liver, heart, head kidney and pancreas tissues were collected in 1,5 Eppendorf microtubes and snap-frozen on dry ice. The pancreas is not a distinct organ in fish, but a layer in close contact with the pyloric ceca, therefore a section of the pyloric ceca was taken. Histology samples from the pancreas (section of pyloric ceca) was also taken from 4 fish from each tank. The histology samples were handled with the same procedure as before.

Table 1: *Solutions used during collections*:

SEI buffer:	
26,67 g sucrose	(Cas nr. 57-50-1)
1,86 g Na_2EDTA	(Cas nr. 6381-92-6)
1,7 g imidazole	(Cas nr. 288-32-4)

Diluted in 475 ml distillated water (dH_2O).

pH adjusted to 7,3 with HCl (hydrochloric acid).

Solution adjusted to 500 ml with dH_2O and stored in 4°C until used.

10%NBF:

100 ml formalin (37-40% stock solution)

900 ml dH_2O

4 g/L NaH_2PO_4 (monobasic)

6.5 g/L Na_2HPO_4 (dibasic / anhydrous)

NBF without formalin/phosphate buffer:

900 ml dH_2O

4 g/L NaH_2PO_4 (monobasic)

6.5 g/L Na_2HPO_4 (dibasic / anhydrous)

2.2 Condition factor

Condition factor from the fork length and weight (g) were calculated using the formula:

Equation 4

$$Condition\ factor = Weight(g) \times \frac{100}{Fork\ lenght^3}$$

2.3 Osmolality

Osmolality of plasma samples (T1-T3) was conducted using the osmometer OSMOMAT® 030 GONOTEC. The osmometer was calibrated using 50 µl GONOTEC 850 calibration standard (Ref: 30.9.0850) and 50 µl dH_2O. 50 µl of each sample were measured in duplicate. For every ~10 sample dH_2O was measured to make sure the readings were correct. An average was taken for each sample and the data was plotted in GraphPad Prism version 9.0.0.

2.4 NKA assay and protein analysis

To test if the salmon had smoltified properly in both group 1 (LL) and group 2 (LD), the change in enzymatic activity of Na^+,K^+-ATPase was measured. This was done by conducting an NKA assay and protein analysis of the gill filaments by the method of McCormick (1993).

Table 2: *Solutions used in NKA assay and protein analysis. All solutions were made the day before or the same day as the assays was performed*:

0,5% SEID:	
0,1 g Sodium deoxycholate	(Cas nr: 302-95-4)
Dissolved in 20 ml SEI-buffer	
Kept in 4°C until used	
Imidazol buffer (IB-buffer)	
3,404 g Imidazol	(Cas nr: 288-32-4)
Dissolved in 950 ml dH2O	
pH adjusted to 7,5 using HCl	
Kept in 4°C until used.	

Salt solution:

5,52 g NaCl (Cas nr: 7647-14-5)

1,07 g $MgCl_2$ x $6H_2O$ (Cas nr: 7791-18-6)

1,57 g KCL (Cas nr: 7791-18-6)

Dissolved in 500 ml Imidazol.

Kept at 4°C until used

PEP:

0,491g Phosphoenolpyruvate (Cas nr: 5541-93-5)

Dissolved in 500 ml Imidazol then divided in 10 ml tubes.

Kept at -80 °C until used.

Ouabain:

0,382 g Ouabain (Cas nr: 11018-89-6)

Dissolved in 50 ml imidazole buffer in boiling water bath, inside fume hood, while stirring.
Kept at 4 °C in darkness until used.

Na Acetate buffer:

0,767 g Na Acetate trihydrate (Cas nr: 6131-90-4)

Dissolved in 100ml dH_2O.pH adjusted to 6,8.

ADP standard:

0,0489 g ADP (Cas nr: 20398-34-9)

Dissolved in 25 ml NA-Acetate buffer. Solution divided in 300 µl Eppendorf microtubes.
Kept at -80 °C util used.

AM medium (Na^+K^+ ATPase Assay mixture for 4 plates)

40 ml start volume IB

48 µl Pyruvate Kinase (SKU: P1506-5KU)

62 µl Lactic dehydrogenase (LDH) (SKU: L2500-5KU)

10 mg NADH (SKU: N9410-15VL)

10 ml Phosphoenolpyruvate (PEP)

0,0290 g ATP

Volume adjusted to 70 ml with IB.

The AM Medium was made in a beaker on ice. First the start volume of IB was added. Pyruvate Kinase and LDH was transferred into Eppendorf tubes and centrifuged at 12000 rpm for 8 minutes. The supernatant was discarded, and the pellet was resuspended in IB before being added. NADH was dissolved in 2 ml of IB buffer before being added to the master mix. ATP was added and then the final solution was adjusted to 70 ml with IB.

The solutions AM and AM-O was made in 50 ml falcon tubes. The AM-O medium were to contain the enzyme inhibitor ouabain, which is light sensitive. Hence, the AM-O tube was coated with aluminium so no light could enter the tube. 35 ml of AM-medium and 2,5 ml of IB was added to the AM tube. 35 ml of AM-medium and 2,5 ml of ouabain was added to the AM-O tube. To make the ADP standard curve 4 different dilutions were made (See Table 3)

Table 3**:** *ADP dilutions for the standard curve*

nmole/10µl	IB (µl	ADP std (µl)
0	200	0
5	175	25
10	150	50
20	100	100

AM salt solution was made by adding 700 µl salt solution to 2,1 ml AM. 10 µl of each standard were put in triplicate on a 96-well microplate. Then 200 µl AM salt solution was added into each well. Then the plate was read (See 2.4.1 Na+, K+ - ATPase activity).

The gill filaments in SEI buffer (T1-T3, see tissue collections), was thawed on ice. 25 µl SEID buffer was added to each tube. The tissue samples were then homogenized with a pellet pestle motor. The samples were centrifuged at 3800 rpm in 30 seconds in a cooling centrifuge.

10 µl of each sample was added to the wells in quintuplicate (See Figure 7). Then 2,7 ml salt solution was added to 8,1 ml AM and 8,1 ml AM-O. 200 µl of AM with the salt solution was added in the AM marked area (See Figure 7), and the same was done for the AM-O.

AM	AM	AMO	AMO	AM	AM	AMO	AMO	AM	AM	AMO	AMO
1	1	1	1	9	9	9	9	17	17	17	17
2	2	2	2	10	10	10	10	18	18	18	18
3	3	3	3	11	11	11	11	19	19	19	19
4	4	4	4	12	12	12	12	20	20	20	20
5	5	5	5	13	13	13	13	21	21	21	21
6	6	6	6	14	14	14	14	24	24	24	24
7	7	7	7	15	15	15	15	25	25	25	25
8	8	8	8	16	16	16	16	26	26	26	26

***Figure 7**: Illustration of ATPase analysis plate. The numbers illustrate sample names.*

For the protein analysis, the BCA Protein Assay Kit from PIERCE (Prod# 23227) was used. The samples used were the same as the ones used in the NKA assay. The samples were thawed on ice. Working solution was made by adding 20 ml of reagent A and 400 µl of reagent B into a new clean tube. Bicinchoninic acid (BCA) dilution standards were made in tubes marked with 0,5,10 and 20 (See Table 4). The tubes containing the samples were vortexed for ~20 seconds and centrifuged in a cooling centrifuge at 3800 rpm for 30 seconds. 10 µl of each BCA standard and 10 µl of each sample were added to a 96-well microplate in triplicate. 200 µl of work solution were added to each well with a multi-pipette. The lid was put on and the plate was covered in aluminum. The plate was incubated in darkness at 37°C for 60 minutes.

***Table 4**: BCA dilution standards*

Std (µg/10µl)	2mg/ml BSA std (µl)	dH_2O (µl)
0	0	100
5	25	75
10	50	50
20	100	0

2.4.1 Na+, K+ - ATPase activity

All plates were read by using the software SOFT MAX PRO. NKA assay plates were read at 25°C for ~10 minutes. BCA assay plates were read at 540 nm for 12 seconds. The data was

exported to Microsoft Excel (Office 365). The known concentrations (ADP nmole/10µl) were plotted against the mOD values to get the slope.

ATPase activity was found for each sample by taking the average of AM values minus the average of AM-O values (Vmax).

However, to find the accurate activity, we also needed the protein concentration of each sample, since inconsistency in sample size will affect the activity level reading. First the average of each triplicate BCA standard was calculated. These values were plotted against the OD values to get the slope and intercept for each concentration (0,5,10 and 20µg/µl). The average for each triplicate individual sample were calculated. Then protein concentration was calculated as follows.

Equation 1

$$Protein\ concentration = Protein\ concentration\ (avg.) - \frac{Protein\ assay\ intercept}{Protein\ assay\ slope}$$

Then ATPase activity per hour were calculated as follows:

Equation 2

$$Activity\ per\ well = \frac{Vmax}{NKA\ Slope}$$

Equation 3

$$Acitivity\ per\ min = \frac{Activity\ per\ well}{Protein\ concentration}$$

The activity per min was multiplied with 60 to get activity per hour.

2.5 Leukocyte Isolation

To test if the salmon had a circadian immune response, leukocytes from the salmon head kidney were isolated and put through an immune challenge at different times of day. Salmon head kidney tissue was collected from spare fish from the SAV-3 T1-T3 cohort. Tissue was collected over two days at four different timepoints, n=8 for each collection point from the

LD smoltified group Day 1, and n=6 each collection point from both LD smoltified fish and LL smoltified fish Day 2 (See Figure 18A). The different timepoints were ~ 12 hours apart.

2.5.1 Percoll gradient

The day prior the first collection 1,5 M NaCl was prepared in a 50 ml falcon tube. The NaCl used had a concentration of 58,44 g/mol. To get a concentration of 1,5 M:

58,44 g/mol x 1,5M = 87,66 g/l.

To get grams per 50 ml: (87,66 g/l :1000) x 50 = 4,383 g.

4,383 g NaCl was dissolved in 50 ml dH_2O. The solution was then 5000 U/ml filter sterilized. Cell culture media, transport media and Percoll gradient solutions were made the same day as the collection (See Table 5).

8 ml of 54% Percoll was added to a 50 ml falcon tube. 10 ml of 25% Percoll was carefully added on top to make gradient. We waited ~ 30 min before adding the homogenized tissue. Head kidney tissue was put in 10 ml of transport media and transported on ice. The tissue was homogenized by 100 mm pore size cell strainers. A syringe plunger was used to force the tissue through. The suspension was carefully put on the Percoll gradient. The Percoll gradient, know containing the cell suspension, was centrifuged for 40 min in a centrifuge at 400xg at 4°C. The top red layer was (containing unwanted cells) was removed with a suction pump. Cells were collected at interface (5 ml) and put into 10 ml transport media. The cell suspension was centrifuged at 400xg for 10 min. The supernatant was removed, and the pellet was resuspended in 2 ml culture media.

Table 5: *Solutions used in Percoll gradient.*

Culture media		
Gilco® L-15:	50 ml	(ThermoFisher, Ref: 11415064)
P/S (1%):	500 µl	
FBS (5%):	2,5 ml	
Transport media		
Gilco® L-15:	500 ml	(ThermoFisher, Ref: 11415064)
FBS (2%):	10 ml	
Heparin 5000U/ml:	2 ml	
P/S (1%):	5 ml	
90% Percoll (for 24 gradients)		
Cytiva Percoll™:	225 ml	(ThermoFisher, Ref: 45-001-747)
1,5 M NaCl:	25 ml	
Heparin (5000U/ml:	1 ml	
54% Percoll (for 24 gradients)		
90% Percoll:	118 ml	
Transport media:	82 ml	
25% Percoll (for 10 gradients)		
90% Percoll:	28 ml	
PBS:	72 ml	
Heparin:	288 µl	

2.5.2 Poly I:C infection

The cells were counted with the cell counting machine TC20 (BioRad). We seeded 2 x 10^6 cells in each well. One sample needed to fill 4 wells due to 4 different treatments (See Figure 8). Cell density was therefore adjusted to 8 x 10^6 in 4 ml culture media. The cells were incubated in 24-well cell culture plates, where 1 ml was put into each well. The cells were treated with 5 mg/ml Poly I: C. The cells were incubated in 20°C.

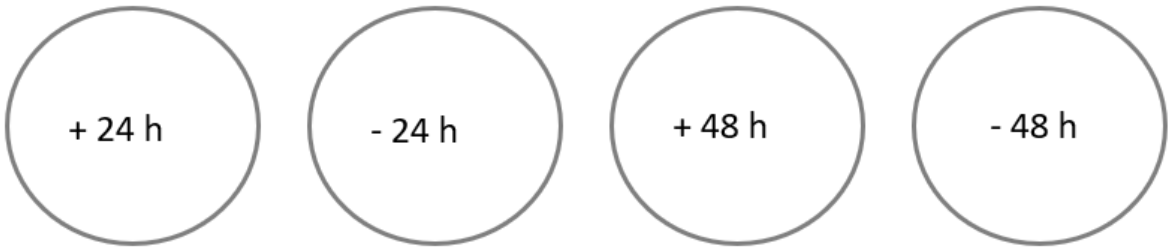

***Figure 8**: Illustration of leukocyte infection setup. + illustrate wells treated with 1 ml 5mg/ml Poly I:C and - wells illustrate the control group where 1 ml of culture media were added. 24 h is the wells containing cells collected after 24 hours incubation and 48 h is the cells collected after 48 hours incubation. This is a schematic setup, in reality the 24-hour cells and 48-hour cells were kept on different plates.*

2.5.3 Leukocyte collection

Leukocyte cell collection occurred 24 hours and 48 hours post infection. The media in the wells was collected and put into 2 ml microtubes and centrifuged at 10 000xg for 5 min at 4°C. Meanwhile 350 µl of RLT buffer (QIAgen) was added into the empty wells. The supernatant from the centrifuged tubes was discarded. The RLT in the wells was washed over the bottom well surface and then put into the tubes containing a pellet of cells. The cells were stored at -80°C.

2.6 RNA analysis

2.6.1 cDNA conversion

RNA was converted to cDNA by using Applied biosystems™ by Thermo Fisher Scientific High-capacity RNA-to-cDNA kit (Ref: 4387406). A master mix was made from 1 µl enzyme mix x number of samples, and 10 µl buffer x number of samples + 2 extra to not fall short while pipetting. The RNA quantity for each tissue sample was normalized to 2 µg, where nuclease free water volume was adjusted accordingly to make the total volume 9 µl. This was done by taking 2000 / RNA ng μl^{-1}. To get volume nuclease free water, the RNA volume (µl) was subtracted from 9 µl.

Since the leukocyte cells contained less RNA than the tissues, the RNA was normalized to 350,1 ng/ µl, which were one of the lowest values (38,9 ng/ µl x9 µl). The enzyme mix and buffer mix were vortexed and spun down before added to the master mix tube. 11 µl of master mix was added to each new sample tube of an 8 strip microtube, then RNA and nuclease free water were added according to the calculations above. See Table 6 for thermal cycling conditions. After the cDNA conversion the tissue cDNA was diluted in a 1:10 dilution by adding 180 µl nuclease free water. The leukocyte cell cDNA was diluted in a 1:2 dilution by adding 20 µl of nuclease free water, this was due to the lower concentration of RNA yield of the leukocyte cells.

***Table 6**: Thermal conditions for RNA to cDNA conversions*

Temperature	Time
37°C	60 min
97°C	5 min
4°C	Hold

2.6.1 RNA extraction

RNA was extracted from 8 of the 16 gill samples per group from the T1-T3 collections (See section 2.1.2 Tissue collections). The reason we did not use all the gill samples was because we wanted to fit all groups at one 96-well qPCR plate in duplicate.

From the SAV3 challenge tissue collections, we decided to extract RNA from one central immune tissue and one site of infection. Hence, we extracted RNA from head kidney tissue samples and heart samples from the mid light infected group (See section 2.1.1 SAV3 Immune Challenge). We extracted RNA only from the mid light infected group to reduce workload, and because we mainly wanted to see if there would be a difference between the immune response between the LL and LD smoltified fish.

For the leukocyte cells, we extracted and analysed data from the LD1 -LD4 48-hour, and the LL1 and LL2 48-hour groups (See Figure 18A). This was to reduce workload due to time limitations

RNA was extracted from gill, head kidney tissues and leukocyte cells by using Qiagen RNeasy® plus mini kit (Ref:74134) following manufactures handbook. RNA from hearts were extracted using Qiagen RNeasy® Universal mini kit, since the RNeasy® plus mini kit column filters clogged and did not yield any usable RNA. All RNA concentrations, including quality, was checked by using the software NanoDrop™ 2000/2000c.

Tissue was homogenized using Tissue Lyser II. Leukocyte cells were homogenized by using Qiagen QIA shredder (Ref: 79654).

2.7 qPCR primers

The primers for the genes *EF1-alpha* (b), *NKA a1b(ii)*, *CFTR1*, *S100A1* and *CAPN2* was the same as used in the Iversen et al. (2020) paper. The *EF1-alpha* (c), *EF1-alpha* (d), *UBA*, *MHCII*, *nsP1* and *IFN alpha 1* sequences was provided by dr. Eva-Stina Isabella Edholm.

***Table 7**: Primers used for qPCR.*

Gene target		Gene ID	Sequences 5' to 3'	Annealing Temp (°C)
EF1-alpha	F	LOC100136525	TCATCATGACTTCTGTGGAG	61
	R		CTTTATCAGGACAGGTCAATG	
EF1-alpha (b)	F	LOC100136525	AGGCTGCTGAGATGGGTAAG	63
	R		AGCAACGATAAGCACAGCAC	
EF1-alpha (c)	F	AF321836	CCCCTCCAGGACGTTTACAAA	60
	R		CACACGGCCCACAGGTACA	
EF1-alpha (d)	F	BG933897	TGCCCCTCCAGGATGTCTAC	60
	R		CACACGGCCCACAGGTACTG	
Cd3e	F	LOC100136516	TCATCATGACTTCTGTGGAG	59
	R		CTTTATCAGGACAGGTCAATG	
CSF1R	F	LOC106611874	TGGACACCAAATTCTACAAG	59
	R		ATCGTATACATCTCTGGAGG	
IL10rb	F	LOC106575150	AAAGATCTCATCGCTGAAAG	61
	R		TCTCAAACACATCCTTCTTG	
NKA a1b (ii)	F	LOC106575572	GGGTGTGGGCATCATTTCTG	65
	R		CATCCAACTGTTCGGCTGAC	
CAPN2	F	LOC106589985	GTTGAGGAGATCGTGGTGGA	65
	R		TGTTCAGAATCCTCCGCAGT	
CFTR1	F	LOC 100136364	CCTTCTCCAATATGGTTGAAGAGGCAAG	63
	R		GCACTTGGATGAGTCAGCAG	
S100A1	F	LOC 106570104	GGATGACCTGATGACGATGC	65
	R		ATCACATACTCCCCACCAGG	
UBA	F	AF504019.1	GACAGTGACACAGCTCAGAAT	60
	R		CATCAGAGTGCTCTTCCCATAG	
nsP1	F	AY604235	AGTTCCAGACTGCGTTTCC	60
	R		GGTAGCCAAGTGGGAGAAAG	
MHC II	F	EF451156.1	GTGGAGCACATCAGCCTCACT	60
	R		GACGCACCGATGGCTATCTTA	
IFN *alpha* 1	F	XM_014187640.1	CCTTTCCCTGCTGGACCA	60
	R		TGTCTGTAAAGGGATGTTGGGAAAA	

2.8 Primer design

The primers for the immune target genes *Cd3e, CSF1R, Il10rb* and reference gene *EF1-alpha* was found by taking the cDNA from the gene databank Salmobase (https://salmobase.org/) using the gene IDs (See Table 7). The cDNA was copied into the software A plasmid Editor version 3.0.4 (ApE). The exons were marked, and the cDNA sequences were put into the software Primer3 (https://primer3.ut.ee/) to find optimal primers for each gene. The primers were set to be 18-25 bp long, so they would be unique in the genome. To avoid contaminating DNA the primers picked were set to read across exon junctions. In Primer3 the amplification size was set to be 75-200 bp and the annealing temperature to be 60°C, max N was set to be 3 and GC% was 40% to 60% respectively. Number to return 500. To double check for optimal annealing temperature, Promega (https://no.promega.com/resources/tools/biomath/tm-calculator/) was used and the temperature in Primer3 adjusted accordingly. Primers ending with C and G were preferred since they have 3 hydrogen bonds and therefore are more stable.

Since the Atlantic salmon has been through multiple genome duplication events (Allendorf & Thorgaard, 1984) we needed to know if the primers sequences were unique in the genome. This was done by searching for the primer sequences in the Atlantic salmon genome using the Blast databank (https://www.ensembl.org/Salmo_salar/Tools/Blast?tl=ZQXlomiTiPwnqhTk-7620399).

2.9 Primer efficiency

To test primer efficiency, 6 different dilutions were made from salmon gill cDNA (See Table 8). qPCR was performed by using the Promega GoTaq® qPCR kit (Ref: A6001). A master mix for each primer pair was made (see Table 9). 19 µl of master mix was put into the wells of a 96-well qPCR plate and 1µl of the dilution templates were added in duplicate. The qPCR was performed using Bio-Rad CFX manager 3.1 in a 3-step manner where the thermal cycling conditions varied with annealing temperature of the primers (See table 7). The general thermal cycling condition were: denaturation of DNA for 2 minutes of 95°C followed by 40 cycles of 15 seconds 95°C, 15 seconds of annealing temperature and 1 minute extension at 60°C.

The Ct values were exported to Microsoft Excel (Office 365) where they were plotted against the LOG of the dilution concentrations. The slope was then calculated for each of the primer

pairs and put into the ThermoFisher Scientific qPCR efficiency calculator (https://www.thermofisher.com/no/en/home/brands/thermo-scientific/molecular-biology/molecular-biology-learning-center/molecular-biology-resource-library/thermo-scientific-web-tools/qpcr-efficiency-calculator.html) . Only primers with a higher efficiency than 90% where used.

***Table 8**: Dilution concentrations of cDNA*

Dilution	cDNA concentration
1	100 %
2	50 %
3	25 %
4	12.5 %
5	6.25 %
6	3.125 %

***Table 9**: Master mix for qPCR x1 and x13 wells. Used x13 and not x12 to not fall short due to inaccuracy pipetting.*

Master mix	x1	x13
GoTaq®	10µl	130µl
Primer F	1µl	13µl
Primer R	1µl	13µl
CXR (reference dye)	0.2µl	2.6µl
H2O (Nuclease free)	6.8µl	88.4µl

2.10 Primer specificity

The primer pairs for the immune genes *Cd3e*, *CSFR1*, *IL10rb* and the reference gene *Ef1-alpha* were validated for target specificity. The primer pair sequence products were therefore cloned and sequenced (See Figure 14). The other primer pairs in Table 7 had already been validated beforehand of the study.

2.10.1 PCR

The primers were amplified by PCR. 10 µl of GoTaq® (Promega, Ref: A6001), 7 µl of nuclease free water, 1 µl of salmon gill cDNA template, 1 µl primer forward and 1 µl primer reverse were put into a PCR tube for each of the primer pairs. The thermal cycling conditions were as follows: denaturation of DNA for 2 minutes at 95°C followed by 40 cycles of 10 seconds at 95°C, 10 seconds annealing at 59°C and 1 minute extension at 60°C.

2.10.2 Ligation – Plasmid integration

The cloning kit Zero Blunt® TOPO® PCR (ThermoFisher, Ref: 450245) was used for ligation. 1 µl of 12M NaCl, 1µl PCR blunt and 4 µl PCR product was added into 8 strip PCR tubes, one primer pair per tube. The tubes were left in room temperature for 5 minutes and then put on ice.

2.10.3 Transformation

Transformation was performed by using NEB 5-alpha Competent *E. coli* cells (NEB, Ref: C2987I) next to a lit bunsen burner practicing an aseptic technique. The cells were thawed on ice until the last ice crystals disappeared. 25 µl *E. coli* cells were added into 1,5 ml Eppendorf microtubes. 2 µl of plasmid mix from ligation were added to each tube while stirring carefully (to mix cells with the plasmid DNA). The tubes were left on ice for 30 minutes, then but in a water bath at 42°C for 30 seconds to facilitate uptake of plasmids into the cells. The tubes were but on ice for 5 minutes and 475 µl SOC Outgrowth Medium (NEB, Ref: B9020) were added. The tubes were placed into a shaking incubator at 37°C for 1 hour and secured with tape. Selection plates were warmed to 37°C. The tubes were flicked and 200 µl of the bacterial mixture from each tube were spread over the agar of the selection plates with a glass spreader sterilized in ethanol. The selection plates were labelled according to target genes of the primers. The plates were incubated to at 37°C until the next day.

2.10.4 Plasmid growth and sequencing preparation

After ~24 hours the plates were examined for colonies. 2 ml LB media containing 50 µg/ml of kanamycin were prepared in 15 ml falcon tubes next to a lit bunsen burner. With the aid of 10 µl sterile pipette tip, single colonies were transferred to the 15 ml falcon tubes prepared, one colony per tube. The lid of each tube was put on, a quarter turn open, allowing air into the tube. The lids were secured with parafilm tape and put into a 37°C shaking incubator overnight. The following day, 2 ml of each falcon tube was transferred to 1,5ml Eppendorf microtubes. The tubes were centrifuged at 8000xg for 3 minutes. The supernatant was discarded and the tube, now containing a pellet, were stored at -20°C until further used. To extract the plasmids from the *E. coli* pellets the QIAprep Spin Miniprep Kit (QIAGEN, Ref: 27106X4) was used following the manufactures handbook. The plasmids were prepared for sequencing by Big Dye™ Terminator v3.1 Cycle sequencing kit (ThermoFisher, Ref: 4337455). A master mix was made (See Table 10). Then 19 µl of master mix and 1µl of

plasmid template were added into each tube of 8-strip PCR tubes. The tubes were put into a thermal cycling machine with 5 minutes at 95°C followed by 40 cycles of 10 seconds at 95°C, 5 seconds at 50°C and 4 minutes at 60°C. The sequence products were sent to the sequencing facility of UNN (Universitestssykehuset Nord-Norge, UNN) and the sequences were sent back by email. The cloning site for the plasmids were found using ApE, the primer sequence and the cloning sequence were aligned using the Multiple sequence alignment tool of Clustal Omega.

***Table 10**: Big Dye master mix. The volumes shown are for one plasmid sequencing reaction. The volumes were multiplied with number of different plasmids and replicates, in addition to 2 extra, for not to fall short during pipetting. There were 4 replicates for each plasmid.*

Big Dye master mix		
Forward primer MB:	0,5 µl	x (Number of plasmids +2)
Big dye:	0,5 µl	x (Number of plasmids +2)
Buffer:	3,0 µl	x (Number of plasmids +2)
Nuclease free water:	15 µl	x (Number of plasmids +2)

2.11 qPCR

For the target genes *NKA a1b (ii*), *CFTR1*, *S100A1* and *CAPN2*, qPCR was performed on gill cDNA by using SSo advanced universal SYBR Green qPCR kit (BioRad, Ref: 1725272) with *Ef1-alpha* (b) as reference gene. A master mix was made for each of the primer pairs (See Table 11). 19 µl of master mix was put into the wells of a 96-well qPCR plate and 1 µl of the gill cDNA templates were added in duplicate. The qPCR was performed using Bio-Rad CFX manager 3.1 in a 2-step manner where the thermal cycling conditions varied with annealing temperature of the primers. The general thermal cycling conditions were: 10 minutes at 50°C and 5 minutes at 95°C followed by 40 cycles of 10 seconds at 95°C and 30 seconds extension phase (See table 7 for annealing temperature of primers).

For the target genes *Cd3e*, *CSF1R*, *IL10rb* and reference gene *EF1-alpha*, the same reagent (GoTaq® qPCR kit) as for the efficiency testing were used with the same procedure and thermal cycling conditions (See section 2.9 Primer efficiency). Instead of gill template dilutions, the cDNA from the gill samples were added in duplicate.

For the head kidney and heart cDNA samples, qPCR was performed using Fast SYBR™ Green master mix (ThermoFisher, Ref: 4385612) as the reagent (See Table 12). For the head kidney cDNA samples, the target genes *UBA* (MHC I), *MHC II*, *IFN alpha 1* and reference genes *EF1-alpha* (c) *and EF1-alpha* (d) were used. The same gene markers were used for the heart cDNA samples, in addition to the SAV3 non-structural protein marker nsP1. 19 µl of master mix were added as before. 1 µl of cDNA template were added as singles, to fit all groups on a single plate to avoid plate effects. The qPCR was performed using Bio-Rad CFX manager 3.1 in a 2-step manner. The thermal cycling conditions were as follows: 2 min of 95°C followed by 40 cycles of 15 seconds at 95°C and 1 minute at 60°C.

***Table 11**: Sso advanced universal SYBR Green master mix for qPCR x1 and x68. Used x68 and not x64 to not fall short due to inaccuracy pipetting.*

Master mix	**x1**	**x68**
Universal sybr green	10µl	680µl
Primer F	1µl	68µl
Primer R	1µl	68µl
H2O (Nuclease free)	7µl	476µl

***Table 12**:Fast SYBR Green master mix for qPCR x1 and x68. Used x68 and not x64 to not fall short due to inaccuracy pipetting.*

Master mix	**x1**	**x98**	**x66**
Fast SYBR green	10µl	980µl	660µl
Primer F	1µl	98µl	66µl
Primer R	1µl	98µl	66µl
H2O (Nuclease free)	7µl	686µl	462µl

2.11.1 qPCR Analysis

The qPCR data were handled in Microsoft Excel (Office 365). An average Ct were calculated for the duplicated samples. The difference between duplicated samples were calculated, samples with a difference over 0,50 were excluded unless the Ct value were generally very high (over 30 cycles). Since we were using 2 reference genes for the head kidney and heart cDNA, a geometric mean was calculated and used in the following calculations. The ΔCt values were calculated for each target gene as in equation 5.

Equation 5

$$\Delta Ct = Target\ gene\ Ct\ value - Reference\ gene\ Ct\ value$$

Then a control mean for each target gene was calculated. The control mean for the T1-T3 group were calculated from the T1 group. The control mean for the SAV3 challenge were calculated from the LD PBS group for each of the individual days' past infection. The ΔΔCt were calculated as in equation 6.

Equation 6

$$\Delta\Delta Ct = \Delta Ct - Control\ mean$$

The ΔΔCT values were logarithmic with base 2 to get the expression fold change the value $2^{-\Delta\Delta CT}$ were calculated.

2.12 Statistical Analysis

All the data results were plotted in GraphPad Prim 9.0.0. Statistical analyses were performed in GraphPad and RStudio version 2022.02.0 (R Core team, 2020). To test if the data were normally distributed the residuals of the data was plotted in RStudio with the function qqnorm() followed by qqline(). Homogeny among variances were tested by the Flinger – Kileen homogeneity of variance test with the R function flinger.test().
The Flinger – Kileen homogeneity of variance test performed on the residuals of each dataset revealed that we could not reject the 0 hypothesis, which is that the variance across the groups is unequal, p>0,05 (Barnard et al., 2017). Visual assessment of qqplots showed that most of the data did not stray from the normal distribution (See Appendix A). If the data strayed too much from the normal distribution line, the data where log transformed in R using the function log(), which is based on the natural logarithm *e*.

To test if there were a significant difference between smoltification status or immune remodelling between the groups (Groups: T1, T2, T3 LL and T3 LD) a Post Hoc comparison were performed with the Tukey Honestly Significant Difference Method with the function TukeyHSD(aov(Data~Groups)) in RStudio.
For the SAV3 data results (3dpi, 8dpi and 14dpi) a 3-way ANOVA were performed in GraphPad.

The assumptions for performing ANOVA were not met for the smolt marker gene *CAPN2*, even after log transformation. Hence, a non-parametric Kruskal rank sum test were performed.

2.13 ECG pilot study

To test how the salmon's circadian physiology was affected by light, we conducted a pilot study using ECG- and temperature bio-loggers.

The experiment was approved by the Norwegian food safety authority (Mattilsynet FOTS 27400) in the fall of 2021. In this experiment we used juvenile Atlantic salmon parr with an average weight of 161,8 g, SD= 19,28. The salmon were kept under constant light (LL) in circular freshwater tanks until they reached at least 132 g. The freshwater tanks were kept at natural water temperature and had circumferential waterflow. ~2 weeks before the experiment started the salmon were moved to a 16-hour light, 8-hour dark cycle (16L:8D). The lights went on at 06:00 and off at 22:00 CET. One week before surgery the salmon were transferred and acclimated to an 8°C 100 L circular tank.

10 Atlantic salmon (*Salmo salar)* were implanted with the ECG bio-loggers (Star Oddi, DST-micro-HRT, Weight: 3,3 g Length: 2,4 cm). These 10 salmon were housed together with 50 others to reduce hierarchal effects. The bio-loggers were programmed by using the mercury software version 5.99 (Star - Oddi). The bio-loggers were programmed to start recording 3 weeks after implantation, the 16.09.2021(experimental day 1) at 02:00. The bio-loggers were set to have a measuring interval of 30 min at 150 Hz, leaving enough time for 6-8 heartbeats to be measured. After 14 days of recording under LD, the salmon was moved into a LL photoperiod until the bio-loggers were retrieved (see Figure 9).

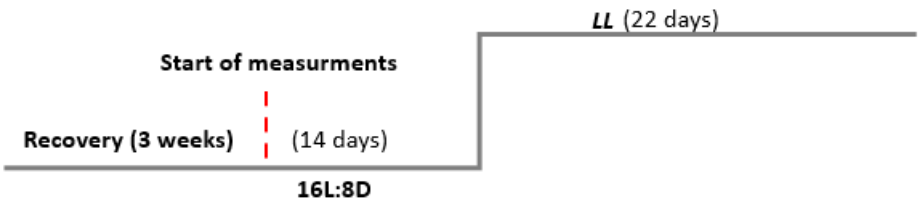

***Figure 9**: ECG experimental set-up.*

2.13.1 Implantation

The day prior to the implantation surgery, the bio-loggers were sterilized in a 1:10 2,5% glutaraldehyde solution in a 50 ml falcon tube, and the surgical tools were autoclaved. The surgery was performed the 26.08.2021 by Dr Anja Striberny. The salmon were anesthetized in a 10 L bucked with 60 ppm benzocaine (60 µl per L), until the operculum stopped moving. The surgical suture (Ethilon suture 6-0, 667H, C-2 needle, 45 cm) was attached at the front of the bio-logger (See Figure 10 A). A small incision was made in between the pelvic fins (See Figure 10 B). A pit tag was placed in the muscle wall in the cavity and then the ECG bio-logger was inserted. The opening was closed with a stitch from the suture attached to the bio-logger, holding it in place at the same time as the wound was closed. The pit tag ID was recorded, and length and weight measurements of the fish were taken. The procedure took ~3min for each fish. After the implantation the fish was put in a bucket filled with water from their tank to recover from the anesthesia. The fish were returned to their tank after recovering balance and swimming ability.

Two weeks after implantation the fish was again anesthetized with the same procedure as before, and weight and length measurements (fork length) were taken. We also observed the surgical site to see how it had healed.

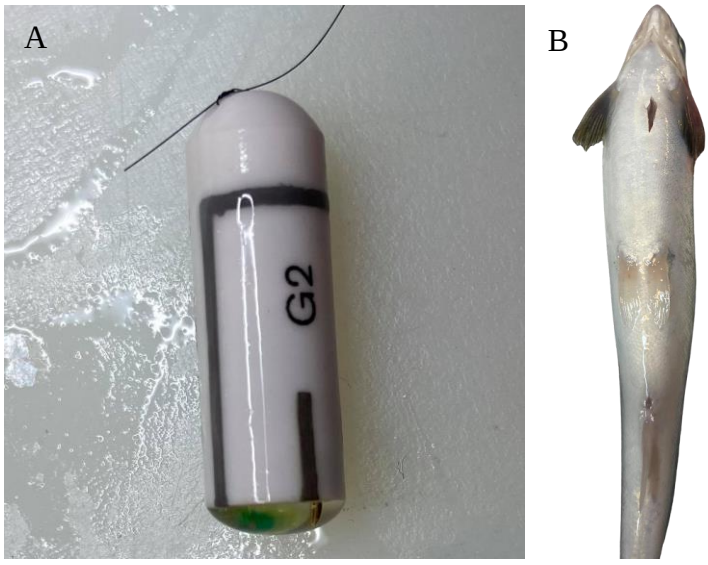

Figure 10: ***A***: *Star Oddi, DST micro-HRT ECG bio-logger and the suture attached.* ***B***: *Salmon surgical site*

2.13.2 ECG-retrieval and Data analysis

On experimental day 37 the bio-loggers were retrieved. The salmon was overdosed on benzocaine, weighted, and then cut open. The position of the bio-logger in the fish was noted and then the bio-loggers were retrieved (see Appendix E, Table S10). The bio-loggers were cleaned with water, and the data was collected using the procedure described in the mercury software user manual (Star-Oddi). The data were then exported to Microsoft Excel (Office 365).

The date and time in the document were changed from the excel timekeeping number system to standard time (CET). The data from each of the ECG bio-loggers were sorted into one document, only values with a quality score of 0 were used. To clean up the dataset a threshold of 90bpm> and 30bpm< was set. The data from each bio-logger were plotted in the software GraphPad Prism 9.0.0.

To make actograms the heart rate values were converted to values between 0 and 1. This was done by taking the heart rate minus the minimum value, then the new value/maximum new value. There was made a 5-hour cutoff in the time series. This was done because missing values displayed themselves as 0, no activity, in the actograms. Actograms was made with the software Image J 1.53e with Java 1.0.8_172 and the plugin ActogramJ. Chi-square periodograms was made. The values were transported to GraphPad version 9.0.0 for visualization.

3 Results

3.1 Smoltification

We hypothesize that the immunosuppression observed in Atlantic salmon during smoltification is due to circadian disruption caused by the aquaculture light environment. We tested this by performing an experiment with two different smoltification protocols, one under LD and one under LL (See Figure 5).

3.1.1 Condition factor and osmolality

Difference in photoperiod treatment may impact non-immune smoltification-related development. Therefore, before comparing immune competence we wanted to characterize a battery of classical smoltification-related factors between LD and LL. As the salmon transforms from a freshwater fish to a marine adapted fish, it changes in shape by becoming longer and narrower, fitting the marine morph. This is due to the change in the weight/length ratio, which is usually calculated by using the condition factor (See Method, section 2.2 Condition factor). Both LD and LL groups showed a decreased condition factor between T1 and T3 during the smoltification timeframe, with no significant difference between T3 LD and T3 LL (See Figure 11A), indicating that the difference in light schedule had no impact on the morphological development of the fish.

For the salmon to survive in seawater it needs to have osmoregulatory capabilities of a marine fish. Hence, as the salmon goes though smoltification it will become sea-water tolerant (Stefansson et al., 2008). Under aquaculture conditions, osmolality measurements of blood plasma from fish challenged for 24-hours in seawater is used as an indicator for osmoregulatory capacity which are linked to smolt status. We wanted to compare the osmoregulatory capacity of fish smoltified under LD and LL. Here both groups received summer-like photoperiodic information to stimulate smoltification, however the LL group lacked a circadian light zeitgeber. Our osmolality measurements of the seawater challenged fish showed that, in line with previous work (Iversen et al., 2020), that the hypo - osmoregulatory capabilities of the LL group changed throughout the smoltification experiment period (T1-T3), with an increase in osmolality during the winter photoperiod followed by a decrease at the end of the smoltification process (Figure 11B). Crucially, there was no significant difference between salmon smoltified under long photoperiod (T3 LD) and

salmon smoltified under constant light (T3 LL), indicating that both groups could tolerate seawater and keep their osmotic pressure stable.

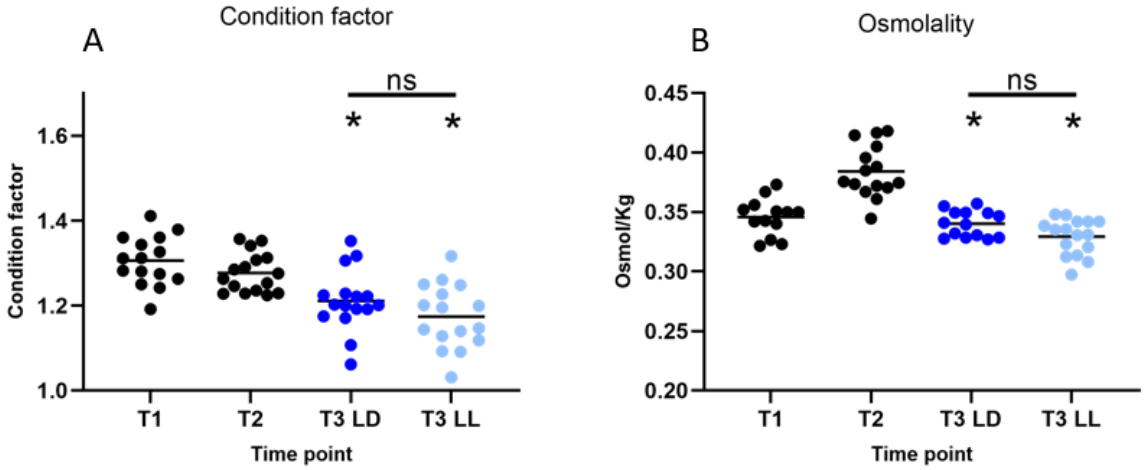

Figure 11*: Plotted values for condition factor values and osmolality measurements. The X axis shows the different time collection points, where T3 LD is the salmon smoltified under a long photoperiod, and T3 LL is the salmon smoltified under constant light. The Y axis shows the condition factor and osmolality (Osmol/kg), respectively. Each group average is represented by horizontal lines.* ***A****: The post hoc Tukey Honestly Significance Difference test (post hoc TukeyHSD) test showed a significant difference between the T1 and T3 groups, p<0,05, which is marked with *. There was no significant difference between T3 LD and T3 LL, p>0,05* ***B:*** *The post hoc TukeyHSD revealed a significant difference between T1 and T2, p<0,05, and T2 and T3, p<0,05, which is marked with *. There was no significant difference between T3 LD and T3 LL, p>0,05, marked with ns.*

3.1.2 NKA assay qPCR smolt marker genes

Osmotic balance is dependent upon the activity of several essential ion pumps. Chief among these pumps is NKA, which is essential for the active transport of sodium and potassium ions, but also essential for motivating the passive transport of a suite of other molecules, including water (Evans et al., 2005). Hence, NKA is associated with seawater tolerance, where an increase in NKA activity is linked to smoltification (McCormick et al., 2013; Zaugg & McLain, 1970). Because of this we wanted to test if there would be a difference in the NKA gill phenotype between LD smoltified and LL smoltified fish. The results from the NKA assay revealed that the NKA activity changed throughout the smoltification experiment period (T1-T3), with a much lower NKA activity during the winter photoperiod (T2) and a higher NKA activity prior to the smoltification experiment (T1) and after 6 weeks of LL or LD (See Figure 12). This corroborates with the findings of Handeland et al. (2013), where it was found that increased NKA activity can also be seen in salmon parr only kept under LL conditions,

without being subjected to a winter photoperiod. As for the osmolality measurements, there was no significant difference between the T3 LD and T3 LL group, hence, NKA activity is not affected if the salmon smoltified under a long photoperiod vs salmon smoltified under constant light

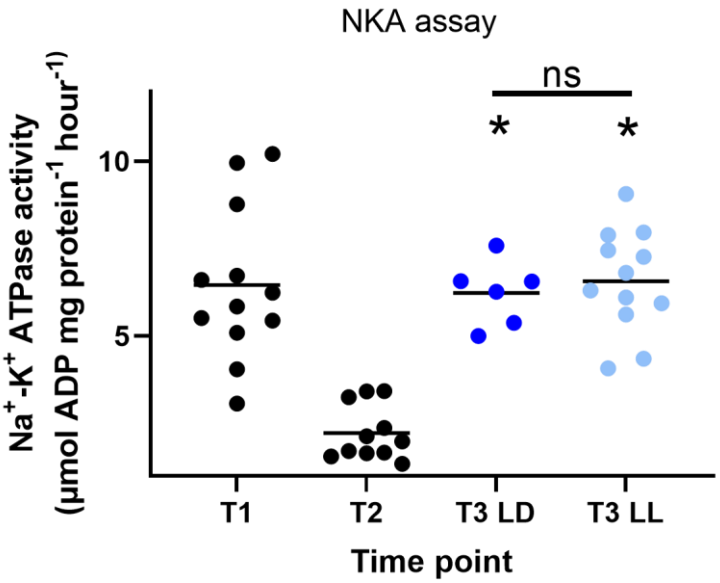

***Figure 12**: Plotted values from the NKA assay. The X axis shows the different time collection points, where T3 LD is the salmon smoltified under a long photoperiod, and T3 LL is the salmon smoltified under constant light. The Y axis shows the the gill Na+-K+ ATPase activity (µmol ADP mg protein^{-1} hour^{-1}). The horizontal lines are the average for each group. The post hoc TukeyHSD showed a significant difference between T1 and T2, $p<0,05$, and T2 and T3 (both LD and LL), $p<0,05$, which is marked with *. There was no significant difference between T3 LD and T3 LL, $p>0,05$, marked with ns.*

The gill undergoes a dramatic cellular remodelling during smoltification which is associated with the change in abundance of genes (West et al., 2021) The gene isoform *NKA a1b (ii*), a sub-unit of the NKA enzyme pump, is shown to have an increase in expression during smoltification and are associated with sea water tolerance (McCormick et al., 2013; Nilsen et al., 2007). The CFTR1 chloride channel also increases in its gene expression throughout smoltification (Nilsen et al., 2007). Here, we performed qPCR analysis to confirm if this change in gill phenotype is consistent between salmon smoltified under long photoperiod (LD) and salmon smoltified under constant light (LL). The qPCR marker gene isoform *NKA a1b (ii)* showed the same pattern as the NKA assay, with a decrease in expression during the T2 winter photoperiod compared to T1 and T3 summer-like photoperiods (See Figure 13A). These data suggest that regulation of NKA activity does not depend on winter photoperiod

exposure, but instead is directly responsive to photoperiod. Unexpectedly, we did not detect a significant difference between *CFTR1* expression during the T2 winter photoperiod and T3 (See Figure 13C).

More recently winter-dependent factors have been identified from the gill of the Atlantic salmon (Iversen et al., 2020) among these are Calpain-2, a protein involved in cytoskeletal remodelling and cell motility (Carragher & Frame, 2002) coded by the *CAPN2* gene, and S100A1 is a calcium protein binding gene involved regulating in many cellular processes (Wright et al., 2009). Expression of these genes are low in LL parr and pre-smolts at the end of winter-photoperiod exposure, but is dramatically stimulated at subsequent exposure to summer-photoperiods (Iversen et al., 2020). Our qPCR analysis of these genes mirrors the findings of the Iversen et al., 2020 paper. Visual interpretation shows that the gene marker *CAPN2* had an expression increase at T3 (See Figure 17B), but due to lack of homogeneity of variance, we could not perform a post hoc test to confirm. The smolt marker *S100A1* showed a significant increase at the T3 LD and LL collection point, there were however no difference between the T3 LD and T3 LL groups (See Figure 13D).

Our results revealed that there was no difference in the non-immune smolt characteristics investigated, between LD and LL smoltified salmon, indicating that the difference in light schedule did not affect smolt status.

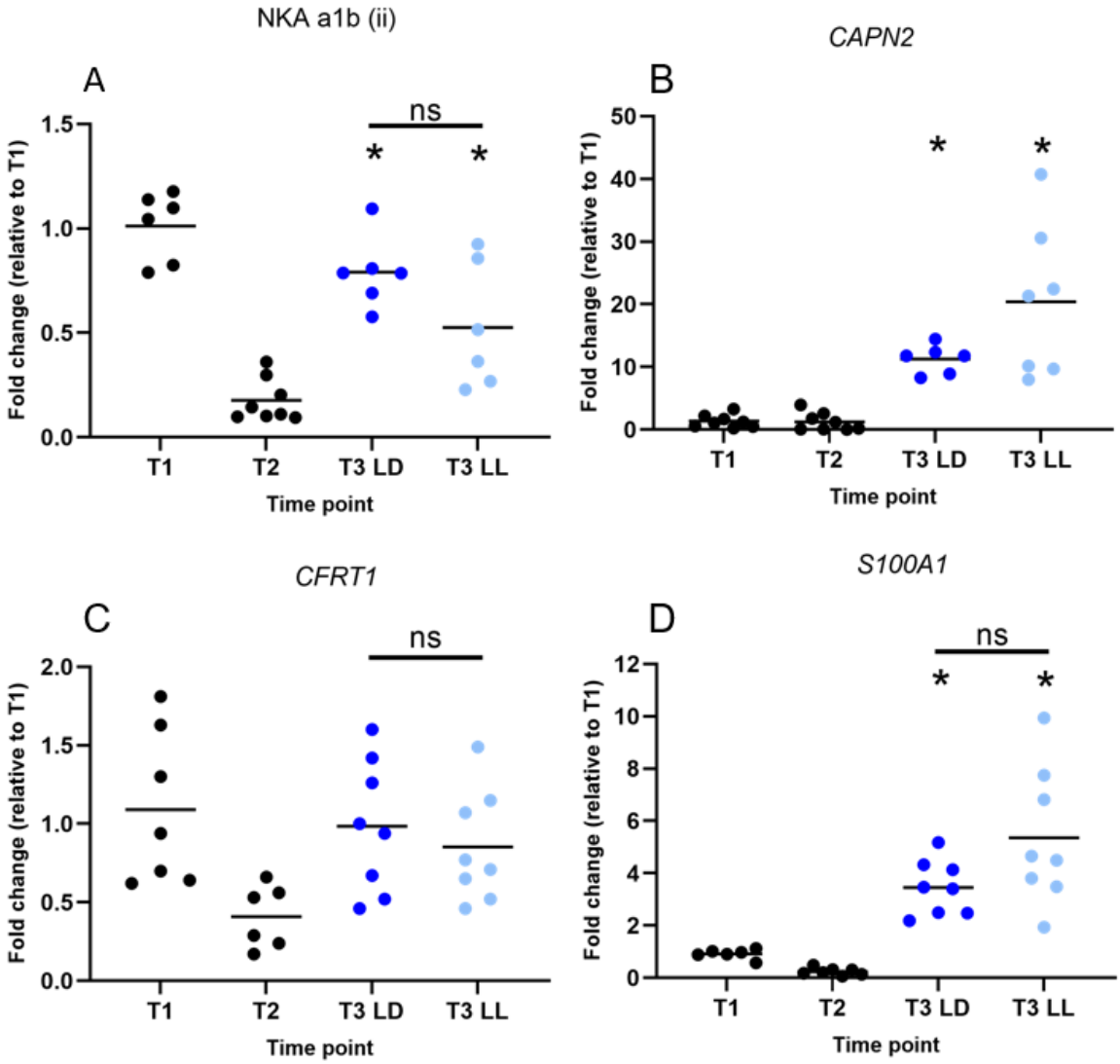

***Figure 13**: Plotted qPCR values for the smolt marker genes (**A**) NKA a1b (ii), (**B**) CAPN2, (**C**) CFTR1 and (**D**) S100A1 where the X axis is the time collection points, where T3 LD is the salmon smoltified under a long photoperiod, and T3 LL is the salmon smoltified under constant light. The Y axis is the fold change relative to the T1 average. The post hoc TukeyHSD revealed a significant expression difference between T2 and T3, p<0,05, for all markers except CFRT1. There was no significant difference between T3 LD and T3 LL for any of the markers, marked with ns.*

3.1.3 Gene expression of immune factors – primer development

The qPCR analysis depends on target specificity and efficiency of the sequence primers. First, to verify target specificity, we cloned the PCR products into a PCR TOPO vector, then aligned the sequencing product with the target sequence gene targets *EF1-alpha*, *Cd3e*, *CSF1R* and *IL10rb.* Each of the alignments was 100% specific, confirming that out primers amplify the desired targets (See Figure 14).

Next, we determined the efficiency of the qPCR reactions. This is important as the qPCR analysis $2^{-\Delta\Delta Ct}$ method assumes that the target sequence and reference sequence both are amplified with high efficiency (Livak & Schmittgen, 2001). To verify the efficiency, we tested the primers using standard cDNA dilutions and confirmed that the amplification efficiency exceeded a 90% threshold (Table 13).

```
Ef1alpha        GGTACTACGTCACAATCATTGATGCCCCTGGGCACAGAGACTTTATCAAGAACATGATCA      60
Insert          GGTACTACGTCACAATCATTGATGCCCCTGGACACAGAGATTTCATCAAGAACATGATCA      60
                ********************************* ******** ** ****************

Ef1alpha        CTGGTACATCTCAGGCTGATTG    82
Insert          CTGGTACATCTCAGGCTGATTG    82
                **********************

CLUSTAL O(1.2.4) multiple sequence alignment


Cd3e            TCATCATGACTTCTGTGGAGGGTGGAGGAGATGTGTCATTCTGGAGAACTACAGTCACAT      60
insert          TCATCATGACTTCTGTGGAGGGTGGAGGAGATGTGTCATTCTGGAGAACTACAGTCACAT      60
                ************************************************************

Cd3e            TGACCTGTCCTGATAAAG  78
insert          TGACCTGTCCTGATAAAG  78
                ******************

CLUSTAL O(1.2.4) multiple sequence alignment


Csf1r           TGGACACCAAATTCTACAAGATGATAGAGTCTGGTTATCAAATGTCCCGGCCAGACTTTG      60
insert          TGGACACCAAATTCTACAAGATGATAGAGTCTGGTTATCAAATGTCCCGGCCAGACTTTG      60
                ************************************************************

Csf1r           CCCCTCCAGAGATGTATACGAT      82
insert          CCCCTCCAGAGATGTATACGAT      82
                **********************
CLUSTAL O(1.2.4) multiple sequence alignment


Il10rb          AAAGATCTCATCGCTGAAAGAAGCCTACAGCAAAGTGGAATACAATATCAGATACTGGAA      60
Insert          AAAGATCTCATCGCTGAAAGAAGCCTACAGCAAAGTGGAATACAATATCAGATACTGGAA      60
                ************************************************************

Il10rb          GAAGACTGACAAGAAGGATGTGTTTGAGA       89
Insert          GAAGACTGACAAGAAGGATGTGTTTGAGA       89
                ******************************
```

Figure 14: *Sequence alignment of cloned primer sequences and target primer sequences by Clustal Omega multiple sequence alignment shows 100% alignment.*

Table 13: *Efficiency of qPCR reaction based on the slope calculated from cDNA dilutions and Ct values.*

Target gene	**Slope**	**Efficiency(%)**
EF1-alpha	-3,518	91,93
Cd3e	-3,3808	97,6
CSF1R	-3,451	94,88
Il10b	-3,485	93,62

3.1.4 Gene expression of Immune markers

Recent work associates smoltification with the downregulation of the immune gene markers in the gill, such as the pan T-cell marker gene *Cd3e*, the macrophage like gene marker *CSF1R* and the interleukin receptor marker *IL10rb* (West et al., 2021). We wanted test if this immune-suppressed phenotype observed was a consequence of the aquaculture light environment, since constant light has proven to have a negative effect on the immune system of mammals (Mizutani et al., 2017; Valdés-Tovar et al., 2015). Therefore, a qPCR study of the immune genes *Cd3e*, *CSF1R* and *IL10rb* were conducted. Surprisingly, our qPCR results revealed that the pan T-cell marker gene *Cd3e* did not show a decrease in expression throughout the smoltification experiment, neither did the macrophage like cell gene marker *CSF1R* or the interleukin receptor gene marker *IL10rb* (See Figure 15). There was no difference in expression between T3 LD and T3 LL for any of the immune gene markers. This suggests that the expression of these three immune genes are not consistently associated with smoltification.

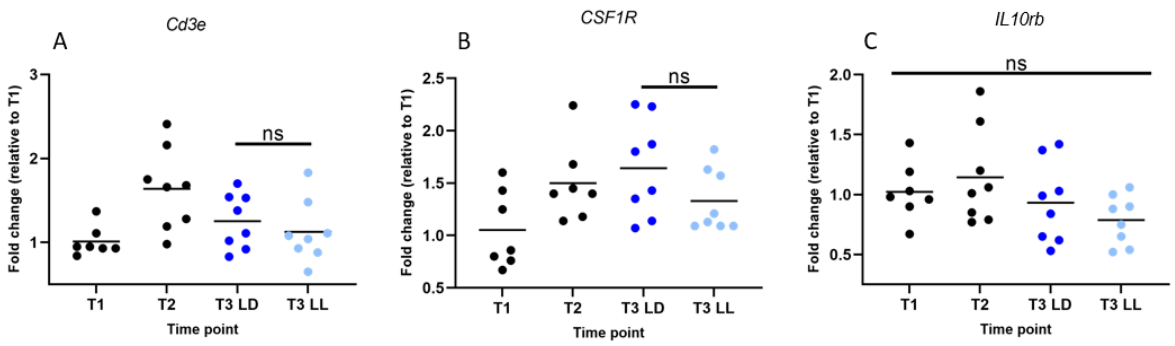

Figure 15*: Plotted qPCR values for the immune marker genes (**A**) Cd3e, (**B**) CSF1R and (**C**) Il10rb, where the X axis is the time collection points, where T3 LD is the salmon smoltified under a long photoperiod, and T3 LL is the salmon smoltified under constant light. The Y axis is the fold change relative to the T1 average. **A:** The post hoc TukeyHSD showed a significant difference between T1 and T2, p<0,05, T2 and T3 LL. There was no significant difference between T3 LD and T3 LL. There was no significant difference between T3 LD and T3 LL. **B:** There were a significant difference between T2 and T3 LL, p<0,05. **C:** There were no significant difference between any of the groups, p>0,05.*

3.2 SAV3 qPCR results – Heart

To test how the salmon immune response is affected by different light conditions, the LD and LL smoltified salmon were put through an immune challenge. The fish were intraperitoneally (i.p) infected with Salmonid alpha virus 3 (SAV3), which is the causative agent of pancreatic disease, a common disease in the aquaculture environment (Deperasińska et al., 2018). To

determine the viral burden of the SAV3 infected fish, we performed qPCR using primers for the SAV3 marker nsP1 on heart cDNA samples, since the heart is known to be one of the main sites of infection (Deperasińska et al., 2018). The nsP1 qPCR Ct results conducted on the cDNA heart samples showed two distinct groups for the SAV3 infected fish, where one of the groups had similar values to the PBS control (See Figure 16A). Because of this, a Ct threshold of 31 was set based on visual interpretation of the data. All fish below the threshold were removed from subsequent analysis as we interpreted them as non-infected. Visual interpretation of plotted Ct values of nsP1 (See Figure 16A), indicates a higher viral burden at 14 days past infection compared to 8 days past infection. This suggests that the viral load increases as time of infection increases. Unpaired T-tests between SAV3 LD and SAV3 LL showed no significant difference in SAV3 burden between the groups.

When a cell is infected by a virus it releases an immune signalling molecule called interferon alpha 1 (IFN alpha 1) to warn other neighbouring cells, so they can prepare antiviral proteins to interfere with viral production (Abbas et al., 2016). Thus, *IFN alpha 1* expression can be seen as the first response of an infected cell. By looking at the qPCR gene marker for *IFN alpha 1* we wanted to detect if there is a difference in immune response between salmon kept under LD and salmon kept under LL. The interferon gene marker *IFN alpha 1* expression had a significant response in the SAV3 infected fish, where there was a distinct difference between the PBS and SAV3 infected groups (Figure 16B). There was, however, no significant difference between 8- and 14-days past infection or between the SAV3 LD and SAV3 LL groups.

Another important response to viral infection is the antigen presenting protein MHCI. Which which marks the cell for CD8 positive T-cell recognition. The MHCI is a marker for antigens origination from within the cell, such as viruses (Abbas et al., 2016). MHCII is also an important part of the immune response but are only expressed by professional antigen precenting cells. Antigens that are presented by these cells originate from the extracellular environment (Abbas et al., 2016). We would therefore expect an expression increase on the MHCI gene marker *UBA*, but not necessarily from MHCII. Surprisingly we failed to detect changes of expression of either *UBA* (MHCI) or MHCII between PBS and SAV3 groups (See Figure 16C and D).

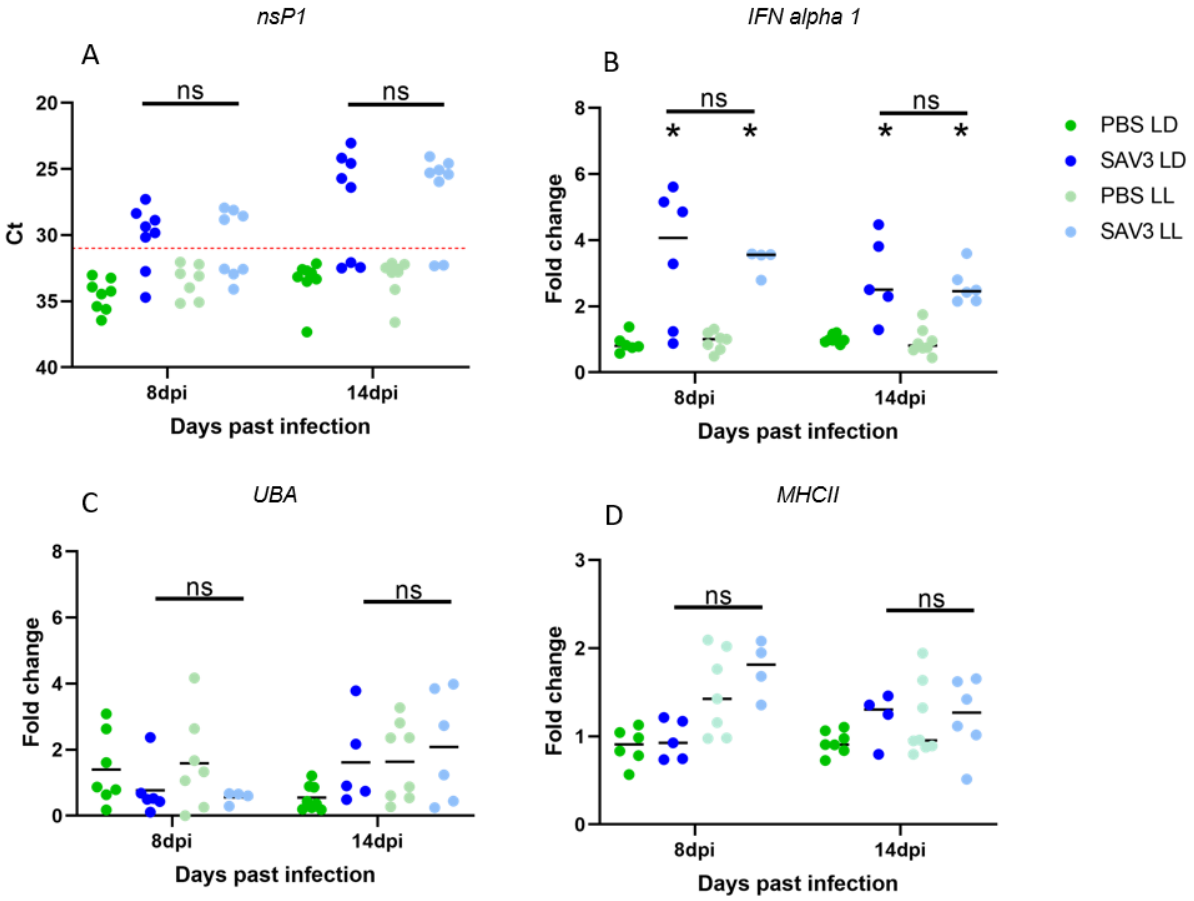

***Figure 16**: Plotted values for (**A**) SAV3 protein marker gene nsP1, (**B**) Interferon marker gene IFN Alpha 1, (**C**) MHCI gene marker UBA and (**D**) MHCII gene marker, performed on cDNA from the heart samples. The X axis is the days past infection. The Y axis for nsP1 is the Ct values from the qPCR and the Y axis for the other marker genes are the fold change relative to the average of the PBS LD group for each of the individual days. The dotted horizontal line on the nsP1 plot is the 31 Ct threshold value, individuals below the line where not included in any of the analysis or plots. The 3-way ANOVA revealed a significant difference in IFN alpha 1 expression between the PBS and SAV3 groups. There was no significant expression change between the PBS and SAV3 infected groups for either MHCI (UBA) or MHCII. Significant differences are marked with *.*

3.3 SAV3 qPCR results – Head Kidney

The head kidney of teleost fishes is a main site of immune cell production and therefore an important immune organ (Zapata, 1979), where expression of immune genes have been shown to change during smoltification (Johansson et al., 2016). Because of this we wanted to observe if there would be an immune response in the head kidney for SAV3 infected fish, and if it would differ between salmon kept under LD compared to LL. Visual inspection of the qPCR results for the SAV3 non-structural protein marker nsP1 in the head kidney revealed no difference in viral burden between the SAV3 treated group and the PBS control group (See

Figure 17A). The Ct values for the SAV3 marker was in general high, with the lowest value being 29,7 cycles, we therefore interpret the data as no virus in the head kidney, and that the readings observed are due to background noise from the qPCR.

To see if there were any immune response occurring, we used the same qPCR *IFN alpha 1* marker as for the heart. There was however no significant difference detected between the SAV3 and PBS control groups, supporting that the virus had not yet spread to the kidney (See Figure 17B). The qPCR results for the MHCI marker *UBA* on the other hand revealed a significant difference between the SAV3 infected and PBS groups and increase in expression as time passed (Dpi), indicating a migration of infected cells to the head kidney. There where however no difference between the LD and LL groups (See Figure 17C). As expected, expression of MHCII was unchanged between the PBS and SAV3 infected groups, $p<0,05$ (See Figure 17D).

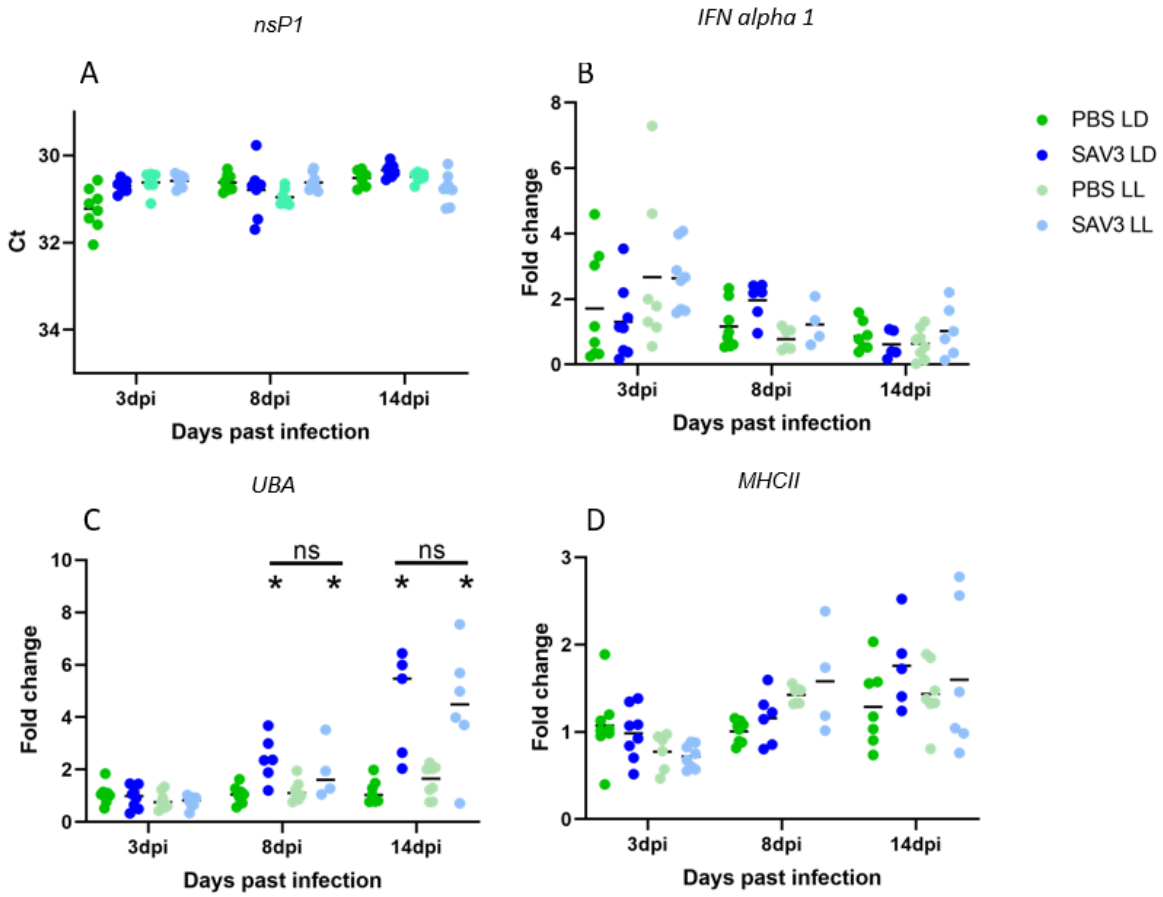

***Figure 17**: Plotted values for (**A**) SAV3 protein marker gene nsP1, (**B**) Interferon marker gene IFN Alpha 1, (**C**) MHCI gene marker UBA and (**D**) MHCII gene marker, performed on head kidney cDNA samples. The X axis is the days past infection. The Y axis for qnsp1 is the Ct values from the qPCR and the Y axis for the other marker genes are the fold change relative to the average of the PBS LD group for each of the individual days. The 3-way ANOVA showed a significant change in expression for the UBA gene marker, between days past infection, $p<0,05$ and between the PBS control groups and SAV3 infected groups, $p<0,05$. There was no significant difference for any of the groups. Significant differences between PBS and SAV3 infected groups are marked with a star.*

3.4 *In vitro* Poly I:C treatment of head kidney leukocytes

The immune system of mammals is under strong circadian control (Prendergast et al., 2013; Scheiermann et al., 2012) and immune challenge studies in mammals show that the immune response is time of day dependant (Ella et al., 2016; Esquifino et al., 1996). We wanted to test if there were an innate difference in immune response between salmon kept under LD and LL, and if the leukocytes of the salmon also displayed this time of day related immune response. We approached this by measuring the relative expression change in *IFN alpha 1* in poly I:C (viral mimetic) treated head kidney leukocytes with different photoperiod history. The qPCR results showed that both the LD and LL group responded to the poly I:C treatment, however, there was no significant difference between the LL and LD groups (See Figure 18B). Visual interpretation of the LD group data suggests a trend toward a higher response during the mid-light phase (LD2) compared to the cells treated during the mid-dark phase (LD1), but there was no significant difference between any of the groups, suggesting that neither light exposure nor circadian phase plays a major role in modulation of the Atlantic salmon immune response in head kidney leukocytes (See Appendix C, Table S9)

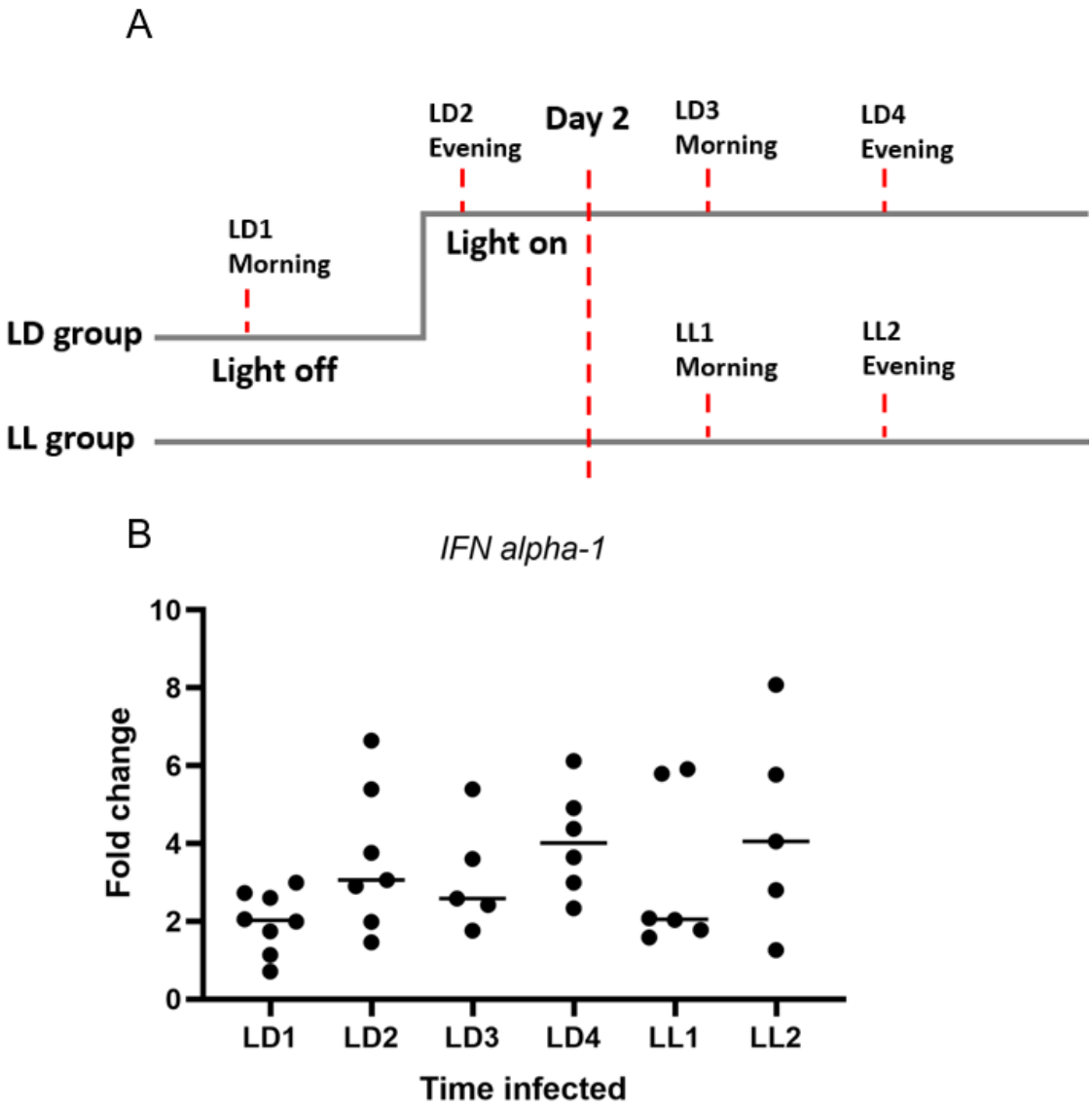

***Figure 18**: **A:** Head kidney collection points for leukocyte isolation and Poly I:C treatment. LD 1 group= timepoint 1 for the LD smoltified salmon, taken in the morning during the dark phase of the salmon LD cycle, LD 2 group= timepoint 2 for the LD smoltified salmon, taken in the evening when the salmon was put into constant light. LD3= Timepoint 3 in the morning Day 2, LD4= timepoint 4 taken in the evening Day 2. LL1 group= timepoint 1 for the LL smoltified salmon taken in the morning. LL 2 group= timepoint 2 for the LL smoltified salmon taken in the evening. **B**: qPCR results from head kidney leukocytes isolated and treated with poly I:C and control 48 hours pre-collection, from the LD smoltified cohort and LL smoltified cohort. The X axis indicates the different collection points, where LD1 being the cells isolated during the mid-dark phase and LD2 during the mid-light phase. LL1 and LL2 is the fish who were under constant light, with ~12 hours sampling interval. The Y axis is the fold change relative to the control (untreated cells) for each individual fish.*

3.5 ECG pilot study:

We hypothesize that the suppression of immune genes observed in the Atlantic salmon during smoltification is a product of circadian disruption caused by chronic exposure to constant light. Little, however, is known about the direct effect of light on the circadian outputs in Atlantic salmon. Here we conduct a pilot study to investigate how heart rate, a major circadian output in mammals and other fish, is affected by daily LD cycles and constant light in Atlantic salmon.

Ten fish were implanted with ECG bio-loggers from Star-Oddi. Measurements were conducted while the fish were entrained to a LD cycle and under constant light (See Figure 9). There were no mortalities caused by the implantation of the bio-loggers. All fish recovered well from anaesthesia and returned to the tank.

After 2 weeks the fish had increased in average weight and length from 161,83 g, SD=19,28, and 22,96 cm, SD= 0,88, to 185,64 g, SD= 22,96, length 23,91 and SD= 0,91 cm. In 3 of the fish the suture had become undone, 2 of the bio-loggers had become partially undone, and the last 5 held. Three of the bio-loggers were found at the bottom of the tank and had fallen out 28, 30 and 36 days after implantation.

When retrieving the bio-loggers, 2 of the bio-loggers were found behind the liver, 4 at the spleen site and one was held in place. We expected poorer data quality from the untethered ECG bio-loggers, however, the location of the ECG bio-loggers did not seem to correlate with the quality of the data (see Appendix E, Table S10). The rupture of the suture where most likely caused by a combination of rapid growth of the salmon and too thin suture, for future reference a stronger suture is needed.

3.5.1 Daily change in heart rate

Recordings were recovered from 7 ECG bio-loggers. Assessment of the data quality showed that 2 loggers collected high quality data throughout the experiment, 4 collected partial data, and 1 collected no useable data.

To determine the relationship between the fish and the light environment, we plotted the heart rate (BPM) data in an actogram style and measured daily and circadian rhythmicity using a chi squared periodogram.

Our analysis showed that the salmon had large individual responses, which were categorized into 3 groups. Group 1 were rhythmic under LD but became arrhythmic once put in LL (See Fish 1227 in Figure 19). Group 2 were rhythmic in LD and LL (See Fish 1221 in Figure 20) and group 3 were arrhythmic both under LL and LD (See Fish 1226 in Figure 21).

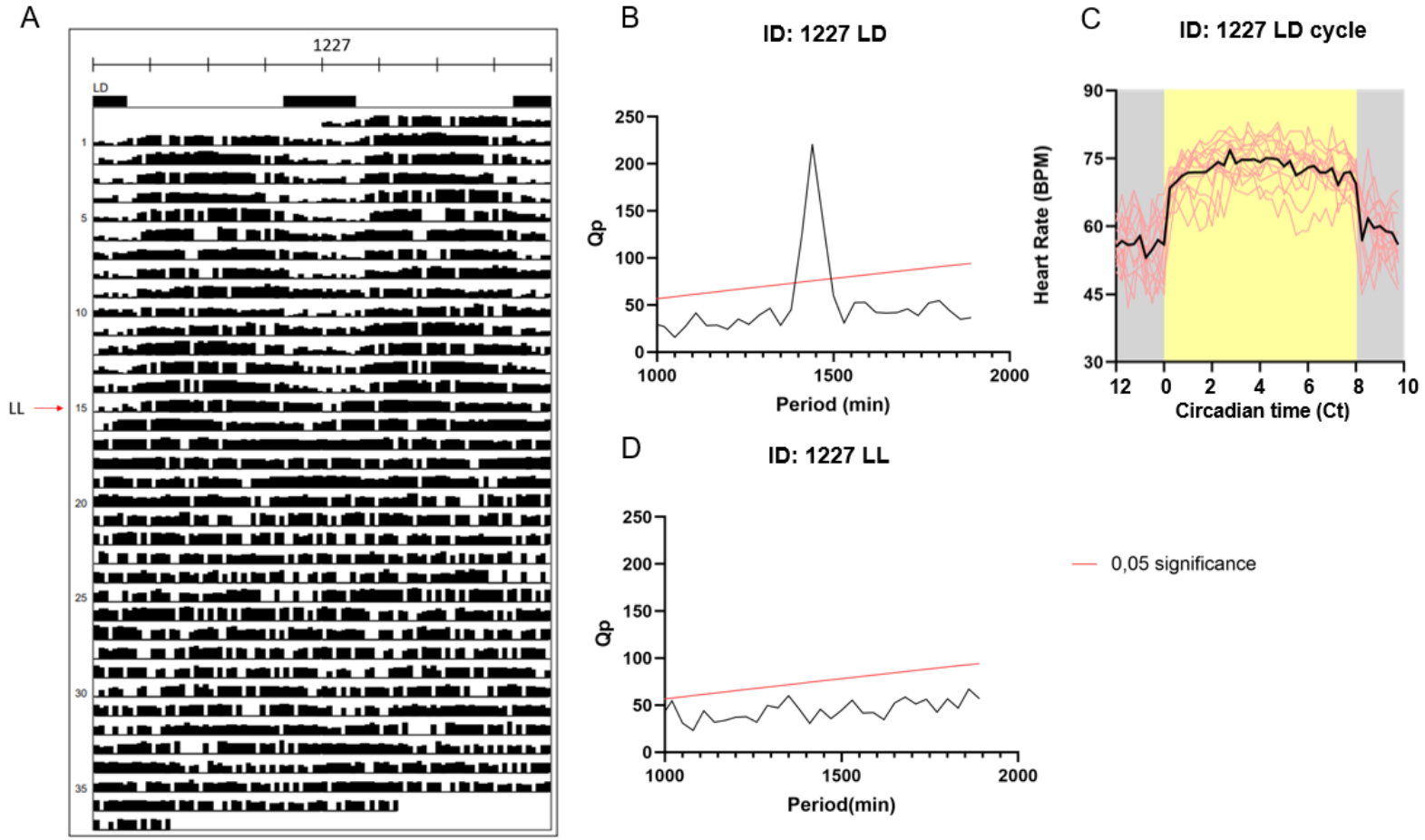

***Figure 19**: **A**: Heart rate (BPM) of representative Atlantic salmon (Fish ID: 1227) double plotted in an actogram style with corresponding chi-square periodograms (**B** and **D**). The black bars are the dark phase during a 24-hour day, and the white bars the light phase. The red arrow shows when the fish went into constant light. The red line in the periodogram is the significance level of p=0,05. The salmon had a significant 24-hour rhythm under LD but become arrhythmic once put in constant light. **C** Daily change in heart rate over 24 hours, where the X axis is put in circadian time. The grey boxes show when it was dark, and the yellow boxes show when it was light. The pink lines are individual days and the black line the average heart rate for all days.*

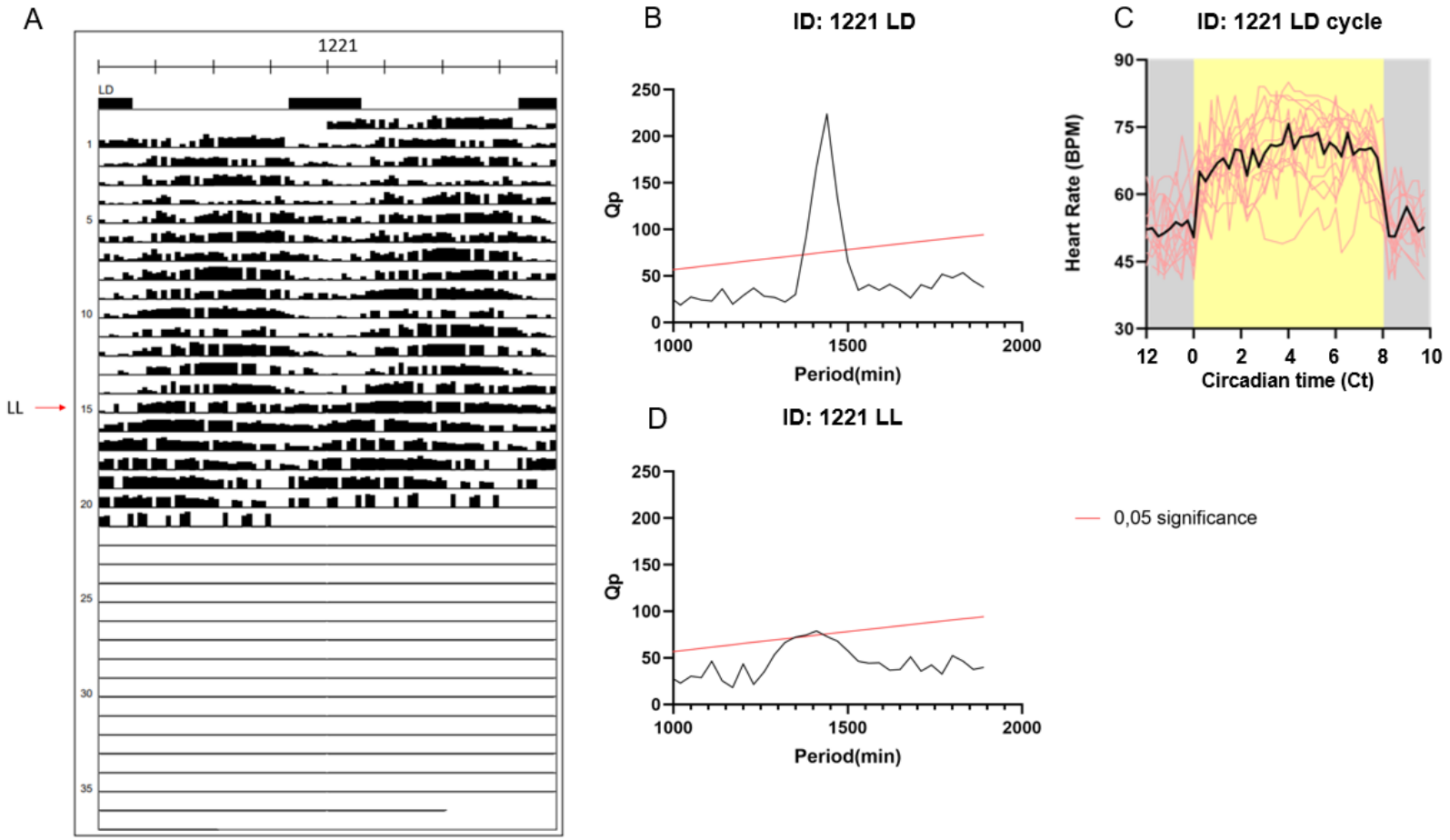

***Figure 20**: **A**: Heart rate (BPM) of representative Atlantic salmon (Fish ID: 1221) double plotted in an actogram style with corresponding chi-square periodograms (**B** and **D**). The black bars are the dark phase during a 24-hour day, and the white bars the light phase. The red arrow shows when the fish went into constant light. The red line in the periodogram is the significance level of p=0,05. The salmon had a significant 24-hour rhythm under LD and has a free running rhythm of 23,5 hours. **C:** Daily change in heart rate over 24 hours, where the X axis is put in circadian time. The grey boxes show when it was dark, and the yellow boxes show when it was light. The pink lines are individual days and the black line the average heart rate for all days.*

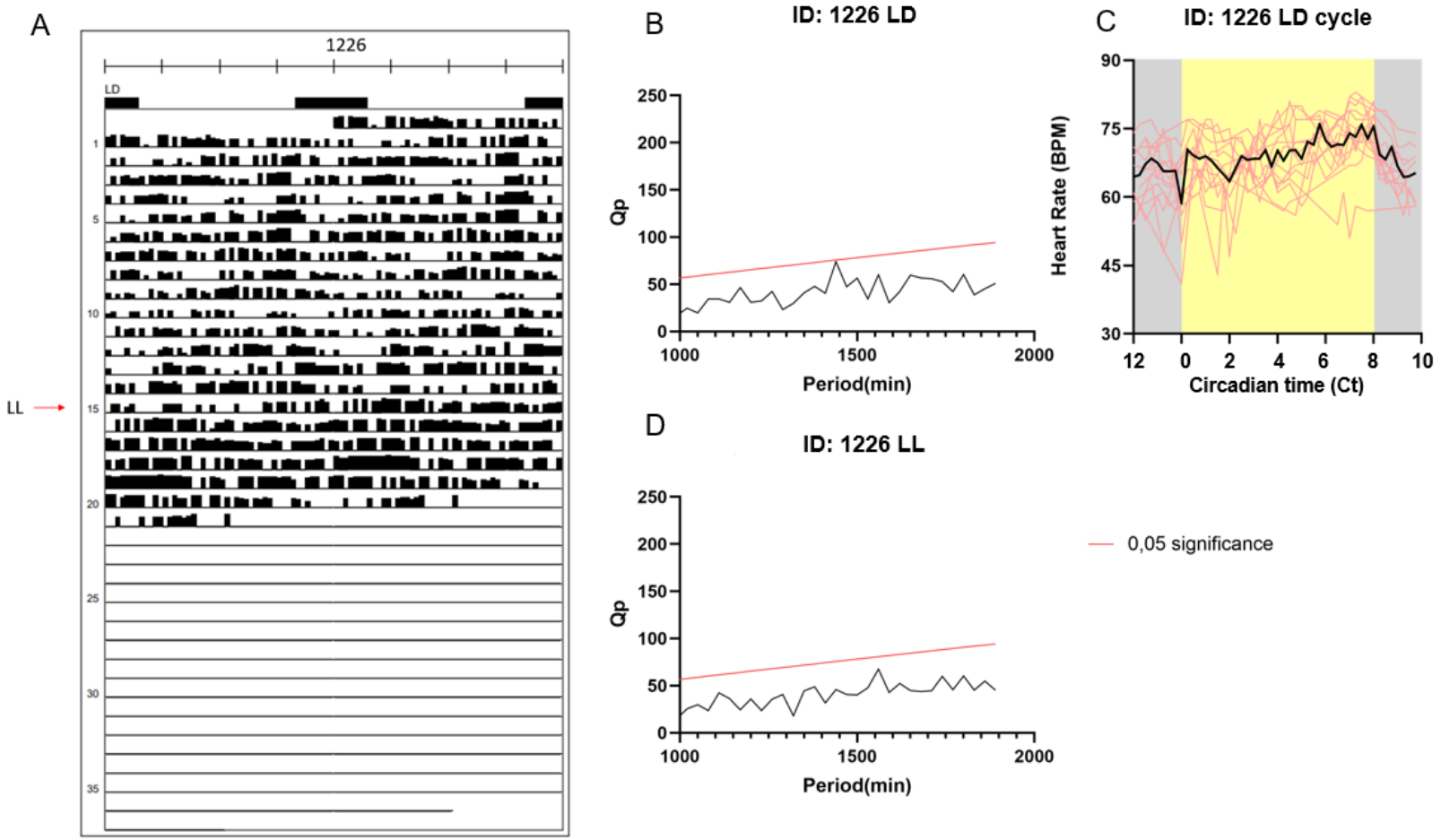

***Figure 21**: **A**: Heart rate (BPM) of representative Atlantic salmon (Fish ID: 1226) double plotted in an actogram style with corresponding chi-square periodograms (**B** and **D**). The black bars are the dark phase during a 24-hour day, and the white bars the light phase. The red arrow shows when the fish went into constant light. The red line in the periodogram is the significance level of p=0,05. The salmon was arrhythmic both under a light/dark cycle and under constant light had a significant. **C:** Daily change in heart rate over 24 hours, where the X axis is put in circadian time. The grey boxes show when it was dark, and the yellow boxes show when it was light. The pink lines are individual days and the black line the average heart rate for all days.*

4 Discussion

4.1 LD and LL photoperiods are equally capable of stimulating classical smolt characteristics

As expected, we observed a decrease in condition factor for both LD and LL smoltified fish. Comparison of average fork length showed that of LL group was longer (18,6 cm, SD: 0,86) compared to the LD group (17,09 cm, SD: 0,9), in keeping with previous work that shows that LL is associated with a higher growth rate compared to salmon kept under other photoperiods (Kråkenes et al., 1991; Strand et al., 2018). The increased growth rate may be a consequence of increased GH in the circulation, as release of this hormone is proportional to day-length (McCormick et al., 1995; Stefansson et al., 1991; Strand et al., 2018), and has a stimulatory effect on fish length and food intake (Johnsson & Björnsson, 1994). However, our results show that condition factor is indistinguishable between the two groups, and therefore that development of marine body shape is conserved between the two experiments.

Consistent with previous studies our osmolality measurements of blood plasma from 24-hour seawater challenged fish revealed a change in seawater tolerance as the salmon went through smoltification, where the short photoperiod supresses, and long photoperiod develops the salmons ability to osmoregulate (Iversen et al., 2020). Short photoperiod suppressed the salmons' osmoregulatory ability as shown by a panel of typical smolt characteristics associated with seawater tolerance in the gill. The results from NKA assays performed on gill filaments from the two smoltification groups (LD vs LL), showed that the salmon groups started with a relatively high ATPase activity, followed by a decrease during the winter photoperiod and then an increase again at the end of the smoltification process, as the salmon developed into its marine phenotype. This pattern could also be seen for the expression of the gene isoform *NKA alpha 1b*. Other studies report increased expression of *NKA alpha 1b* with smoltification and seawater transfer, and have therefore constructed a narrative in which upregulation of NKA activity is linked to smoltification (Nilsen et al., 2007). However, unlike our study, these experiments do not take into account the timepoints prior to smoltification. Therefore, the results do not contradict those observed in other studies but includes an additional time point that challenge the usual narrative that osmoregulatory capacity, NKA activity and expression of NKA *alpha* 1b follows winter exposure. Our data suggests, instead, that this is a passive response to daylength.

The qPCR analysis of the expression of the anion channel CFTR1 gave unexpected results. CFTR1 is involved in chloride secretion and is associated with seawater tolerance (Nilsen et al., 2007). Previous work reports significant increase in CFTR1 expression as the salmon develops into a smolt, however, although our data fits this trend, there is no significant difference between timepoints and light treatment. We know that the primers have been properly verified for its sequence specificity and qPCR efficiency. The thermal cycling condition of the qPCR were double checked as well as analysis of the data. Therefore, our results are unlikely to be a consequence of technical error, and suggests that, in our cohort, CFTR1 is only weakly regulated by photoperiod.

S100A1 and *CAPN2* had an expression increase only after being exposed to a short winter-like photoperiod, which coincides with the results observed in Iversen et al., 2020. These results confirm the regulatory framework for these genes, whose expression depends on winter photoperiod exposure, and shows that the photoperiod of the LD group (18 h L: 6 h D) and LL are both equally capable of stimulating the expression of *S100A1* and *CAPN2*. Although not significant, there is a clear trend toward a higher expression in these markers in LL compared LD which could point to other influential factors such as size.

There are several other factors beyond simply photoperiod change that have been shown to stimulate the development of the smolt phenotype. In nature, the annual cycle of temperature is shown to be an important factor controlling growth and development rates in juvenile salmonids (Stefansson et al., 2008), thereby together with photoperiod, temperature controls the age of when the salmon undergo smoltification. Smoltification is related to size, as the salmon parr do not respond to change photoperiod before it has reached a threshold size (Wedemeyer et al., 1980). In a study by Handeland et al. (2013) it was shown that NKA activity is linked to size, where salmon reared under different photoperiods and temperature regimes, and hence had differed in growth rates, had a peak of NKA activity at different times, and that all were in the same size range during this peak, suggesting that even though a long photoperiod is associated with increased NKA activity the fish size also plays a role. It has even been shown that dietary treatments with salt mixture can develop smolt like ion secreting ability (Striberny et al., 2021). How these non-photoperiod factors influence the immune system and ultimately the seawater survival in aquaculture smolts is presently unknown but are important variables to consider in future studies.

Taken together, our data shows that there were no major differences in the observes smolt characteristics between the two groups, demonstrating that the LD (18 h L:6h D) photoperiod has an indistinguishable effect on most smolt characteristics compared to LL. This corroborates a study from Strand et al. (2018), where they investigated if there is a critical daylength needed for complete smoltification. They showed that the salmon needs 16 hours of light under a light/dark cycle to complete smoltification, and that a photoperiod of 20 hours stimulated smoltification in a manner indistinguishable from their LL group. Our data complements this study and suggests that an LD photoperiod of 18 hours results in comparable smolts to an LL treatment.

4.1.1 Suppression of the immune cell markers CD3e, CSF1R and IL10rb are not robustly associated with smoltification

In contrast to other studies, we did not see an expression decrease in any of our three immune marker genes of the gill, in neither of the smoltification protocols. The pan T-cell marker *CD3e* has been reported in several studies to show a decrease in expression during smoltification, which infer a reduction of T-cells in the gill (Johansson et al., 2016; West et al., 2021). Because this we hypothesised that it might be associated with the smoltification protocol used in aquaculture. The macrophage like cell marker *CSF1R* and interleukin receptor marker *IL10rb* genes has also shown a decrease in expression during smoltification (West et al., 2021). The primers used has been validated for target specificity and qPCR efficiency, and the results are not likely due to technical errors. The immune system is complex and there are thousands of immune gene markers. Since we only investigated the expression of three genes, it does not necessarily mean that the downregulation of the immune system does not occur, rather it might be that the markers we chose are not robustly associated with smoltification. Studies which have linked smoltification to immune downregulation has used other methods, such as RNA-seq and microarrays (Johansson et al., 2016; West et al., 2021) which measure the abundance of all transcripts in the tissue and therefore dramatically increase the detail with which general trends in the transcriptomic landscape are measured. For future studies it might be better to investigate the transcripts of a larger number of immune genes, rather than focus on only a few selected genes.

We did not observe any difference in immune gene expression between LD and LL smoltified fish. Showing that neither constant light or LD conditions differentially regulated genes

associated with T-cells, dendritic cells, and Interleukin receptor 10 beta. Our current research efforts include a better characterisation of the immune gene landscape in these groups which we anticipate will provide a more holistic picture of immune status.

4.2 SAV3 – heart, the main site of infection

Pancreatic disease is caused by the Salmonid alphavirus (SAV) and is a big problem in aquaculture as it causes increased morbidity and mortality (Deperasińska et al., 2018). There are reported several different types of SAV, including SAV type 3 (SAV 3), which is a major issue in Norwegian aquaculture (Hodneland et al., 2005) and is therefore the viral type we used for our immune challenge in this study. To determine viral load we performed a qPCR analysis of the SAV non-structural protein (nsP1) which is proven to be an effective way to quantify infection (Hodneland & Endresen, 2006). Based on qPCR on heart cDNA with nsP1 as a marker, we were able to see that the SAV3 infection were successful for both LD and LL groups, and comparison between LD and LL groups show that there was no difference in viral burden between the infected groups, suggesting that the difference in photoperiod does not affect infection rate of the salmon heart. The qnsP1 readings for some infected fish were in same line as PBS control, suggesting that the fish were not infected, and hence removed from analysis conducted. This might be due to technical issues during the injection of the virus into the peritoneal cavity, meaning that some fish might not have received the virus. During the design phase of the project, we considered alternative methods of infection, such as bath immersion, where the virus is put in the water of the fish tank and the virus enters the fish through the gills, or co-habitation, where non-infected fish are exposed to the virus by introducing infected fish to the tank. Although these alternatives are arguably more comparable to the aquaculture environment as it includes a more-typical infection strategy, we chose to use intraperitoneal infection under the rationale that this allowed us to strictly control of the dosage of virus delivered to each fish. In future experiments, we will test different infection strategies including injection location to achieve the most consistent viral treatments.

We also measured the expression of key genes to indicate the stimulation of the viral immune response. The *IFN alpha 1* expression increased in the heart in both infected groups, indicating that the innate immune response were activated in both groups. Unexpectedly we did not see an expression increase for *UBA* (MHCI). However, many viruses have evolved

characteristic to interfere with the host's immune system, where some viruses has evolved proteins which are capable of repressing MHCI by downregulation (Hewitt, 2003). This has as far as we know not been reported for SAV3 and therefore remains speculative. We also measured MHCII expression in response to SAV3 challenge. Antigens presented by MHCII derive form the external environment, therefore as expected, we did not observe significant expression increase for MHCII (Abbas et al., 2016)

4.3 SAV 3 – head kidney, primary immune tissue

The nsP1 Ct data of the head kidney did not differ between the PBS and SAV3 groups. We are confident that the PBS group where not subjected to the virus, so the fact that we got readings from the PBS control group are likely due to "background noise" from the qPCR procedure, as the readings from the PBS control had in general high Ct values. Hence, we interpret the results as no virus present in the head kidney. This was supported by *IFN alpha* 1 result, as there was no significant difference in expression between the PBS and SAV3 groups, suggesting that little to no IFN type 1 antiviral response was taking place.

The head kidney is not only a primary immune organ where leucocytes are produced, but is also, together with the spleen, an important secondary immune organ, as it is one of the main sites for antigen presentation (Press & Evensen, 1999). Hence, it is possible that the MHCI expression increase detected in the SAV3 infected fish may be due to migration of cells into the head kidney. However, the results observed may also be due to that individual cells express more MHCI which are regulated by other mechanisms, or due to migration of cells out of the head kidney. As expected, we did not observe an increase in MHCII expression.

4.3.1 Photoperiod and the innate immune response

Our results revealed that there was no difference in the viral immune response between the LD and LL group, in either of the tissues observed, indicating that constant light effect on the circadian clock may not have the immunosuppressive effect as reported in mammals.

Although the physiology and molecular biology of the circadian clock is well conserved in mammals, recent work shows that the Atlantic salmon clock is quite different, even from other teleosts. In an expression study of clock genes on Atlantic salmon gill, saccus vasculosus (SV) and optic tectum tissues, fewer clock genes cycled in gill and SV, compared to the optic tectum of brain under a light/dark cycle. Furthermore, the cycling of clock genes

were completely abolished in the gill when moved into LL, and only one clock gene continued to cycle in the SV (West et al., 2020). The circadian clock, therefore, appears to be strong and consistent in the brain but not in peripheral tissues. These data contrast with work in zebrafish which show robust circadian rhythms of all tissues tested (Whitmore et al., 1998). The data presented in this thesis supports a narrative of weakened peripheral clocks in Atlantic salmon by demonstrating that neither exposure to constant light, nor stimulating an immune challenge at different time-points within the daily light-dark and circadian cycles has an effect on the immune system. Our data, therefore, suggest a fundamental difference in the relationship between the circadian clock and viral immune defence in Atlantic salmon compared to mammals. Which may either be a consequence of a weakened circadian clock in immune tissues, or alternatively a weakened interaction between the circadian clock and immune system.

Most of what we know about circadian immunology comes from studies conducted on humans and rodents, who show strong circadian patterns in immunology with different immune cell types being in circulation at different times of the day (Scheiermann et al., 2018). These animals typically experience daily cycles in their exposure to novel pathogens as a consequence of their robust sleep-wake cycles (Tognini et al., 2017); distinctly different to salmon who likely experience less daily variation in their exposure to pathogens. Therefore, the ultimate drivers for circadian regulation of human and rodent immune systems are likely to be stronger than those in Atlantic salmon. We speculate that relatively weaker daily fluctuations in the exposure of salmon to different pathogens may have fundamentally changed the evolution of the salmon immune system compared to rodents and humans, with much diminished emphasis on circadian regulation.

4.4 *In vitro* – Does salmon leukocytes display a time-of-day dependent immune response?

The LD and LL head kidney leukocytes all responded to the poly I:C treatment, as can be seen from the *IFN alpha 1* expression response. However, the response did not differ between the LD and LL group.

The value of using immune stimulates directly on leukocytes is that one can see if there is a change in immune response in the absence of the context to the animal and get an overview if there is light or clock dependent changes in their responses to immune stimulation. In mice

there have been reported a circadian gated difference in pro-inflammatory cytokine IL6 induction in peritoneal derived macrophages stimulated with lipopolysaccharide (LPS), which mimics a bacterial assault, where rhythmic IL6 was shown to be regulated in a time-of-day matter (Gibbs et al., 2012). In zebrafish there has also been reported an connection between core clock genes (per1 and per2) and the secretion of cytokines from leukocytes (Ren et al., 2018). There have also been cell culture studies who has linked BMAL1, another core clock gene, to have an antiviral role in different mammalian cells (Edgar et al., 2016; Majumdar et al., 2017). In contrast, although our LD and LL head kidney leukocytes all responded to the poly I:C treatment, as can be seen from the *IFN alpha 1* expression response, the response did not differ between the LD and LL group. However, the head kidney leukocyte experiment we conducted consists of a mixed population of leukocyte which are treated outside the experimental animal. Thus, our results do not necessarily rule out the possibility that different immune cell populations respond differently depending on light or clock factors. Indeed, we observed a trend towards a lower response of cells collected in the dark which could conceivably correspond to the diminished response of a specific cell type. It is also possible that another immune stimulus, such as LPS, could influence the cells differently as it may activate other parts of the immune system.

This *in vitro* study was to be complemented by *in vivo* data from tissue from the SAV3 experiment, where we infected the salmon during the mid-dark- and mid-light phase, but time limitations have not allowed for mid-dark data to be processed during my masters. These data will give a better understanding of how the immune system responds to an immune stimulus at different times of day in an *in vivo* setting. In rodents the numbers of lymphocytes circulation in the blood and in lymph nodes are dynamic, and oscillates in a time-of-day matter, as peak of lymphocytes in the blood are 5 hours after light onset in contrast to lymph nodes where the peak is delayed (Druzd et al., 2017). As a teleost the salmon does not have lymph nodes, antigen presentation occurs in the head kidney and spleen, but it might be that there are cycles in leukocyte recruitment, but this has to our knowledge not been investigated. There has also been reported a link between clock genes and immune cells in zebrafish, where rhythmic migration of neutrophils appear to depend on the core clock genes (Ren et al., 2018). Hence, even though we did not see a time-of-day related difference in our poly I:C leukocytes, the response to immune stimulus in the Atlantic salmon could still be light or circadian based as number of circulation immune cells and tissue infiltration could be

conceivably different depending on the environmental conditions and perceived circadian phase.

4.4.1 Summary and future directions

Overall, we did not see any big differences in the antiviral response between the LD and LL groups, neither in our *in vivo* SAV3 challenge or in our *in vitro* leukocyte experiment. These data suggests that the smoltification-associated immunosuppression in Atlantic salmon is not a consequence of circadian disruption, and instead suggests that it is naturally occurring. The migration from a fresh- to a seawater environment exposes the smolts to dramatically different environments with an entirely different pathogen ecologies. We speculate that smoltification-associated immunosuppression could either indicate a re-programming of the immune system, which must now prime itself against an entirely new complement of pathogens; or suggest a protective response which prevents an overstimulation of the immune system when the smolts are entering a dramatically different habitat. To investigate these theories, future studies could test the sea-cage survival of smolts reserved in holding aquaculture tanks for different periods. The functional response to SAV3 is typically low at 3 weeks after sea-water transfer but recovers to a higher capacity after 9 weeks (Moore et al., 2018). If smoltification-associated immune reprogramming is adaptive, as we hypothesise above, then we would expect that salmon transferred to sea-caged after 9 weeks may have higher mortality than those transferred at earlier timepoints. We also suggest that thorough characterization of the immune system of wild smolts could be insightful to the adaptive context of smoltification-associated immune reprogramming. Wild fish could be caught at different stages of the parr-smolt transition then brought into the lab where the state of their immune system could be characterized by transcriptomics then, by performing a controlled pathogen challenge, the functional state of their immune capacity could be tested. These data would allow us to better understand the natural progression of the immune system during smoltification in a semi-controlled environment.

4.5 ECG pilot study reveals large inter-individual variation in heart rate

Our ECG results revealed that the Atlantic salmon has large inter-individual variation in response to different light conditions. This is consistent with activity studies conducted on pink salmon (Godin, 1981). In contrast to mammals whose activity patterns can often be

categorized into nocturnal, diurnal, or crepuscular, within and across species, fish has a higher plasticity in their rhythms as the same species and individual can display both diurnal and nocturnal patterns (Reebs, 2002). It has been suggested that these changes in activity patterns is a consequence of food availability, predation risk and temperature (Reebs, 2002). It is also not uncommon for juveniles and adults to display opposed activity phases (Reebs, 2002). Half of the salmon (3 of 6) displayed a ~24-hour rhythm in heart rate output, with an elevated heart rate during the light phase. In mammals there has been reported a sex difference in the ability to entrain to a light/dark cycle (Davis et al., 1983). In our study we did not investigate male and female differences, but since half of the fish displayed an arrhythmic pattern in heart rate, it would be interesting to check for sex specific differences in future studies.

Our experimental design allowed us to be able to distinguish between diel and circadian rhythms in heart rate. A circadian rhythm arises from an endogenous clock within the animal; however, an animal may display a 24-hour rhythm as a direct response to the environment rather than being clock driven (Pittendrigh, 1960). One way to find if the rhythm observed is a consequence of an intrinsic endogenous clock, is to see if the rhythm persists under constant conditions. One of our six salmon displayed a significant free running rhythm in heart rate (See Figure 20). However, due to low quality scores, we only have 6 days in LL, therefore, we don't know if the rhythm would have persisted over a longer timeframe.

Overall, the pilot study conducted revealed a large individual variety in response to light, this may be due to circadian plasticity which has been observed in fish, and could be due to a more opportunistic lifestyle, but can also be sex related or related to life stage.

From a technical standpoint the ECG pilot showed that the procedure for anaesthesia, implantation and recovery was a success, however, the suture tethering several of the implants broke before the end of the experiment which led to the loss of three implants and internal displacement of several others. We recommend use of thicker suture will such as 4-0 polypropylene monofilament suture in future which will reduce the chance that the implant will be released while not compromising wound healing (Wagner et al., 2000). This pilot has therefore highlighted important details for technical refinement that will improve future data acquisition using the Star-Oddi or equivalent-sized implants.

5 Conclusion

We have demonstrated that the LD and LL protocols both stimulated smoltification of our Atlantic salmon as measured by condition factor, osmoregulatory capacity and smolt related gill-gene expression. We did not observe a decrease in expression for our chosen immune markers during smoltification, indicating that the pan T-Cell marker CD3e, the macrophage-like cell marker CSF1R and the interleukin receptor marker IL10rb, might not be associated with the immunosuppression observed during smoltification.

The SAV3 immune challenge demonstrated that the viral response did not differ between LD and LL groups, suggesting that LL don't have the immunosuppressive effect as seen in mammals, which may be a consequence of a fundamentally different circadian system. This finding was supported by our *in vitro* leukocyte experiment, which showed that LL and LD were similarly stimulated by the viral mimic poly I:C and that there were no distinct time-of-day difference in response to treatment. Overall, our results do not support our hypothesis that immunosuppression observed during smoltification is a consequence of circadian disruption. We suggest that the phenomenon may instead be an adaptive response, perhaps better described as immune-reprogramming, which may be important for the successful migration of the Atlantic salmon from their freshwater natal streams to the ocean.

Lastly, despite technical issues surrounding implant placement, our ECG pilot study suggests that, similar to other salmonids, Atlantic salmon have a large inter-individual in heart rate output in response to light. These findings require further data to interpret, and we suggest improvements to the procedure which will secure better quality longitudinal readings from our fish under controlled lighting and feeding schedules.

References

Abbas, A. K., Lichtman, A. H., & Pillai, S. (2016). *Basic immunology: Funcrions and Disorders of the immune system* (5th ed.). Elsevier Inc.

Allendorf, F. W., & Thorgaard, G. H. (1984). Tetraploidy and the evolution of salmonid fishes. In *Evolutionary genetics of fishes* (pp. 1-53). Springer.

Barnard, C. J., Gilbert, F. S., & McGregor, P. K. (2017). *Asking questions in biology: A guide to hypothesis-testing, analysis and presentation in practical work and research* (5th ed.). Pearson Education.

Bisbal, G. A., & Specker, J. (1991). Cortisol stimulates hypo‐osmoregulatory ability in Atlantic salmon, Salmo salar L. *Journal of Fish Biology*, *39*(3), 421-432.

Björnsson, B. T., Stefansson, S. O., & McCormick, S. D. (2011). Environmental endocrinology of salmon smoltification. *General and Comparative Endocrinology*, *170*(2), 290-298. https://doi.org/10.1016/j.ygcen.2010.07.003

Boeuf, G., Marc, A. M., Prunet, P., Le Bail, P. Y., & Smal, J. (1994). Stimulation of parr-smolt transformation by hormonal treatment in Atlantic salmon (Salmo salar L.). *Aquaculture*, *121*(1-3), 195-208.

Bolton, C., Bekaert, M., Eilertsen, M., Helvik, J. V., & Migaud, H. (2021). Rhythmic clock gene expression in Atlantic salmon parr brain. *Frontiers in physiology*. https://doi.org/10.3389/fphys.2021.761109

Carragher, N. O., & Frame, M. C. (2002). Calpain: a role in cell transformation and migration. *The international journal of biochemistry & cell biology*, *34*(12), 1539-1543.

Dardente, H., Hazlerigg, D. G., & Ebling, F. J. (2014). Thyroid hormone and seasonal rhythmicity. *Frontiers in endocrinology*, *5*, 1-11. https://doi.org/10.3389/fendo.2014.00019

Davis, F. C., Darrow, J. M., & Menaker, M. (1983). Sex differences in the circadian control of hamster wheel-running activity. *American Journal of Physiology-Regulatory, Integrative and Comparative Physiology*, *244*(1), R93-R105.

Deperasińska, I., Schulz, P., & Siwicki, A. K. (2018). Salmonid alphavirus (SAV). *Journal of Veterinary Research, 62*(1), 1-6. https://doi.org/10.2478/jvetres-2018-0001

Dickhoff, W. W., Folmar, L. C., & Gorbman, A. (1978). Changes in plasma thyroxine during smoltification of coho salmon, Oncorhynchus kisutch. *General and Comparative Endocrinology, 36*(2), 229-232.

Druzd, D., Matveeva, O., Ince, L., Harrison, U., He, W., Schmal, C., Herzel, H., Tsang, A. H., Kawakami, N., & Leliavski, A. (2017). Lymphocyte circadian clocks control lymph node trafficking and adaptive immune responses. *Immunity, 46*(1), 120-132.

Du, L. Y., Darroch, H., Keerthisinghe, P., Ashimbayeva, E., Astin, J. W., Crosier, K. E., Crosier, P. S., Warman, G., Cheeseman, J., & Hall, C. J. (2017). The innate immune cell response to bacterial infection in larval zebrafish is light-regulated. *Scientific reports, 7*(1), 1-13.

Edgar, R. S., Stangherlin, A., Nagy, A. D., Nicoll, M. P., Efstathiou, S., O'Neill, J. S., & Reddy, A. B. (2016). Cell autonomous regulation of herpes and influenza virus infection by the circadian clock. *Proceedings of the National Academy of Sciences, 113*(36), 10085-10090.

Ella, K., Csépányi-Kömi, R., & Káldi, K. (2016). Circadian regulation of human peripheral neutrophils. *Brain, behavior, and immunity, 57*, 209-221.

Ellison, A. R., Wilcockson, D., & Cable, J. (2021). Circadian dynamics of the teleost skin immune-microbiome interface. *Microbiome, 9*(1), 1-18.

Esquifino, A. I., Selgas, L., Arce, A. n., Della Maggiore, V., & Cardinali, D. P. (1996). Twenty-four-hour rhythms in immune responses in rat submaxillary lymph nodes and spleen: effect of cyclosporine. *Brain, behavior, and immunity, 10*(2), 92-102.

Evans, D. H., Piermarini, P. M., & Choe, K. P. (2005). The multifunctional fish gill: dominant site of gas exchange, osmoregulation, acid-base regulation, and excretion of nitrogenous waste. *Physiological reviews, 85*(1), 97-177. https://doi.org/10.1152/physrev.00050.2003

Flajnik, M. F. (2018). A cold-blooded view of adaptive immunity. *Nature Reviews Immunology, 18*(7), 438-453.

Garseth, Å., Silva de Oliveira, V. H., Grave, K., Helgesen, K. O., Dverdal Jansen, M., Jarp, J., Nilsen, A., Patel, S., Stige, L. C., & Brun, E. (2021). *2 Endringer i smitterisiko* (Fiskehelserapporten 2021, Issue 2a/2022). Veterinærinstituttet.

Gibbs, J. E., Blaikley, J., Beesley, S., Matthews, L., Simpson, K. D., Boyce, S. H., Farrow, S. N., Else, K. J., Singh, D., & Ray, D. W. (2012). The nuclear receptor REV-ERBα mediates circadian regulation of innate immunity through selective regulation of inflammatory cytokines. *Proceedings of the National Academy of Sciences, 109*(2), 582-587.

Godin, J. (1981). Circadian rhythm of swimming activity in juvenile pink salmon (Oncorhynchus gorbuscha). *Marine Biology, 64*(3), 341-349.

Handeland, S., Imsland, A., Björnsson, B. T., & Stefansson, S. (2013). Long‐term effects of photoperiod, temperature and their interaction on growth, gill Na+, K+‐ATPase activity, seawater tolerance and plasma growth‐hormone levels in Atlantic salmon Salmo salar. *Journal of Fish Biology, 83*(5), 1197-1209. https://doi.org/10.1111/jfb.12215

Handeland, S., Järvi, T., Fernö, A., & Stefansson, S. (1996). Osmotic stress, antipredatory behaviour, and mortality of Atlantic salmon (Salmo salar) smolts. *Canadian Journal of Fisheries and Aquatic Sciences, 53*(12), 2673-2680.

Haugarvoll, E., Bjerkås, I., Nowak, B. F., Hordvik, I., & Koppang, E. O. (2008). Identification and characterization of a novel intraepithelial lymphoid tissue in the gills of Atlantic salmon. *Journal of Anatomy, 213*(2), 202-209.

Hewitt, E. W. (2003). The MHC class I antigen presentation pathway: strategies for viral immune evasion. *Immunology, 110*(2), 163-169.

Hoar, W. S. (1939). The weight-length relationship of the Atlantic salmon. *Journal of the Fisheries Board of Canada, 4*(5), 441-460.

Hodneland, K., Bratland, A., Christie, K., Endresen, C., & Nylund, A. (2005). New subtype of salmonid alphavirus (SAV), Togaviridae, from Atlantic salmon Salmo salar and rainbow trout Oncorhynchus mykiss in Norway. *Diseases of aquatic organisms, 66*(2), 113-120.

Hodneland, K., & Endresen, C. (2006). Sensitive and specific detection of Salmonid alphavirus using real-time PCR (TaqMan®). *Journal of virological methods, 131*(2), 184-192.

Houde, A. L. S., Günther, O. P., Strohm, J., Ming, T. J., Li, S., Kaukinen, K. H., Patterson, D. A., Farrell, A. P., Hinch, S. G., & Miller, K. M. (2019). Discovery and validation of candidate smoltification gene expression biomarkers across multiple species and ecotypes of Pacific salmonids. *Conservation physiology, 7*(1), 1-21.

Hvas, M., Folkedal, O., & Oppedal, F. (2020). Heart rate bio-loggers as welfare indicators in Atlantic salmon (Salmo salar) aquaculture. *Aquaculture, 529*, 1-7. https://doi.org/10.1016/j.aquaculture.2020.735630

Iversen, M. (2020). *Photoperiodic history-dependent preadaptation of the smolting gill: Novel players and SW immediate response as markers of growth and welfare* [PhD. thesis, Norges arktiske Univeristet, UiT].

Iversen, M., Mulugeta, T., Gellein Blikeng, B., West, A. C., Jørgensen, E. H., Rød Sandve, S., & Hazlerigg, D. (2020). RNA profiling identifies novel, photoperiod-history dependent markers associated with enhanced saltwater performance in juvenile Atlantic salmon. *PloS one, 15*(4), 1-21. https://doi.org/10.1371/journal.pone.0237623

Johansson, L.-H., Timmerhaus, G., Afanasyev, S., Jørgensen, S. M., & Krasnov, A. (2016). Smoltification and seawater transfer of Atlantic salmon (Salmo salar L.) is associated with systemic repression of the immune transcriptome. *Fish & shellfish immunology, 58*, 33-41.

Johnsson, J. I., & Björnsson, B. T. (1994). Growth hormone increases growth rate, appetite and dominance in juvenile rainbow trout, Oncorhynchus mykiss. *Animal Behaviour, 48*(1), 177-186.

Johnston, C. E., & Eales, J. G. (1967). Purines in the integument of the Atlantic salmon (Salmo salar) during parr–smolt transformation. *Journal of the Fisheries Board of Canada, 24*(5), 955-964.

Jørgensen, J. B. (2014). The innate immune response in fish. In A. L. Roar Gudding, Øystein Evensen (Ed.), *Fish vaccination* (pp. 85-103). https://doi.org/10.1002/9781118806913.ch8

Koppang, E. O., Kvellestad, A., & Fischer, U. (2015). Fish mucosal immunity: gill. In *Mucosal health in aquaculture* (pp. 93-133). Elsevier.

Koronowski, K. B., & Sassone-Corsi, P. (2021). Communicating clocks shape circadian homeostasis. *Science, 371*(6530).

Kråkenes, R., Hansen, T., Stefansson, S. O., & Taranger, G. L. (1991). Continuous light increases growth rate of Atlantic salmon (Salmo salar L.) postsmolts in sea cages. *Aquaculture, 95*(3-4), 281-287. https://doi.org/10.1016/0044-8486(91)90093-M

Livak, K. J., & Schmittgen, T. D. (2001). Analysis of relative gene expression data using real-time quantitative PCR and the 2− ΔΔCT method. *methods, 25*(4), 402-408.

Logan, R. W., & McClung, C. A. (2019). Rhythms of life: circadian disruption and brain disorders across the lifespan. *Nature Reviews Neuroscience, 20*(1), 49-65.

Lorgen, M., Casadei, E., Król, E., Douglas, A., Birnie, M. J., Ebbesson, L. O., Nilsen, T. O., Jordan, W. C., Jørgensen, E. H., & Dardente, H. (2015). Functional divergence of type 2 deiodinase paralogs in the Atlantic salmon. *Current Biology, 25*(7), 936-941.

Majumdar, T., Dhar, J., Patel, S., Kondratov, R., & Barik, S. (2017). Circadian transcription factor BMAL1 regulates innate immunity against select RNA viruses. *Innate immunity, 23*(2), 147-154.

McCormick, S., Björnsson, B. T., Sheridan, M., Eilerlson, C., Carey, J., & O'dea, M. (1995). Increased daylength stimulates plasma growth hormone and gill Na+, K+-ATPase in Atlantic salmon (Salmo salar). *Journal of Comparative Physiology B, 165*(4), 245-254.

McCormick, S. D. (1993). Methods for nonlethal gill biopsy and measurement of Na+, K+-ATPase activity. *Canadian Journal of Fisheries and Aquatic Sciences, 50*(3), 656-658.

McCormick, S. D., Regish, A. M., Christensen, A. K., & Björnsson, B. T. (2013). Differential regulation of sodium–potassium pump isoforms during smolt development and seawater exposure of Atlantic salmon. *Journal of Experimental Biology, 216*(7), 1142-1151.

Mizutani, H., Tamagawa-Mineoka, R., Minami, Y., Yagita, K., & Katoh, N. (2017). Constant light exposure impairs immune tolerance development in mice. *Journal of dermatological science, 86*(1), 63-70.

Montero, R., Strzelczyk, J. E., Tze Ho Chan, J., Verleih, M., Rebl, A., Goldammer, T., Köllner, B., & Korytář, T. (2019). Dawn to dusk: Diurnal rhythm of the immune response in rainbow trout (Oncorhynchus mykiss). *Biology, 9*(1), 1-13. https://doi.org/10.3390/biology9010008

Moore, L., Jarungsriapisit, J., Nilsen, T., Stefansson, S., Taranger, G., Secombes, C., Morton, H., & Patel, S. (2018). Atlantic salmon adapted to seawater for 9 weeks develop a robust immune response to salmonid alphavirus upon bath challenge. *Fish & shellfish immunology, 74*, 573-583.

Mutoloki, S., Jørgensen, J. B., & Evensen, Ø. (2014). The adaptive immune response in fish. In A. L. Roar Gudding, Øystein Evensen (Ed.), *Fish vaccination* (pp. 104-115). https://doi.org/10.1002/9781118806913.ch9

Nelson, R. J., & Zucker, I. (1981). Absence of extraocular photoreception in diurnal and nocturnal rodents exposed to direct sunlight. *Comparative Biochemistry and Physiology Part A: Physiology, 69*(1), 145-148.

Nilsen, T. O., Ebbesson, L. O., Madsen, S. S., McCormick, S. D., Andersson, E., Björnsson, B. r. T., Prunet, P., & Stefansson, S. O. (2007). Differential expression of gill Na+, K+-ATPaseα-and β-subunits, Na+, K+, 2Cl-cotransporter and CFTR anion channel in juvenile anadromous and landlocked Atlantic salmon Salmo salar. *Journal of Experimental Biology, 210*(16), 2885-2896.

Nuñez-Ortiz, N., Moore, L., Jarungsriapisit, J., Nilsen, T. O., Stefansson, S., Morton, H. C., Taranger, G. L., Secombes, C. J., & Patel, S. (2018). Atlantic salmon post-smolts adapted for a longer time to seawater develop an effective humoral and cellular immune response against Salmonid alphavirus. *Fish & shellfish immunology, 82*, 579-590.

Pittendrigh, C. S. (1960). Circadian rhythms and the circadian organization of living systems. Cold Spring Harbor symposia on quantitative biology,

Prendergast, B. J., Cable, E. J., Patel, P. N., Pyter, L. M., Onishi, K. G., Stevenson, T. J., Ruby, N. F., & Bradley, S. P. (2013). Impaired leukocyte trafficking and skin inflammatory responses in hamsters lacking a functional circadian system. *Brain, behavior, and immunity, 32*, 94-104.

Press, C. M., & Evensen, Ø. (1999). The morphology of the immune system in teleost fishes. *Fish & shellfish immunology*, *9*(4), 309-318.

R Core team. (2020). *A language and environment for statistical computing.* In https://www.R-project.org/

Reebs, S. G. (2002). Plasticity of diel and circadian activity rhythms in fishes. *Reviews in Fish Biology and Fisheries*, *12*(4), 349-371.

Reed, L. J., & Muench, H. (1938). A simple method of estimating fifty per cent endpoints. *American journal of epidemiology*, *27*(3), 493-497.

Ren, D.-l., Zhang, J.-l., Yang, L.-q., Wang, X.-b., Wang, Z.-y., Huang, D.-f., Tian, C., & Hu, B. (2018). Circadian genes period1b and period2 differentially regulate inflammatory responses in zebrafish. *Fish & shellfish immunology*, *77*, 139-146.

Rességuier, J., Dalum, A. S., Du Pasquier, L., Zhang, Y., Koppang, E. O., Boudinot, P., & Wiegertjes, G. F. (2020). Lymphoid tissue in teleost gills: variations on a theme. *Biology*, *9*(6), 127.

Robertsen, B. (2018). The role of type I interferons in innate and adaptive immunity against viruses in Atlantic salmon. *Developmental & Comparative Immunology*, *80*, 41-52.

Scheiermann, C., Gibbs, J., Ince, L., & Loudon, A. (2018). Clocking in to immunity. *Nature Reviews Immunology*, *18*(7), 423-437.

Scheiermann, C., Kunisaki, Y., Lucas, D., Chow, A., Jang, J.-E., Zhang, D., Hashimoto, D., Merad, M., & Frenette, P. S. (2012). Adrenergic nerves govern circadian leukocyte recruitment to tissues. *Immunity*, *37*(2), 290-301.

Sigholt, T., Staurnes, M., Jakobsen, H. J., & Åsgård, T. (1995). Effects of continuous light and short-day photoperiod on smolting, seawater survival and growth in Atlantic salmon (Salmo salar). *Aquaculture*, *130*(4), 373-388.

Stefansson, S., Björnsson, B., Ebbesson, L., & McCormick, S. (2008). Smoltification. In *Fish Larval Physiology* (pp. 639–681). . https://doi.org/10.1201/9780429061608-27

Stefansson, S. O., Björnsson, B. T., Hansen, T., Haux, C., Taranger, G. L., & Saunders, R. L. (1991). Growth, parr–smolt transformation, and changes in growth hormone of Atlantic salmon (Salmo salar) reared under different photoperiods. *Canadian Journal of Fisheries and Aquatic Sciences*, *48*(11), 2100-2108.

Strand, J. E., Hazlerigg, D., & Jørgensen, E. H. (2018). Photoperiod revisited: is there a critical day length for triggering a complete parr–smolt transformation in Atlantic salmon Salmo salar? *Journal of Fish Biology*, *93*(3), 440-448.

Strandskog, G., Villoing, S., Iliev, D. B., Thim, H. L., Christie, K. E., & Jørgensen, J. B. (2011). Formulations combining CpG containing oliogonucleotides and poly I: C enhance the magnitude of immune responses and protection against pancreas disease in Atlantic salmon. *Developmental & Comparative Immunology*, *35*(2011), 1116-1127. https://doi.org/10.1016/j.dci.2011.03.016

Striberny, A., Lauritzen, D. E., Fuentes, J., Campinho, M. A., Gaetano, P., Duarte, V., Hazlerigg, D. G., & Jørgensen, E. H. (2021). More than one way to smoltify a salmon? Effects of dietary and light treatment on smolt development and seawater growth performance in Atlantic salmon. *Aquaculture*, *532*, 1-16.

Svendsen, E., Føre, M., Økland, F., Gräns, A., Hedger, R. D., Alfredsen, J. A., Uglem, I., Rosten, C., Frank, K., & Erikson, U. (2021). Heart rate and swimming activity as stress indicators for Atlantic salmon (Salmo salar). *Aquaculture*, *531*, 735804.

Tamai, T. K., Young, L. C., & Whitmore, D. (2007). Light signaling to the zebrafish circadian clock by Cryptochrome 1a. *Proceedings of the National Academy of Sciences*, *104*(37), 14712-14717.

Tognini, P., Thaiss, C. A., Elinav, E., & Sassone-Corsi, P. (2017). Circadian coordination of antimicrobial responses. *Cell host & microbe*, *22*(2), 185-192.

Valdés-Tovar, M., Escobar, C., Solís-Chagoyán, H., Asai, M., & Benítez-King, G. (2015). Constant light suppresses production of Met-enkephalin-containing peptides in cultured splenic macrophages and impairs primary immune response in rats. *Chronobiology international*, *32*(2), 164-177.

Varanelli, C. C., & Mccleave, J. D. (1974). Locomotor activity of Atlantic salmon parr (Salmo salar L.) in various light conditions and in weak magnetic fields. *Animal Behaviour*, *22*(1), 178-186.

Wagner, G. N., Stevens, E. D., & Byrne, P. (2000). Effects of suture type and patterns on surgical wound healing in rainbow trout. *Transactions of the American Fisheries Society, 129*(5), 1196-1205. https://doi.org/10.1577/1548-8659(2000)129<1196:EOSTAP>2.0.CO;2

Wedemeyer, G. A., Saunders, R. L., & Clarke, W. C. (1980). Environmental factors affecting smoltification and early marine survival of anadromous salmonids. *Marine Fisheries Review*.

West, A. C., Iversen, M., Jørgensen, E. H., Sandve, S. R., Hazlerigg, D. G., & Wood, S. H. (2020). Diversified regulation of circadian clock gene expression following whole genome duplication. *PLoS genetics, 16*(10), 1-21. https://doi.org/10.1371/journal.pgen.1009097

West, A. C., Mizoro, Y., Wood, S. H., Ince, L. M., Iversen, M., Jørgensen, E. H., Nome, T., Sandve, S. R., Martin, S. A., & Loudon, A. S. (2021). Immunologic profiling of the Atlantic salmon gill by single nuclei transcriptomics. *Frontiers in Immunology, 12*. https://doi.org/10.3389/fimmu.2021.669889

Whiting, J. R., Mahmud, M. A., Bradley, J. E., & MacColl, A. D. (2020). Prior exposure to long-day photoperiods alters immune responses and increases susceptibility to parasitic infection in stickleback. *Proceedings of the Royal Society B, 287*(1930), 1-10. https://doi.org/10.1098/rspb.2020.1017

Whitmore, D., Foulkes, N. S., & Sassone-Corsi, P. (2000). Light acts directly on organs and cells in culture to set the vertebrate circadian clock. *Nature, 404*(6773), 87-91.

Whitmore, D., Foulkes, N. S., Strähle, U., & Sassone-Corsi, P. (1998). Zebrafish Clock rhythmic expression reveals independent peripheral circadian oscillators. *Nature neuroscience, 1*(8), 701-707.

Wright, N. T., Cannon, B. R., Zimmer, D. B., & Weber, D. J. (2009). S100A1: structure, function, and therapeutic potential. *Current chemical biology, 3*(2), 138-145.

Xie, Y., Tang, Q., Chen, G., Xie, M., Yu, S., Zhao, J., & Chen, L. (2019). New insights into the circadian rhythm and its related diseases. *Frontiers in physiology*, 1-19. https://doi.org/10.3389/fphys.2019.00682

Yoo, S.-H., Yamazaki, S., Lowrey, P. L., Shimomura, K., Ko, C. H., Buhr, E. D., Siepka, S. M., Hong, H.-K., Oh, W. J., & Yoo, O. J. (2004). PERIOD2:: LUCIFERASE real-time reporting of circadian dynamics reveals persistent circadian oscillations in mouse peripheral tissues. *Proceedings of the National Academy of Sciences, 101*(15), 5339-5346.

Young, G., Björnsson, B. T., Prunet, P., Lin, R. J., & Bern, H. A. (1989). Smoltification and seawater adaptation in coho salmon (Oncorhynchus kisutch): plasma prolactin, growth hormone, thyroid hormones, and cortisol. *General and Comparative Endocrinology, 74*(3), 335-345.

Zapata, A. (1979). Ultrastructural study of the teleost fish kidney. *Developmental & Comparative Immunology, 3*, 55-65.

Zaugg, W. S., & McLain, L. R. (1970). Adenosinetriphosphatase activity in gills of salmonids: seasonal variations and salt water influence in coho salmon, Oncorhynchus kisutch. *Comparative Biochemistry and Physiology, 35*(3), 587-596.

Zaugg, W. S., & Wagner, H. (1973). Gill ATPase activity related to parr-smolt transformation and migration in steelhead trout (Salmo gairdneri): influence of photoperiod and temperature. *Comparative Biochemistry and Physiology Part B: Comparative Biochemistry, 45*(4), 955-965. https://doi.org/10.1016/0305-0491(73)90156-9

Zrini, Z. A., & Gamperl, A. K. (2021). Validating Star-Oddi heart rate and acceleration data storage tags for use in Atlantic salmon (Salmo salar). *Animal Biotelemetry, 9*(1), 1-15.

Appendix A: qqplots

All the qqplots are based on the residuals from the one-way ANOVA.

T1-T3 – qqplots

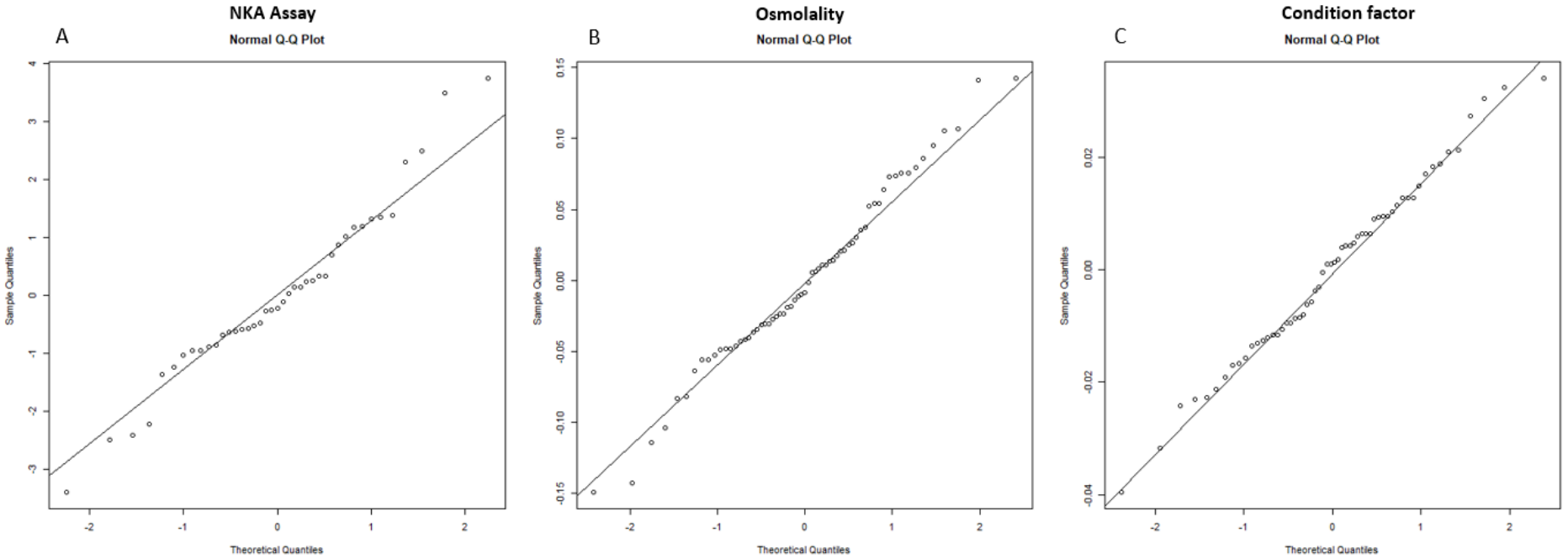

Figure S1: qqplot for (A) NKA assay data, (B) osmolality and (C)condition factor.

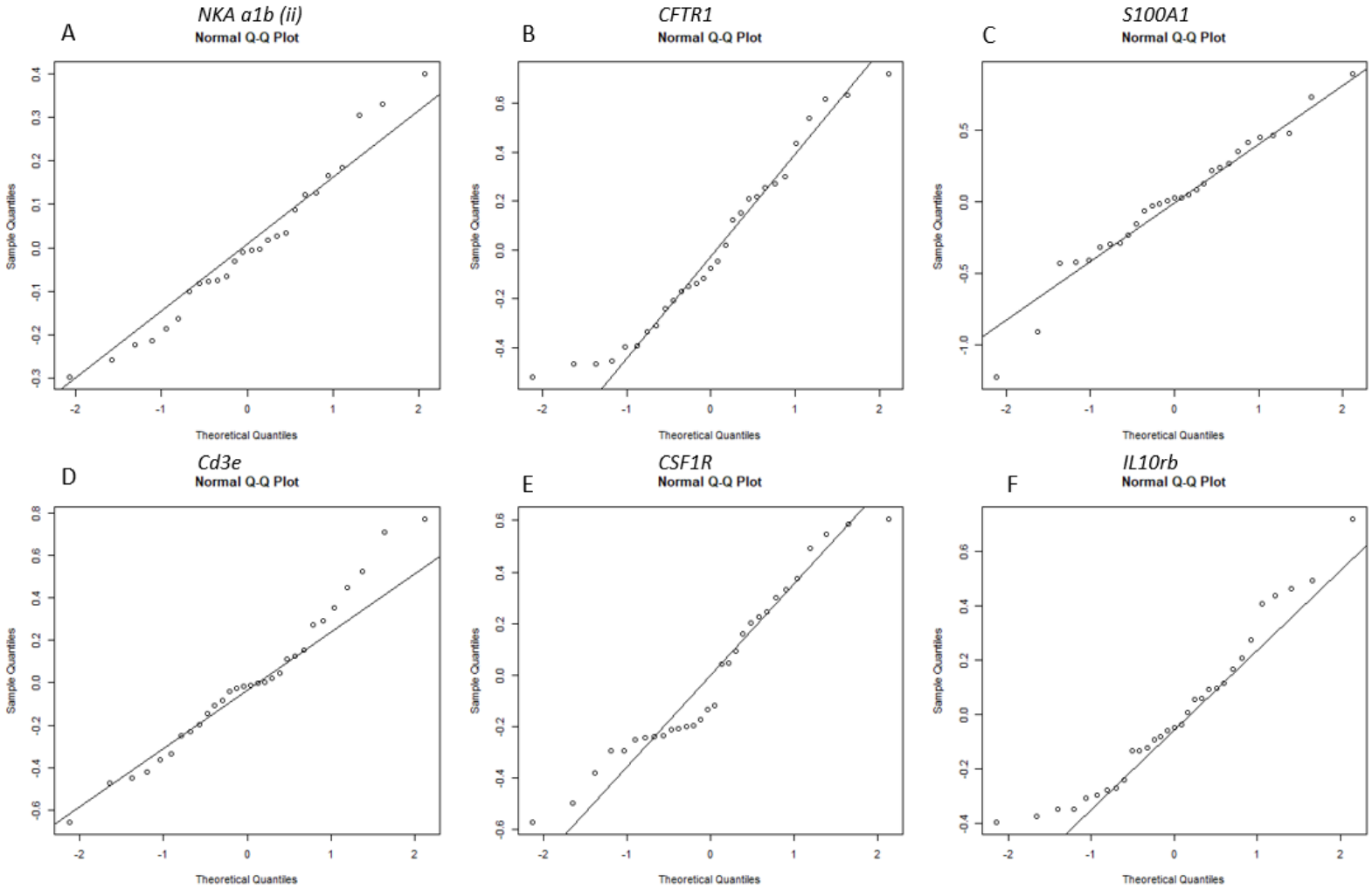

Figure S2: qqplot for qPCR results from gill for (A) NKA a1b (ii), (B) CFTR1 (C) S100A1, (D) Cd3e (E) CSF1R and (F) IL10rb.

Heart qPCR markers – qqplots

All the qqplots for the heart marker genes.

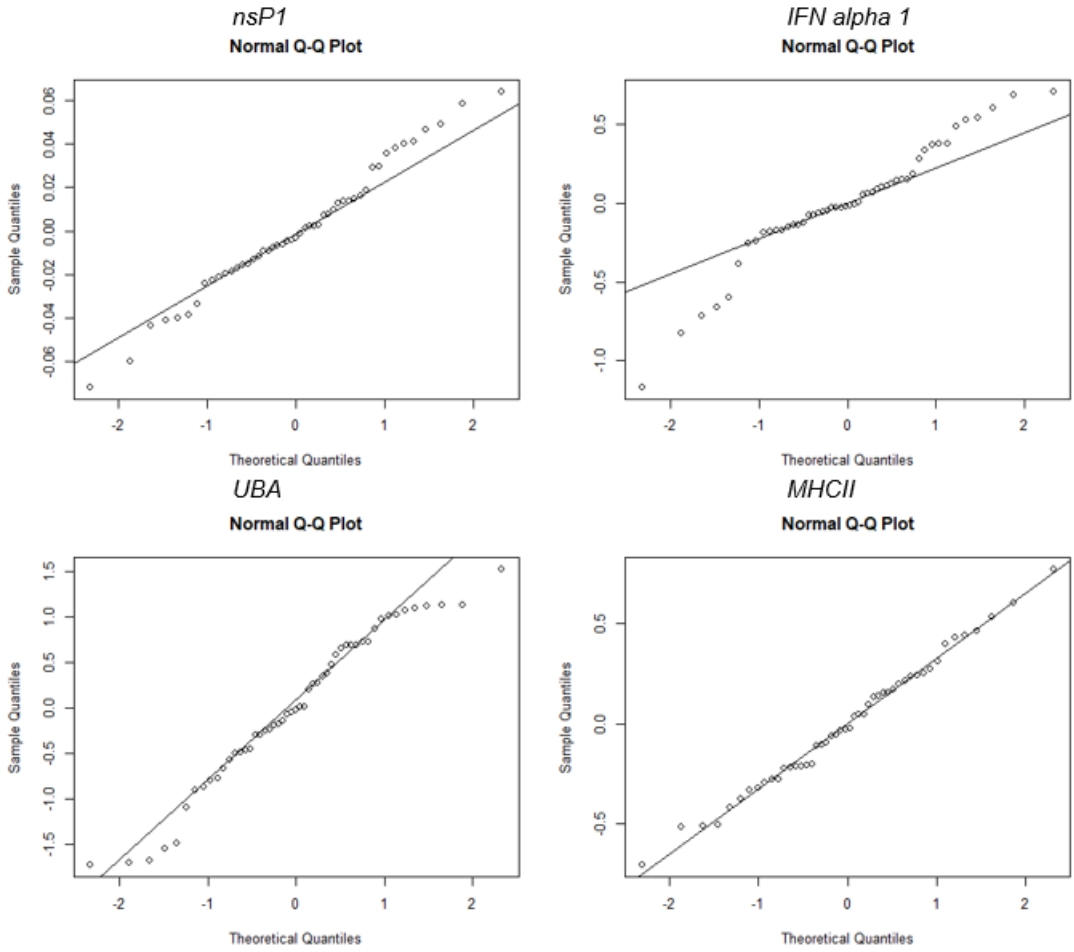

Figure S3: qqplots for heart qPCR gene markers nsP1, IFN alpha 1, MHCI (UBA) and MHCII.

Head kidney qPCR markers – qqplots

All the qqplots for the head kidney marker genes seems to follow a normal distribution based on visual interpretation (See Figure S4).

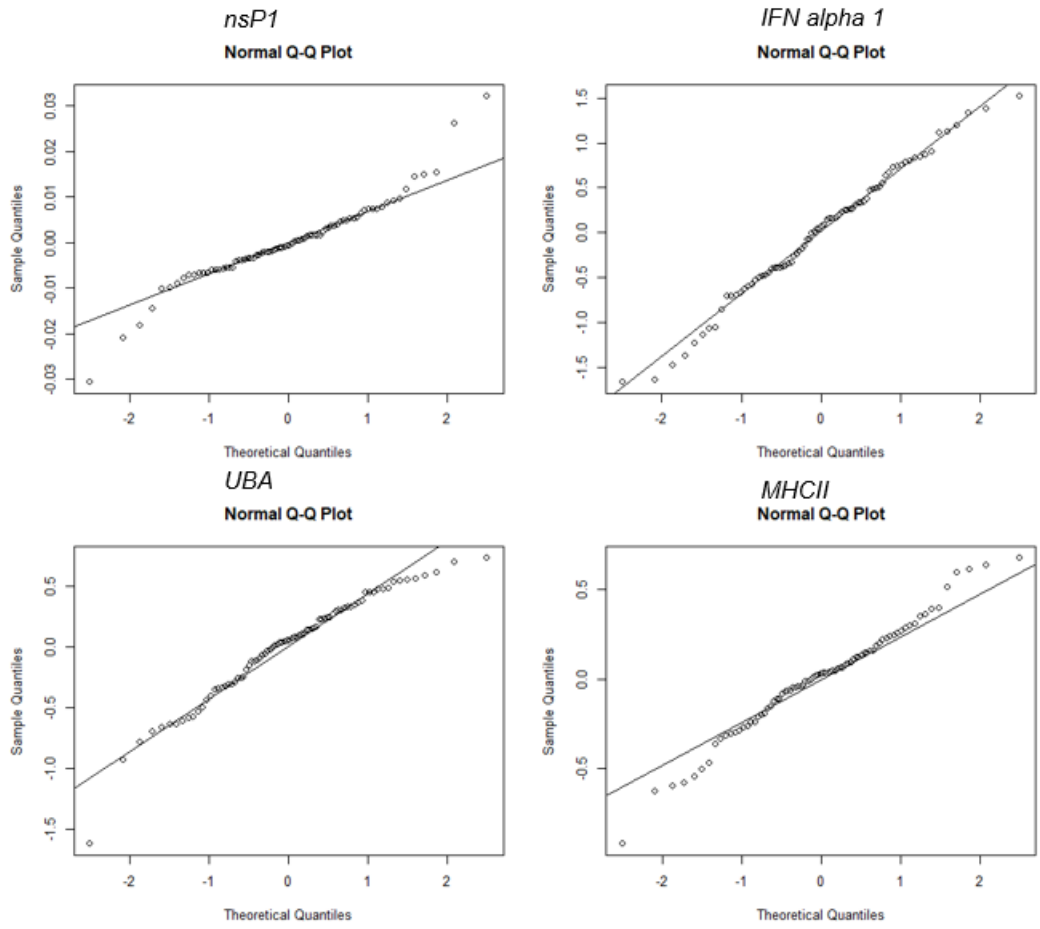

Figure S4: qqplots for head kidney qPCR gene markers nsP1, IFN alpha 1, MHCI (UBA) and MHCII.

Leukocyte – *IFN alpha* qqplot

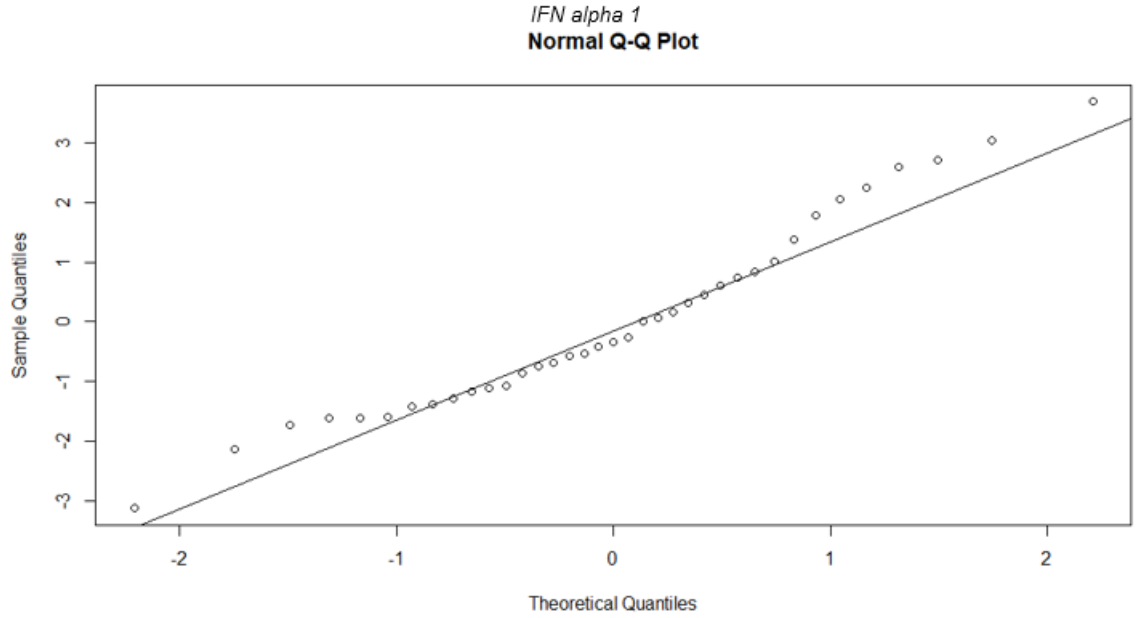

Figure S5: qqplot for isolated head kidney leukocytes qPCR gene marker IFN alpha 1.

Appendix B: Leukocyte Poly I:C cohort weights

Weights from LD and LL fish cohorts from the head kidney leukocyte isolation experiment shows that the fish in the LL group had a general trend of being bigger, LD cohort mean: 144,3 g, SD: 34,72 and LL cohort mean: 199,63 g, SD: 38,5. See table A2 for individual weights.

Table S1: Weights in grams from head kidney leukocyte isolation LD and LL fish cohorts. The weights are not from the fish the leukocytes were extracted from, but fish from the same cohort with the same photoperiod.

LD cohort weights (g)	LL cohort weights (g)
119,5	184
168,5	148
98	180,5
163,5	291
125	193
205	199
125,5	195
160	253
134,5	201
106,5	158
199,5	201
126,5	192

Appendix C: Supplementary Tables

T1-T3 ANOVA Tables

```
Tukey multiple comparisons of means
    95% family-wise confidence level

Fit: aov(formula = condition_factor ~ TimePoint, data = smolt)

$TimePoint
                    diff         lwr          upr     p adj
T2-T1       -0.02904013 -0.09011193  0.032031679 0.5934937
T3_LD-T1    -0.09501632 -0.15608813 -0.033944519 0.0006922
T3_LL-T1    -0.13143090 -0.19250271 -0.070359095 0.0000025
T3_LD-T2    -0.06597620 -0.12605490 -0.005897495 0.0259578
T3_LL-T2    -0.10239077 -0.16246948 -0.042312072 0.0001831
T3_LL-T3_LD -0.03641458 -0.09649328  0.023664126 0.3851700



Tukey multiple comparisons of means
    95% family-wise confidence level

Fit: aov(formula = osmolality ~ TimePoint, data = smolt)

$TimePoint
                     diff         lwr           upr     p adj
T2-T1        0.038374359  0.02183360  0.0549151154 0.0000006
T3_LD-T1    -0.005620879 -0.02243367  0.0111919130 0.8119805
T3_LL-T1    -0.016504808 -0.03280381 -0.0002058066 0.0461110
T3_LD-T2    -0.043995238 -0.06021644 -0.0277740370 0.0000000
T3_LL-T2    -0.054879167 -0.07056721 -0.0391911196 0.0000000
T3_LL-T3_LD -0.010883929 -0.02685854  0.0050906818 0.2817024



  Tukey multiple comparisons of means
    95% family-wise confidence level

Fit: aov(formula = NKA_activity ~ TimePoint, data = NKA_Assay)

$TimePoint
                   diff       lwr       upr     p adj
T2-T1       -4.2317761 -5.958755 -2.504798 0.0000006
T3_LD-T1    -0.2306113 -2.299228  1.838005 0.9904733
T3_LL-T1     0.1096831 -1.579335  1.798701 0.9980714
T3_LD-T2     4.0011649  1.901440  6.100890 0.0000548
T3_LL-T2     4.3414593  2.614481  6.068438 0.0000003
T3_LL-T3_LD  0.3402944 -1.728322  2.408911 0.9706559
```

```
Tukey multiple comparisons of means
    95% family-wise confidence level

Fit: aov(formula = NKA_a1b ~ TimePoint, data = qPCR_gill)

$TimePoint
                  diff         lwr         upr     p adj
T2-T1       -0.8354818 -1.12294689 -0.54801671 0.0000003
T3_LD-T1    -0.2217946 -0.52910771  0.08551851 0.2168260
T3_LL-T1    -0.4859757 -0.79328880 -0.17866258 0.0012352
T3_LD-T2     0.6136872  0.32622211  0.90115229 0.0000322
T3_LL-T2     0.3495061  0.06204102  0.63697120 0.0134343
T3_LL-T3_LD -0.2641811 -0.57149420  0.04313202 0.1091801
```

```
  Tukey multiple comparisons of means
    95% family-wise confidence level

Fit: aov(formula = CFTR1 ~ TimePoint, data = qPCR_gill)

$TimePoint
                  diff           lwr         upr     p adj
T2-T1       -0.6835635 -1.2770800018 -0.09004706 0.0196476
T3_LD-T1    -0.1081608 -0.6602857554  0.44396411 0.9486672
T3_LL-T1    -0.2391757 -0.7913006349  0.31294923 0.6376646
T3_LD-T2     0.5754027 -0.0007387676  1.15154419 0.0503807
T3_LL-T2     0.4443878 -0.1317536471  1.02052931 0.1738409
T3_LL-T3_LD -0.1310149 -0.6644182399  0.40238848 0.9053351
```

```
  Tukey multiple comparisons of means
    95% family-wise confidence level

Fit: aov(formula = logS100A1 ~ TimePoint, data = qPCR_gill)

$TimePoint
                  diff        lwr        upr     p adj
T2-T1       -1.5085832 -2.2366544 -0.7805119 0.0000348
T3_LD-T1     1.3108288  0.6040716  2.0175860 0.0001592
T3_LL-T1     1.6797417  0.9729845  2.3864989 0.0000043
T3_LD-T2     2.8194120  2.1421160  3.4967079 0.0000000
T3_LL-T2     3.1883249  2.5110290  3.8656208 0.0000000
T3_LL-T3_LD  0.3689129 -0.2854171  1.0232430 0.4237493
```

```
      Kruskal-Wallis rank sum test

data:  CAPN by TimePoint
Kruskal-Wallis chi-squared = 22.7, df = 3, p-value = 4.663e-05
```

```
Tukey multiple comparisons of means
    95% family-wise confidence level

Fit: aov(formula = cd3e ~ TimePoint, data = qPCR_gill)

$TimePoint
                  diff        lwr         upr     p adj
T2-T1        0.6869929  0.1523155  1.22167021 0.0081334
T3_LD-T1     0.3019983 -0.2326790  0.83667563 0.4238816
T3_LL-T1     0.1724632 -0.3622141  0.70714056 0.8126587
T3_LD-T2    -0.3849946 -0.8800096  0.11002045 0.1691330
T3_LL-T2    -0.5145297 -1.0095447 -0.01951463 0.0394396
T3_LL-T3_LD -0.1295351 -0.6245501  0.36547995 0.8890863


  Tukey multiple comparisons of means
    95% family-wise confidence level

Fit: aov(formula = csf1r ~ TimePoint, data = qPCR_gill)

$TimePoint
                   diff         lwr       upr     p adj
T2-T1        0.30102381 -0.20832726 0.8103749 0.3846893
T3_LD-T1     0.58795965  0.09478259 1.0811367 0.0150277
T3_LL-T1     0.27657265 -0.21660440 0.7697497 0.4300689
T3_LD-T2     0.28693584 -0.20624122 0.7801129 0.3982303
T3_LL-T2    -0.02445116 -0.51762822 0.4687259 0.9990777
T3_LL-T3_LD -0.31138700 -0.78784130 0.1650673 0.2993190
```

Il10rb ANOVA table

```
            Df Sum Sq Mean Sq F value Pr(>F)
TimePoint    3 0.5348 0.17827   1.909  0.152
Residuals   27 2.5214 0.09338
```

SAV 3 supplementary tables

Table S2: Three – way ANOVA table from GraphPad Prism v 9.0.0 based on IFN alpha 1 $2^{-\Delta\Delta CT}$ values from qPCR analysis for SAV3 heart cDNA samples

Table Analyzed	**Heart IFN *alpha* 1**				
Three-way ANOVA	Ordinary				
Alpha	0.05				
Source of Variation	% of total variation	P value	P value summary	Significant?	
Days past infection	1.348	0.2112	ns	No	
(LD vs LL)	0.1419	0.6826	ns	No	
(PBS vs SAV3)	61.33	<0,0001	****	Yes	
Day past infection x (LD vs LL)	0.06387	0.7837	ns	No	
Days past infection x (PBS vs SAV3)	1.906	0.1387	ns	No	
(LD vs LL) x (PBS vs SAV3)	0.126	0.6999	ns	No	
Days past infection x (LD vs LL) x (PBS vs SAV3)	6.618E-07	0.9993	ns	No	
ANOVA table	SS (Type III)	DF	MS	F (DFn, DFd)	P value
Days past infection	1.211	1	1.211	F (1, 42) = 1,612	P=0,2112
(LD vs LL)	0.1275	1	0.1275	F (1, 42) = 0,1696	P=0,6826
(PBS vs SAV3)	55.09	1	55.09	F (1, 42) = 73,31	P<0,0001
Day past infection x (LD vs LL)	0.05737	1	0.05737	F (1, 42) = 0,07634	P=0,7837
Days past infection x (PBS vs SAV3)	1.712	1	1.712	F (1, 42) = 2,278	P=0,1387
(LD vs LL) x (PBS vs SAV3)	0.1131	1	0.1131	F (1, 42) = 0,1506	P=0,6999
Days past infection x (LD vs LL) x (PBS vs SAV3)	5.945E-07	1	5.945E-07	F (1, 42) = 7,911e-007	P=0,9993
Residual	31.56	42	0.7515		

Table S3: Three – way ANOVA table from GraphPad Prism v 9.0.0 based on MHCI (UBA) $2^{-\Delta\Delta CT}$ values from qPCR analysis for SAV3 heart cDNA samples

Table Analyzed	**Heart MHCI (UBA)**				
Three-way ANOVA	Ordinary				
Alpha	0.05				
Source of Variation	% of total variation	P value	P value summary	Significant?	
Days past infection	2.707	0.233	ns	No	
(LD vs LL)	2.559	0.246	ns	No	
(PBS vs SAV3)	0.02399	0.9099	ns	No	
Day past infection x (LD vs LL)	2.71	0.2328	ns	No	
Days past infection x (PBS vs SAV3)	11.06	0.0187	*	Yes	
(LD vs LL) x (PBS vs SAV3)	1.165	0.4318	ns	No	
Days past infection x (LD vs LL) x (PBS vs SAV3)	0.05294	0.8665	ns	No	
ANOVA table	SS (Type III)	DF	MS	F (DFn, DFd)	P value
Days past infection	1.878	1	1.878	F (1, 43) = 1,463	P=0,2330
(LD vs LL)	1.776	1	1.776	F (1, 43) = 1,383	P=0,2460
(PBS vs SAV3)	0.01664	1	0.01664	F (1, 43) = 0,01297	P=0,9099
Day past infection x (LD vs LL)	1.881	1	1.881	F (1, 43) = 1,465	P=0,2328
Days past infection x (PBS vs SAV3)	7.673	1	7.673	F (1, 43) = 5,977	P=0,0187
(LD vs LL) x (PBS vs SAV3)	0.8084	1	0.8084	F (1, 43) = 0,6297	P=0,4318
Days past infection x (LD vs LL) x (PBS vs SAV3)	0.03674	1	0.03674	F (1, 43) = 0,02862	P=0,8665
Residual	55.2	43	1.284		

Table S4: Three – way ANOVA table from GraphPad Prism v 9.0.0 based on MHCII $2^{-\Delta\Delta CT}$ values from qPCR analysis for SAV3 heart cDNA samples

Table Analyzed	**Heart MHCII**				
Three-way ANOVA	Ordinary				
Alpha	0.05				
Source of Variation	% of total variation	P value	P value summary	Significant?	
Days past infection	2.78	0.1821	ns	No	
(LD vs LL)	24.16	0.0003	***	Yes	
(PBS vs SAV3)	4.106	0.1068	ns	No	
Day past infection x (LD vs LL)	11.79	0.008	**	Yes	
Days past infection x (PBS vs SAV3)	0.001259	0.9771	ns	No	
(LD vs LL) x (PBS vs SAV3)	0.005001	0.9544	ns	No	
Days past infection x (LD vs LL) x (PBS vs SAV3)	1.723	0.2914	ns	No	
ANOVA table	SS (Type III)	DF	MS	F (DFn, DFd)	P value
Days past infection	0.2185	1	0.2185	F (1, 39) = 1,845	P=0,1821
(LD vs LL)	1.898	1	1.898	F (1, 39) = 16,03	P=0,0003
(PBS vs SAV3)	0.3226	1	0.3226	F (1, 39) = 2,725	P=0,1068
Day past infection x (LD vs LL)	0.9266	1	0.9266	F (1, 39) = 7,827	P=0,0080
Days past infection x (PBS vs SAV3)	0.00009896	1	0.00009896	F (1, 39) = 0,0008359	P=0,9771
(LD vs LL) x (PBS vs SAV3)	0.0003929	1	0.0003929	F (1, 39) = 0,003319	P=0,9544
Days past infection x (LD vs LL) x (PBS vs SAV3)	0.1354	1	0.1354	F (1, 39) = 1,144	P=0,2914
Residual	4.617	39	0.1184		

Correlation between nsP1 and IFN *alpha 1* in heart

Table S5: Pearson correlation analysis between the SAV3 protein marker nsP1 and IFN alpha 1 dCT values from qPCR conducted on cDNA heart samples.

	nsP1 vs. IFNa1
Pearson r	
r	-0.005572
95% confidence interval	-0,4362 to 0,4271
R squared	0.00003104
P value	
P (two-tailed)	0.9809
P value summary	ns
Significant? (alpha = 0.05)	No
Number of XY Pairs	21

Table S6: Three – way ANOVA table from GraphPad Prism v 9.0.0 based on IFN alpha 1 $2^{-\Delta\Delta CT}$ values from qPCR analysis for SAV3 head kidney cDNA samples

Table Analyzed	**Head kidney IFN *alpha* 1**				
Three-way ANOVA	Ordinary				
Alpha	0.05				
Source of Variation	% of total variation	P value	P value summary	Significant?	
Days past infection	19.4	0.0002	***	Yes	
(LD vs LL)	0.7848	0.3749	ns	No	
(PBS vs SAV3)	0.389	0.5316	ns	No	
Day past infection x (LD vs LL)	8.083	0.0206	*	Yes	
Days past infection x (PBS vs SAV3)	1.901	0.3858	ns	No	
(LD vs LL) x (PBS vs SAV3)	0.1888	0.6627	ns	No	
Days past infection x (LD vs LL) x (PBS vs SAV3)	0.6327	0.7262	ns	No	
ANOVA table	SS (Type III)	DF	MS	F (DFn, DFd)	P value
Days past infection	24	2	12	F (2, 69) = 9,857	P=0,0002
(LD vs LL)	0.9707	1	0.9707	F (1, 69) = 0,7975	P=0,3749
(PBS vs SAV3)	0.4812	1	0.4812	F (1, 69) = 0,3953	P=0,5316
Day past infection x (LD vs LL)	9.999	2	4.999	F (2, 69) = 4,107	P=0,0206
Days past infection x (PBS vs SAV3)	2.351	2	1.176	F (2, 69) = 0,9658	P=0,3858
(LD vs LL) x (PBS vs SAV3)	0.2336	1	0.2336	F (1, 69) = 0,1919	P=0,6627
Days past infection x (LD vs LL) x (PBS vs SAV3)	0.7826	2	0.3913	F (2, 69) = 0,3215	P=0,7262
Residual	83.99	69	1.217		

Table S7: Three – way ANOVA table from GraphPad Prism v 9.0.0 based on MHCI (UBA) $2^{-\Delta\Delta CT}$ values from qPCR analysis for SAV3 head kidney cDNA samples

Table Analyzed	**Head kidney MHCI (UBA)**				
Three-way ANOVA	Ordinary				
Alpha	0.05				
Source of Variation	% of total variation	P value	P value summary	Significant?	
Days past infection	32.69	<0,0001	****	Yes	
(LD vs LL)	0.04827	0.7529	ns	No	
(PBS vs SAV3)	20.91	<0,0001	****	Yes	
Day past infection x (LD vs LL)	0.2811	0.7484	ns	No	
Days past infection x (PBS vs SAV3)	20.66	<0,0001	****	Yes	
(LD vs LL) x (PBS vs SAV3)	0.328	0.4127	ns	No	
Days past infection x (LD vs LL) x (PBS vs SAV3)	0.253	0.7704	ns	No	
ANOVA table	SS (Type III)	DF	MS	F (DFn, DFd)	P value
Days past infection	56.95	2	28.47	F (2, 70) = 33,84	P<0,0001
(LD vs LL)	0.08408	1	0.08408	F (1, 70) = 0,09991	P=0,7529
(PBS vs SAV3)	36.42	1	36.42	F (1, 70) = 43,29	P<0,0001
Day past infection x (LD vs LL)	0.4897	2	0.2448	F (2, 70) = 0,2910	P=0,7484
Days past infection x (PBS vs SAV3)	35.98	2	17.99	F (2, 70) = 21,38	P<0,0001
(LD vs LL) x (PBS vs SAV3)	0.5714	1	0.5714	F (1, 70) = 0,6790	P=0,4127
Days past infection x (LD vs LL) x (PBS vs SAV3)	0.4407	2	0.2204	F (2, 70) = 0,2619	P=0,7704
Residual	58.9	70	0.8415		

Table S8: Three – way ANOVA table from GraphPad Prism v 9.0.0 based on MHCII $2^{-\Delta\Delta CT}$ values from qPCR analysis for SAV3 head kidney cDNA samples

Table Analyzed	**Head kidney MHCII**				
Three-way ANOVA	Ordinary				
Alpha	0.05				
Source of Variation	% of total variation	P value	P value summary	Significant?	
Days past infection	30.48	<0,0001	****	Yes	
(LD vs LL)	0.2044	0.6269	ns	No	
(PBS vs SAV3)	1.809	0.1509	ns	No	
Day past infection x (LD vs LL)	8.877	0.0081	**	Yes	
Days past infection x (PBS vs SAV3)	2.815	0.2011	ns	No	
(LD vs LL) x (PBS vs SAV3)	0.2108	0.6215	ns	No	
Days past infection x (LD vs LL) x (PBS vs SAV3)	0.6356	0.6916	ns	No	
ANOVA table	SS (Type III)	DF	MS	F (DFn, DFd)	P value
Days past infection	5.583	2	2.792	F (2, 68) = 17,78	P<0,0001
(LD vs LL)	0.03744	1	0.03744	F (1, 68) = 0,2385	P=0,6269
(PBS vs SAV3)	0.3313	1	0.3313	F (1, 68) = 2,110	P=0,1509
Day past infection x (LD vs LL)	1.626	2	0.813	F (2, 68) = 5,178	P=0,0081
Days past infection x (PBS vs SAV3)	0.5156	2	0.2578	F (2, 68) = 1,642	P=0,2011
(LD vs LL) x (PBS vs SAV3)	0.03862	1	0.03862	F (1, 68) = 0,2460	P=0,6215
Days past infection x (LD vs LL) x (PBS vs SAV3)	0.1164	2	0.05821	F (2, 68) = 0,3707	P=0,6916
Residual	10.68	68	0.157		

Table S9: ANOVA table summary for IFN alpha 1 from GraphPad Prism v 9.0.0 based on IFN alpha 1 $2^{-\Delta\Delta CT}$ values from qPCR analysis of poly I:C treated leulocytes

Table Analyzed	Leukocyte IFN alpha 1 qPCR results
Data sets analyzed	A-F
ANOVA summary	
F	1.619
P value	0.1843
P value summary	ns
Significant diff. among means (P < 0.05)?	No
R squared	0.2071

Appendix D: SAV3 infection - Reference gene EF1-alpha

The expression of the geometric mean of reference gene EF1 alpha did not appear to differ between the different groups (Figure S6 and S7).

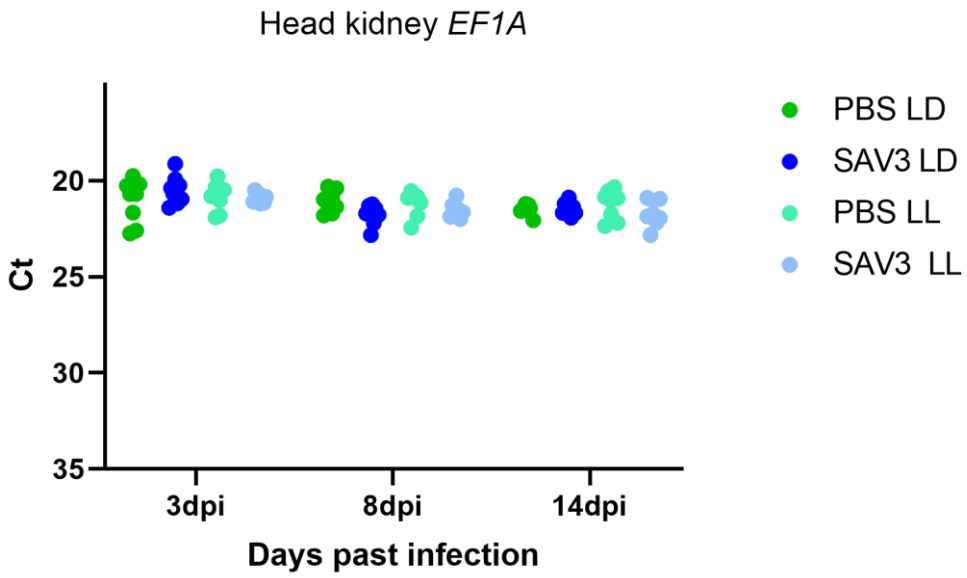

Figure S6: Plotted Ct values for geometric mean of the two reference genes of EF1 alpha in the cDNA head kidney samples.

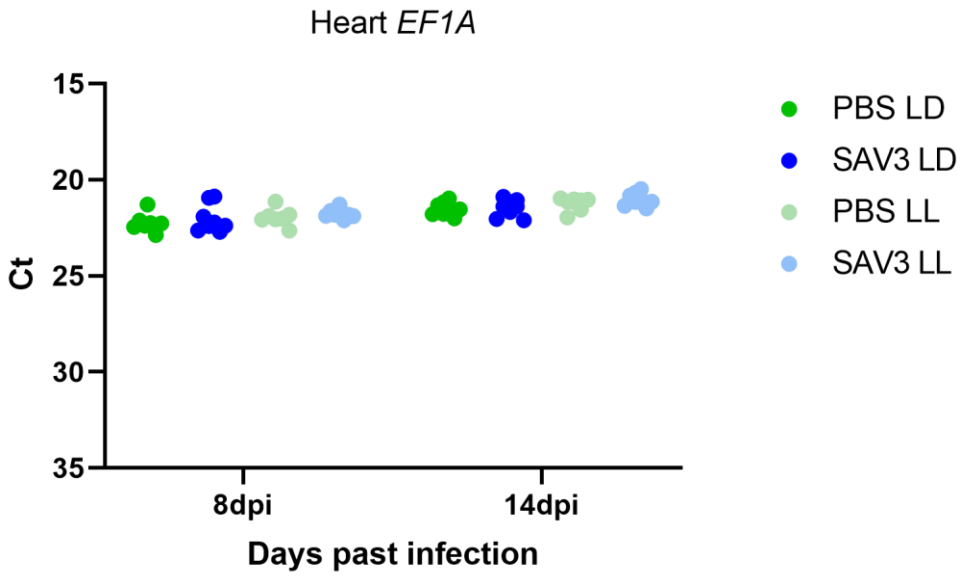

Figure S7: Plotted Ct values for geometric mean of the two reference genes of EF1 alpha in the cDNA heart sample

Appendix E: ECG study

Table S10: Position of ECG bio-logger at collection.

Fish ID	Position
1216	Spleen
1218	Spleen
1220	In place
1221	Spleen
1225	Liver
1226	Spleen
1227	Liver

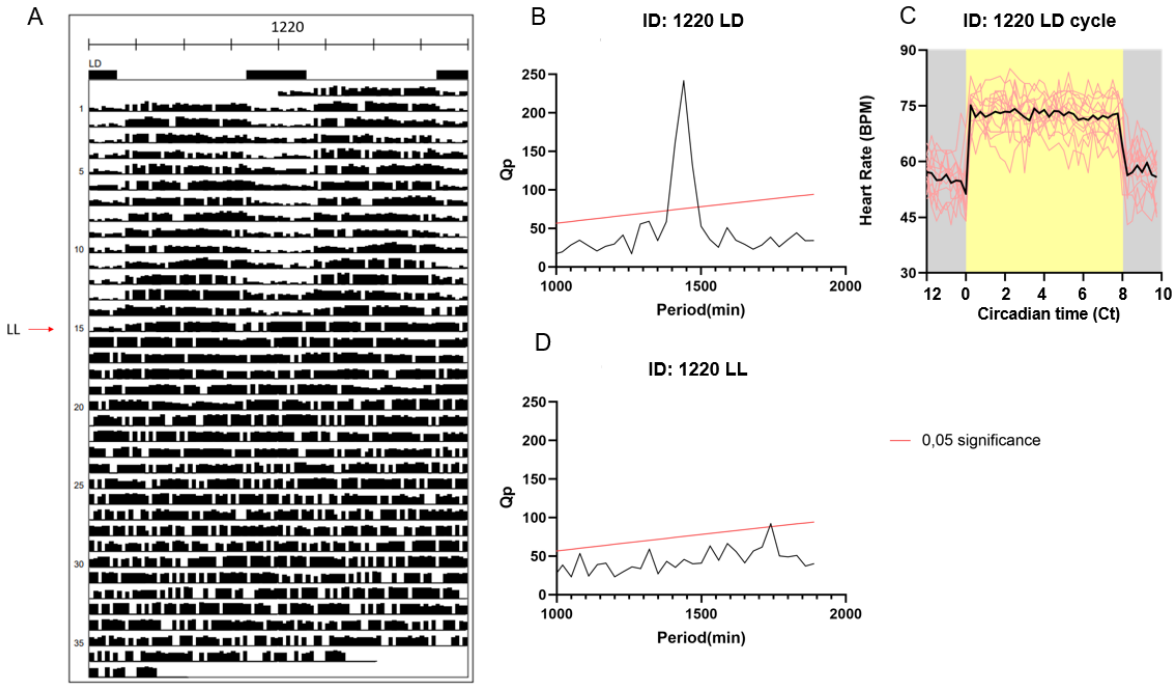

*Figure S8: **A**: Heart rate (BPM) of representative Atlantic salmon (Fish ID: 1220) double plotted in an actogram style with corresponding chi-square periodograms (**B** and **D**). The black bars are the dark phase during a 24-hour day, and the white bars the light phase. The red arrow shows when the fish went into constant light. The red line in the periodogram is the significance level of p=0,05. The salmon had a significant 24-hour rhythm under LD but become arrhythmic once put in constant light. **C** Daily change in heart rate over 24 hours, where the X axis is put in circadian time. The grey boxes show when it was dark, and the yellow boxes show when it was light. The pink lines are individual days and the black line the average heart rate for all days.*

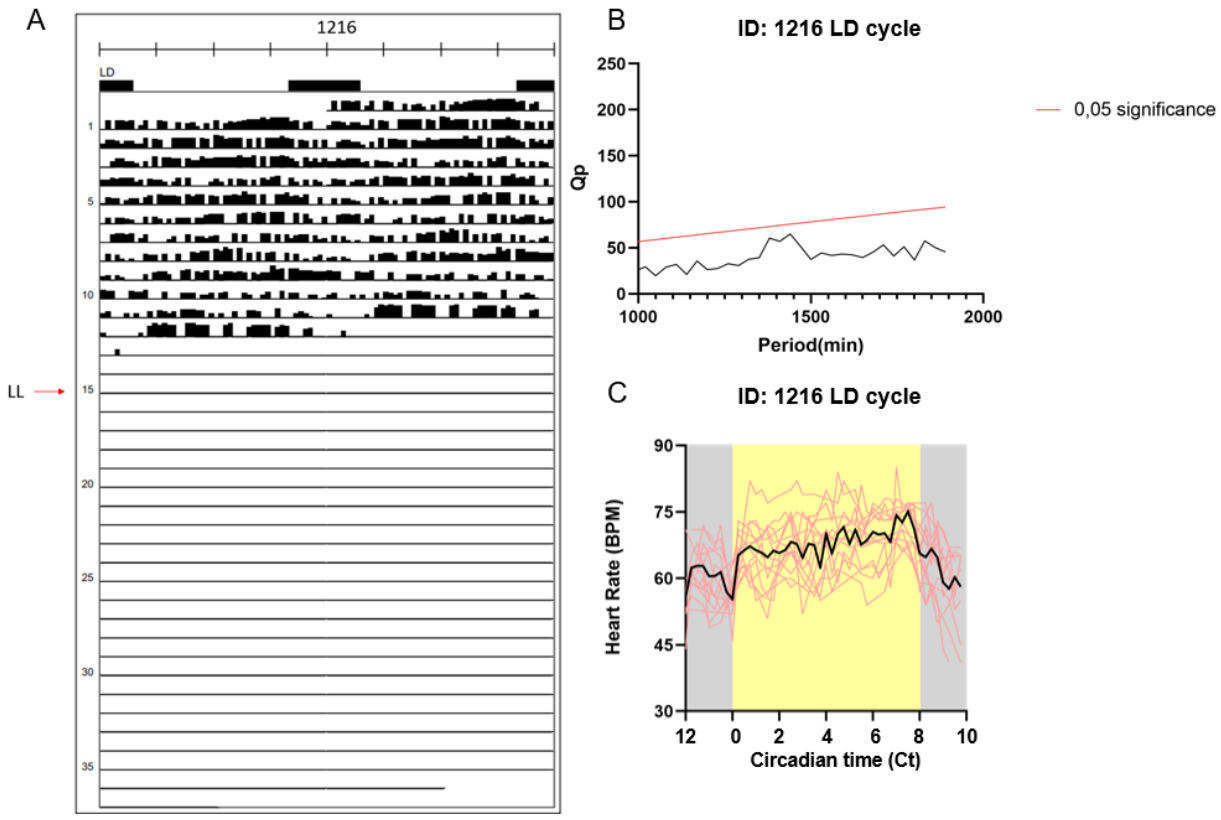

*Figure S9: **A**: Heart rate (BPM) of representative Atlantic salmon (Fish ID: 1216) double plotted in an actogram style with corresponding chi-square periodograms (**B** and **D**). The black bars are the dark phase during a 24-hour day, and the white bars the light phase. The red arrow shows when the fish went into constant light. The red line in the periodogram is the significance level of p=0,05. The salmon was arrhythmic under LD. **C** Daily change in heart rate over 24 hours, where the X axis is put in circadian time. The grey boxes show when it was dark, and the yellow boxes show when it was light. The pink lines are individual days and the black line the average heart rate for all days.*

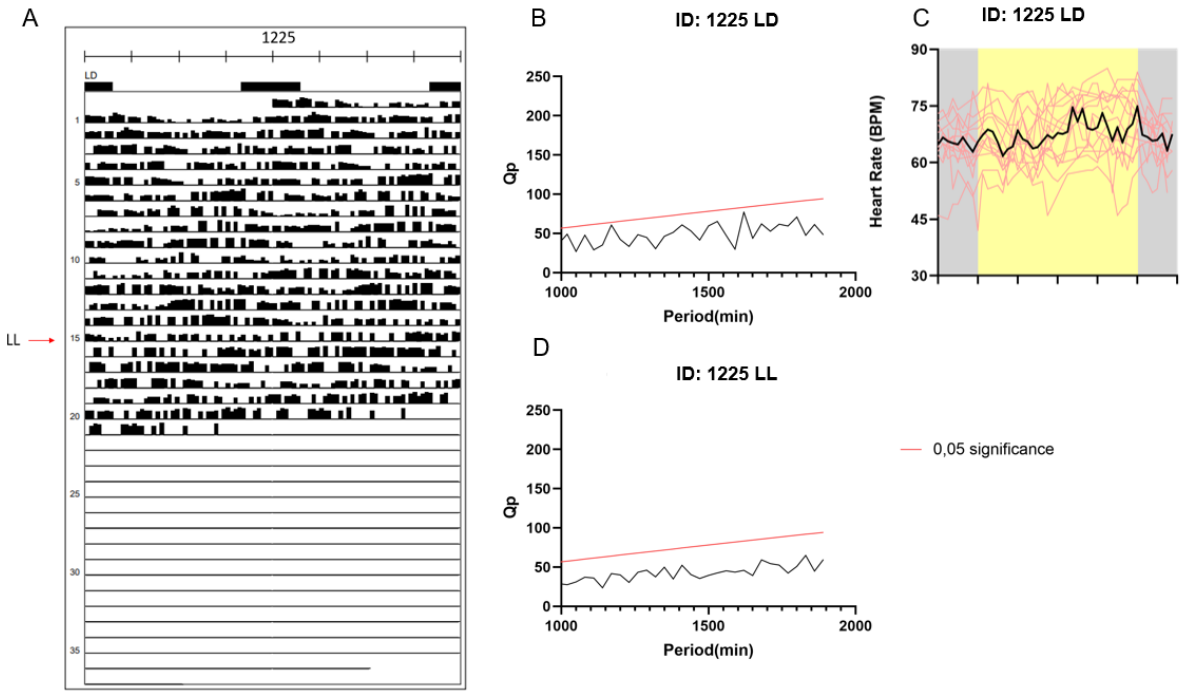

Figure S10: ***A****: Heart rate (BPM) of representative Atlantic salmon (Fish ID: 1226) double plotted in an actogram style with corresponding chi-square periodograms (****B*** *and* ***D****). The black bars are the dark phase during a 24-hour day, and the white bars the light phase. The red arrow shows when the fish went into constant light. The red line in the periodogram is the significance level of p=0,05. The salmon was arrhythmic both under a light/dark cycle and under constant light had a significant.* ***C:*** *Daily change in heart rate over 24 hours, where the X axis is put in circadian time. The grey boxes show when it was dark, and the yellow boxes show when it was light. The pink lines are individual days and the black line the average heart rate for all days.*